SUPPORTING INFORMATION

for

Biosynthesis of the Allylmalonyl-CoA Extender Unit for the FK506 PKS (Polyketide Synthase) Proceeds Through a Dedicated PKS and Facilitates the Mutasynthesis of New Analogs

SangJoon Mo,[1,8] Dong Hwan Kim,[2,3,8] Jong Hyun Lee,[1] Je Won Park,[1] Devi B. Basnet,[1] Yeon Hee Ban,[1] Young Ji Yoo,[1] Shu-wei Chen,[1] Sung Ryeol Park,[1] Eun Ae Choi,[1] Eunji Kim,[1] Ying-Yu Jin,[4] Sung-Kwon Lee,[4] Ju Yeol Park,[5] Yuan Liu,[6] Mi Ok Lee,[2] Keum Soon Lee,[2] Sang Jun Kim,[2] Dooil Kim,[7] Byoung Chul Park,[7] Sang-gi Lee,[1] Ho Jeong Kwon,[5] Joo-Won Suh,[4] Bradley S. Moore,[6] Si-Kyu Lim,[,2] and Yeo Joon Yoon*[,1]*

[1]Department of Chemistry and Nano Science, Ewha Womans University, Seoul 120-750, Republic of Korea. [2]GenoTech Corporation, Daejeon 305-343, Republic of Korea. [3]Department of Microbiology and Molecular Biology, Chungnam National University, Daejeon 305-764, Republic of Korea, [4]Division of Bioscience and Bioinformatics, Myongji University, Gyeonggi 449-728, Republic of Korea. [5]Department of Biotechnology, The Translational Research Center for Protein Function Control, Yonsei University, Seoul 120-746, Republic of Korea. [6]Scripps Institution of Oceanography and Skaggs School of Pharmacy and Pharmaceutical Sciences, University of California at San Diego, La Jolla, CA 92093-0204, USA. [7]Korea Research Institute of Bioscience and Biotechnology, Daejeon 305-600, Republic of Korea. [8]These authors contributed equally to this work.

EMAIL: slim@genotech.co.kr; joonyoon@ewha.ac.kr

Contents

Table S1. Deduced functions of ORFs in the FK506 biosynthetic gene cluster from *Streptomyces* sp. KCTC 11604BP[a]

Protein (residues)	**Homology in related organism**			**Best match**		**Proposed function**
	Streptomyces kanamyceticus KCTC 9225[b]	*Streptomyces* sp. ATCC 55098[c]	*Streptomyces tsukubaensis* NRRL 18488	Source	Percent identity/similarity (residues)	
	Percent identity/similarity (residues)			Organism/GenBank accession no.		
TcsA			AllA[d]			
AT (300)	86 / 92 (300)	83 / 91 (300)	100 / 100 (431)	*Nakamurella multipartita* DSM 44233 / YP_003203169	41 / 52 (578)	Acyl transferase domain
ACP (99)	67 / 78 (99)	74 / 82 (99)	100 / 100 (431)	*N. multipartita* DSM 44233 / YP_003203169	39 / 50 (578)	Acyl carrier protein (ACP)
TcsB			AllK[e]			
KS-$_{N\ term}$ (448)	82 / 87 (448)	81 / 87 (448)	100 / 100 (796)	*N. multipartita* DSM 44233 / YP_003203170	48 / 62 (2014)	β-ketoacyl synthase
KS-$_{C\ term}$ (320)	78 / 84 (320)	75 / 82 (320)	100 / 100 (796)	*Burkholderia thailandensis* E264 / ZP_05589458	34 / 49 (2126)	
TcsC (445)	90 / 94 (445)	87 / 94 (443)	AllR[f] 100 / 100 (445)	*Streptomyces lasaliensis* / CAQ64684	66 / 76 (454)	Crotonyl-CoA reductase
TcsD (386)	87 / 92 (386)	86 / 92 (386)	AllD[g] 99 / 100 (386)	*Catenulispora acidiphila* DSM 44928 / YP_003117666	71 / 81 (386)	Acyl-CoA/ACP dehydrogenase
Tcs1 (384)	—[h]	—[h]	AllM[i] 100 / 100 (384)	*Streptomyces pristinaespiralis* ATCC 25486 / ZP_05010287	66 / 77 (405)	Methionine gamma lyase

Tcs2 (155)	—[h]	—[h]	AllN[j] 100 / 100 (155)	*Streptomyces griseoflavus* Tu4000 / ZP_05542633	52 / 65 (163)	AsnC-family transcriptional regulatory protein
Tcs3 (409)	—[h]	—[h]	AllP[k] 99 / 100 (409)	*Streptomyces peucetius* ATCC 27952 / CAE53706	61 / 74 (410)	Cytochrome P450
Tcs4 (395)	—[h]	—[h]	AllO[l] 99 / 100 (395)	*Rhodococcus opacus* B4 / YP_002780495	38 / 55 (404)	Oxidoreductase
Tcs5 (250)	—[h]	—[h]	AllS[m] 99 / 100 (218)	*Corynebacterium glutamicum* / BAD84134	42 / 60 (249)	3-oxoacyl-ACP reductase
FkbG (222)	86 / 89 (222)	86 / 90 (99; frameshift found)	FkbG[n] 100 / 100 (222)	*Streptomyces hygroscopicus* var. *ascomyceticus* / AAF86386	81 / 86 (222)	Hydroxymalonyl-ACP methyltransferase
FkbH (362)	86 / 90 (362)	86 / 91 (362)	—[o]	*S. hygroscopicus* var. *ascomyceticus* / AAF86387	79 / 86 (360)	Formation of glyceryl-ACP
FkbI (366)	87 / 92 (366)	85 / 89 (366)	—[o]	*S. hygroscopicus* var. *ascomyceticus* / AAF86388	85 / 90 (366)	Acyl-CoA dehydrogenase
FkbJ (86)	85 / 89 (86)	80 / 88 (86)	—[o]	*S. hygroscopicus* var. *ascomyceticus* / AAF86389	73 / 84 (86)	Acyl carrier protein
FkbK (291)	88 / 90 (283)	86 / 89 (282)	—[o]	*S. hygroscopicus* var. *ascomyceticus* / AAF86390	83 / 89 (282)	Glyceryl-ACP C3 oxidation
FkbL (345)	89 / 94 (345)	88 / 92 (345)	—[o]	*S. hygroscopicus* var. *ascomyceticus* / AAF86391	86 / 93 (345)	Lysine cyclodeaminase
FkbC (3598)	82 / 86 (3597)	Recombination found	—[o]	*S. hygroscopicus* var. *ascomyceticus* / AAF86392	77 / 84 (3591)	FK506 polyketide synthase

FkbB (7646)	83 / 87 (7591)	Recombination found	—[o]	*Streptomyces* sp. MA6548 / AAC68815	81 / 86 (7576)	FK506 polyketide synthase
FkbO (330)	85 / 90 (332)	84 / 90 (333)	—[o]	*Streptomyces* sp. MA6548 / AAC68817	86 / 90 (332)	DHCHC biosynthetic protein
FkbP (1532)	83 / 87 (1506)	77 / 81 (1592)	—[o]	*Streptomyces* sp. MA6548 / AAC68816	82 / 87 (1504)	FK506 peptide synthetase
FkbA (6418)	84 / 89 (6408)	82 / 87 (6445)	—[o]	*Streptomyces* sp. MA6548 / T30283	81 /87 (6420)	FK506 polyketide synthase
FkbD (388)	89 / 92 (388)	88 / 91 (388)	—[o]	*S. hygroscopicus* var. *ascomyceticus* / AAF86397	88 / 93 (388)	FK506 C9 hydroxylase
FkbM (260)	82 / 90 (212)	85 / 91 (260)	—[o]	*Streptomyces* sp. MA6548 / AAC44360	84 / 91 (260)	31-*O*-demethyl-FK506 methyltransferase
FkbN (923)	82 / 89 (934)	82 / 89 (934)	—[o]	*S. hygroscopicus* var. *ascomyceticus* / AAF86399	71 / 82 (913)	ATP dependent transcriptional regulator
FkbQ (262)	84 / 90 (255)	81 / 89 (255)	—[o]	*S. hygroscopicus* var. *ascomyceticus* / AAF86400	83 / 88 (247)	Thioesterase II
Tcs6 (69)	—[h]	—[h]	—[o]	*Pectobacterium carotovorum* WPP14 / ZP_03831823	34 / 58 (276)	Putative lipoprotein
Tcs7 (474)	—[h]	—[h]	—[o]	*Streptomyces clavuligerus* ATCC 27064 / EDY53357	77 / 84 (304)	LysR-family transcriptional regulator

[a]GenBank accession no. HM116537; [b]HM116536; [c]HM116538; [d]ADG39431; [e]ADG39432; [f]ADG39433; [g]ADG39434; [h]not present; [i]ADG39435; [j]ADG39436; [k]ADG39437; [l]ADG39438; [m]ADG39439; [n]ADG39440; [o]not reported.

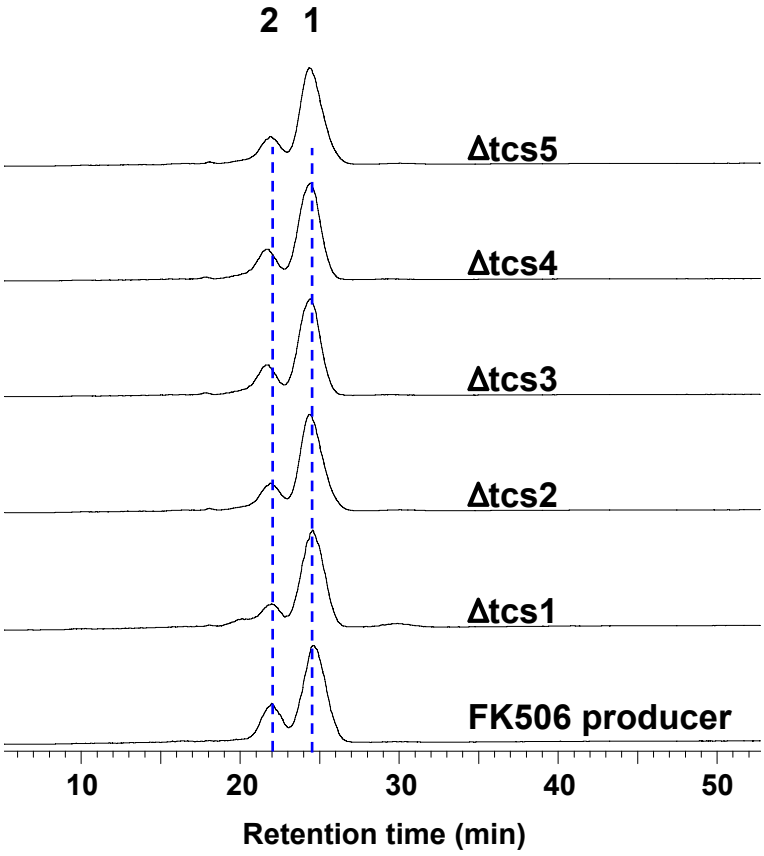

Figure S1. HPLC-ESI-MS/MS analysis of FK506 congeners obtained from wild-type FK506 (**1**)-producing *Streptomyces* sp. KCTC 11604BP and five mutant strains from which *tcs1*, *tcs2*, *tcs3*, *tcs4* or *tcs5* had been in-frame-deleted. The vertical blue dotted lines indicate the identity of the FK506 congeners **1** and FK520 (**2**). Tracing of both **1** and **2** was done in multiple reactions monitoring mode by selecting mass transit from the ammonium-adducted molecular ion to the specific fragmented product ion: 821 > 576 for **1** and 809 > 564 for **2**.

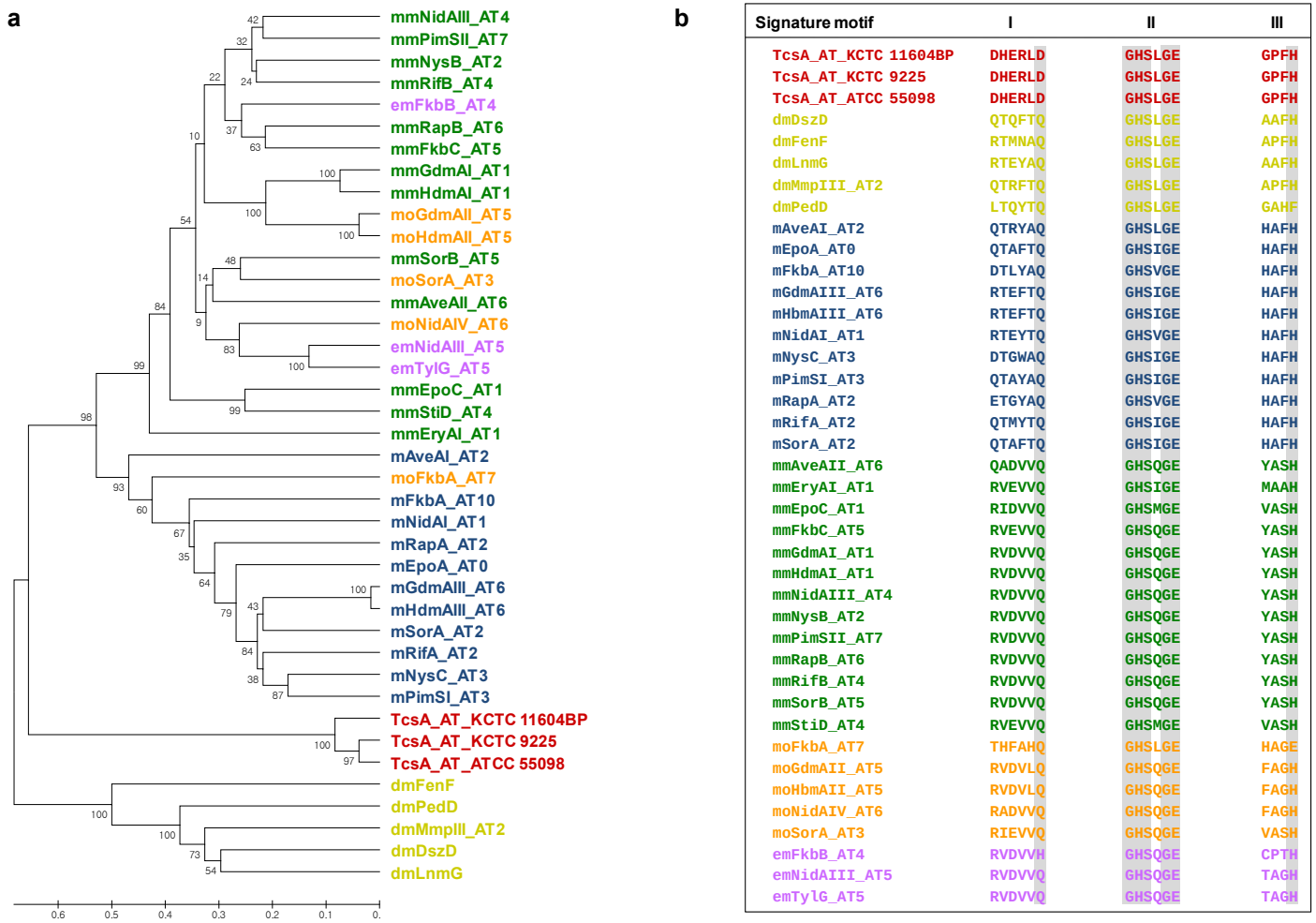

Figure S2. Phylogenetic analysis of TcsA AT domains and their signature motifs. (**a**) Phylogenetic tree of the acyl transferase (AT) domains obtained by comparing the amino acid sequence of each TcsA AT domain derived from three **1**-producing strains with those in the NCBI non-redundant (nr) protein database. (**b**) TcsA AT domain signature motifs. Three dominant motifs, composed of 6, 6, and 4 amino acid residues, are assigned with a group of ATs. Color codes used in this figure are: yellow, discrete malonyl (dm)-specific ATs; blue, malonyl (m)-specific ATs; green, methylmalonyl (mm)-specific ATs; orange, methoxylmalonyl (mo)-specific ATs; purple, ethylmalonyl (em)-specific ATs. See **Table S2**.

***Table S2*.** Sequences used in **Figures S2** and **S37**

Protein	Organism	GenBank accession no	AT no. (position)	Substrate specificity
TcsA_AT	*Streptomyces* sp. KCTC 11604BP	HM116537	4..303	
TcsA_AT	*Streptomyces kanamyceticus* KCTC 9225	HM116536	8..307	
TcsA_AT	*Streptomyces* sp. ATCC 55098	HM116538	8..307	
FkbB	*Streptomyces* sp. KCTC 11604BP	HM116537	AT4 (6571..6853)	
FkbB	*S. kanamyceticus* KCTC 9225	HM116536	AT4 (6516..6798)	
DszD	*Sorangium cellulosum*	AAY32968	1..291	Discrete malonyl-CoA-specific AT
FenF	*Bacillus subtilis*	AAF08794	1..303	
LnmG	*Streptomyces atroolivaceus*	AAN8520	1..276	
MmpIII	*Pseudomonas fluorescens*	AAM12912	AT2 (327..607)	
PedD	symbiont bacterium of *Paederus fuscipe*	AAS47563	1..276	
AveAI	*Streptomyces avermitilis*	BAA84474	AT2 (2641..2910)	
EpoA	*So. cellulosum*	AAF62880	AT0 (545..841)	
FkbA	*Streptomyces hygroscopicus* var. *ascomyceticus* ATCC 14891	AAF86396	AT10 (5904..6160)	
GdmAIII	*Streptomyces hygroscopicus*	AAO06918	AT6 (585..886)	
HdmAIII	*S. hygroscopicus*	AAY28227	AT6 (585..886)	Malonyl-CoA-specific AT
NidAI	*Streptomyces caelestis*	AAC46024	AT1 (1532..1821)	
NysC	*Streptomyces noursei* ATCC 11455	AAF71776	AT3 (546..835)	
PimSI	*Streptomyces natalensis*	CAC20931	AT3 (3831..4120)	
RapA	*S. hygroscopicus*	CAA60460	AT2 (3798..4061)	
RifA	*Amycolatopsis mediterranei*	AAC01710	AT2 (2718..2976)	
SorA	*So. cellulosum*	AAK19883	AT2 (2629..2930)	

AveAII	*S. avermitilis*	BAA84475	AT6 (4825..5114)	
EpoC	*So. cellulosum*	AAF62882	AT1 (541..836)	
EryAI	*Saccharopolyspora erythraea* NRRL 2338	CAM00062	AT1 (109..425)	
FkbC	*S. hygroscopicus* var. *ascomyceticus* ATCC 14891	AAF86392	AT5 (531..807)	
GdmAI	*S. hygroscopicus*	AAO06916	AT1 (1645..1941)	Methylmalonyl-CoA-specific AT
HdmAI	*S. hygroscopicus*	AAY28225	AT1 (1630..1925)	
NidAIII	*S. caelestis*	AAC46026	AT4 (571..868)	
NysB	*S. noursei* ATCC 11455	AAF71775	AT2 (2117..2416)	
PimSII	*S. natalensis*	CAC20921	AT7 (3862..4138)	
RapB	*S. hygroscopicus*	CAA60459	AT6 (2138..2418)	
RifB	*A. mediterranei*	AAC01711	AT4 (564..851)	
SorB	*So. cellulosum*	AAA79984	AT5 (2128..2422)	
StiD	*Stigmatella aurantiaca* Sg a15	CAD19088	AT4 (583..878)	
FkbB	*S. hygroscopicus* var. *ascomyceticus* ATCC 14891	AAF86393	AT4 (6479..6761)	Ethylmalonyl-CoA-specific AT
NidAIII	*S. caelestis*	AAC46026	AT5 (2011..2306)	
TylG	*Streptomyces fradiae*	AAB66506	AT5 (2099..2394)	
FkbA	*S. hygroscopicus* var. *ascomyceticus* ATCC 14891	AAF86396	AT7 (523..774)	
GdmAII	*S. hygroscopicus*	AAO06917	AT5 (2352..2650)	Methoxymalonyl-CoA-specific AT
HdmAII	*S. hygroscopicus*	AAY28226	AT5 (2350..2648)	
NidAIV	*S. caelestis*	AAC46027	AT6 (576..872)	
SorA	*So. cellulosum*	AAK19883	AT3 (4710..5002)	

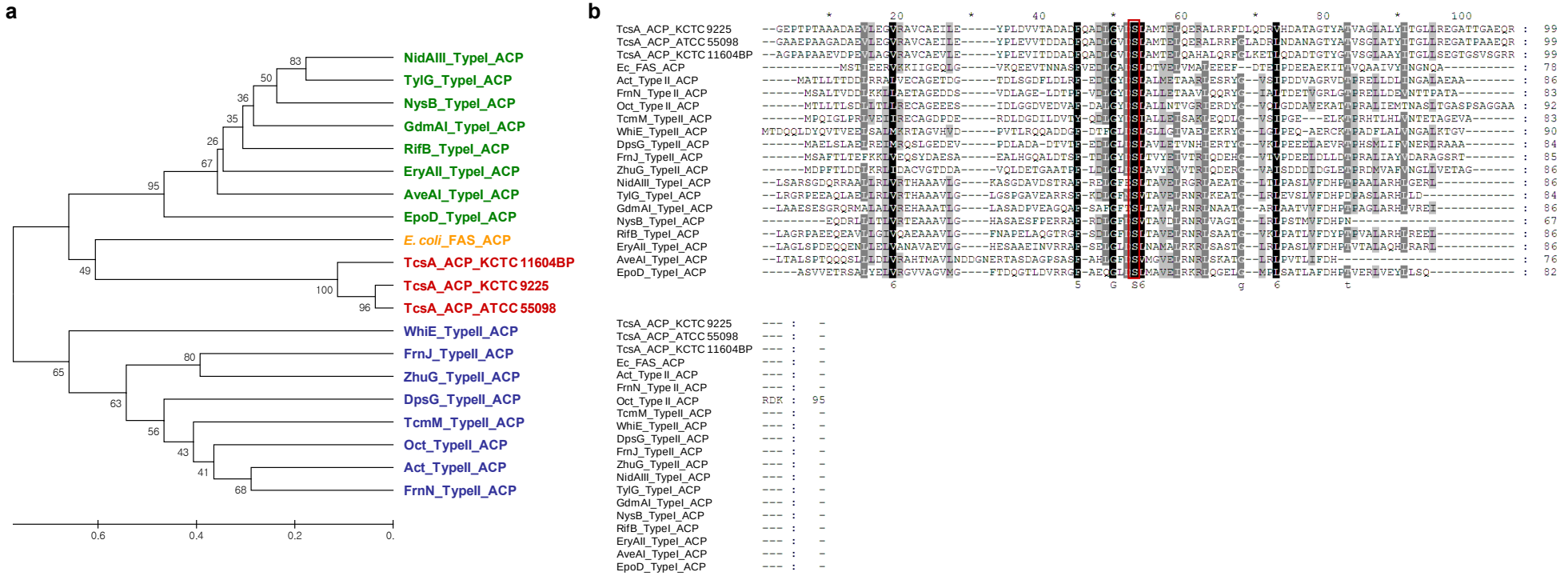

Figure S3. Phylogenetic analysis of TcsA ACP domains and their sequence alignment. (**a**) Phylogenetic tree of the acyl carrier protein (ACP) domains obtained by comparing the amino acid sequence of each TcsA ACP domain derived from three **1**-producing strains with those in the NCBI nr protein database. Color codes used in this figure are: green, ACP domains from type I PKSs; blue, ACP domains from type II PKSs; orange, ACP from *E. coli* FAS. (**b**) Sequence alignment of TcsA ACP domains with other ACPs from PKSs and FAS. The conserved active site is framed in red. See **Table S3**.

***Table S3*.** Sequences used in **Figure S3**

Protein	Organism	GenBank accession no	ACP position	Description
TcsA_ACP	*Streptomyces* sp. KCTC 11604BP	HM116537	329..427	
TcsA_ACP	*Streptomyces kanamyceticus* KCTC 9225	HM116536	328..426	
TcsA_ACP	*Streptomyces* sp. ATCC 55098	HM116538	331..429	
AveAI	*Streptomyces avermitilis*	BAA84474	366..441	Type I PKS
EpoD	*Sorangium cellulosum*	AAF62883	1424..1505	
EryAII	*Saccharopolyspora erythraea* NRRL 2338	CAM00064	1385..1470	
GdmAI	*Streptomyces hygroscopicus*	AAO06916	1000..1085	
NidAIII	*Streptomyces caelestis*	AAC46026	1352..1437	
NysB	*Streptomyces noursei* ATCC 11455	AAF71775	1480..1546	
RifB	*Amycolatopsis mediterranei*	AAC01711	1612..1697	
TylG	*Streptomyces fradiae*	AAB66506	1450..1533	
Act	*Streptomyces coelicolor* A3(2)	ACPCAA45045	1..86	Type II PKS
DpsG	*Streptomyces peucetius*	AAD04718	1..84	
FrnJ	*Streptomyces roseofulvus*	AAC18105	1..85	
FrnN	*S. roseofulvus*	AAC18109	1..83	
Oct	*Streptomyces rimosus*	P43677	1.. 95	
TcmM	*Streptomyces glaucescens*	AAA67517	1..83	
WhiE	*Streptomyces coelicolor*	P23153	1..90	
ZhuG	*Streptomyces* sp. R1128	AAG30194	1..86	
EcACP	*Escherichia coli*	AAB27925	1..78	FAS

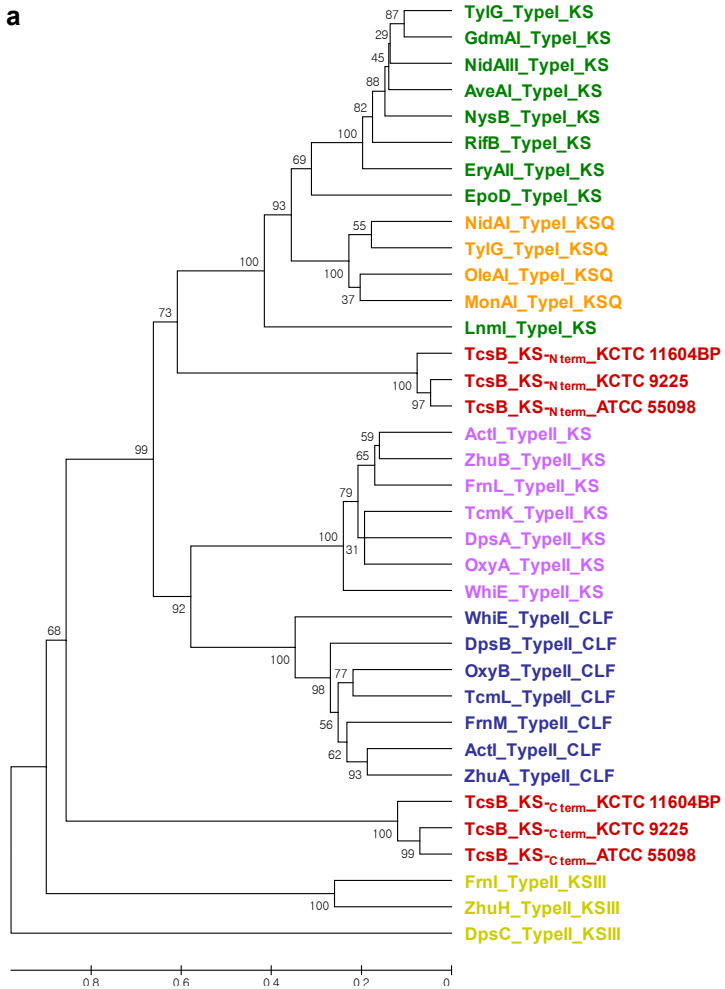

b

Signature motif	I	II	III	IV
TcsB_KS-N term_KCTC 11604BP	AACSS	IAHGT	KSLLGH	AFGFG
TcsB_KS-N term_KCTC 9225	AACSS	IAHGT	KSLLGH	AFGFG
TcsB_KS-N term_ATCC 55098	AACSS	IAHGT	KSLLGH	AFGFG
AveAI_TypeI_KS	TGCSA	EGHGT	KSNIGH	SFGIG
EpoD_Type I_KS	TACSS	ECHGT	KANVAH	AFGLS
EryAII_TypeI_KS	TACSS	EAHGT	KSNIGH	AFGIS
GdmAI_TypeI_KS	TACSS	EAHGT	KSNIGH	SFGVS
LnmI_TypeI_KS	TSCSS	ECAAA	KPNIGH	AVGAT
NidAIII_TypeI_KS	TACSS	EAHGT	KSNIGH	AFGVS
NysB_TypeI_KS	TACSS	EAHGT	KSNIGH	SFGIS
RifB_TypeI_KS	TMCSS	EGHGT	KSVVGH	SFGAS
TylG_TypeI_KS	TACSS	EAHGT	KSNIGH	AFGVS
ActI_TypeII_KS	TGCTS	NAHGS	KSMVGH	GSGFG
DpsA_TypeII_KS	AGCTS	NAHGT	KSMIGH	GSGFG
FrnL_TypeII_KS	TGCTS	NAHGS	KSMIGH	GSGFG
OxyA_TypeII_KS	AGCTS	NAHGS	KSMIGH	ASGFG
TcmK_TypeII_KS	TGCTS	NAHGS	KSMIGH	GSGFG
WhiE_TypeII_KS	TGCTS	NAHGS	KSMVGH	GSGFG
ZhuB_TypeII_KS	SGCTS	NAHGS	KSMIGH	GSGFG
MonAI_TypeI_KSQ	TAQSS	ELHGT	KTNVGH	SFGMG
NidAI_TypeI_KSQ	TGQSS	ELHGT	KTNIGH	AFGMG
OleAI_TypeI_KSQ	TGQSS	ELHGT	KTNIGH	SFGMG
TylG_TypeI_KSQ	SAQSA	ELHGT	KTNVGH	SFGMG
ActI_TypeII_CLF	AEQAG	FADGA	KTTTGR	ARGRW
DpsB_TypeII_CLF	AEQAG	FADGA	KTLTGR	ARGYG
FrnM_TypeII_CLF	ADQAG	FADAA	KTQTGR	ARGHG
OxyB_TypeII_CLF	AEQAG	FADAM	KTMTGR	ARGHG
TcmL_TypeII_CLF	TEQAG	YADAA	KTMTGR	ARGMG
WhiE_TypeII_CLF	ADEAG	FADAL	KTGTGR	ARGLM
ZhuA_TypeII_CLF	GEQAG	FADAA	KSLVGR	ARGHG
TcsB_KS-C term_KCTC 11604BP	TGTTS	VPGGP	DVAVGP	-----
TcsB_KS-C term_KCTC 9225	TGATS	TCGAA	DVAVGP	-----
TcsB_KS-C term_ATCC 55098	TGATS	TCGAA	GVTVGP	-----
DpsC_TypeII_KSIII	QVSNG	SVARV	MGWRRL	SVGAG
FrnI_TypeII_KSIII	GACAG	TPRAA	QANLRM	GFGAG
ZhuH_TypeII_KSIII	AACAG	VPAAR	QANLRI	GFGAG

Figure S4. Phylogenetic analysis of TcsB KS domains and their signature motifs. (**a**) Phylogenetic tree of the β-keto-acyl synthase (KS) domains obtained by comparing the amino acid sequence of each TcsB KS domain derived from three **1**-producing strains into the NCBI nr protein database. (**b**) TcsB KS domain signature motifs. Four dominant motifs, composed of 5, 5, 6, and 5 amino acid residues, are assigned with a group of KSs. Color codes used in this figure are: green, typical KS domains from type I PKSs; orange, typical KS^Q domains from type I PKSs; purple, KSs from type II PKSs; blue, CLF subunits from type II PKSs; yellow, KSIII subunits from type II PKSs. See **Table S4**.

Table S4. Sequences used in **Figure S4**

Protein	Organism	GenBank accession no	KS position	Description
TcsB_KS-$_{N\ term}$	*Streptomyces* sp. KCTC 11604BP	HM116537	16..463	
TcsB_KS-$_{N\ term}$	*Streptomyces kanamyceticus* KCTC 9225	HM116536	16..463	
TcsB_KS-$_{N\ term}$	*Streptomyces* sp. ATCC 55098	HM116538	16..463	
TcsB_KS-$_{C\ term}$	*Streptomyces* sp. KCTC 11604BP	HM116537	477..796	
TcsB_KS-$_{C\ term}$	*S. kanamyceticus* KCTC 9225	HM116536	477..796	
TcsB_KS-$_{C\ term}$	*Streptomyces* sp. ATCC 55098	HM116538	477..796	
AveAI	*Streptomyces avermitilis*	BAA84474	483..913	
EpoD	*Sorangium cellulosum*	AAF62883	3026..3452	
EryAII	*Saccharopolyspora erythraea* NRRL2338	CAM00064	33..457	
GdmAI	*Streptomyces hygroscopicus*	AAO06916	1103..1530	
LnmI	*Streptomyces atroolivaceus*	AAN85522	1931..2345	Type I KS
NidAIII	*Streptomyces caelestis*	AAC46026	38..463	
NysB	*Streptomyces noursei* ATCC 11455	AAF71775	44..464	
RifB	*Amycolatopsis mediterranei*	AAC01711	37..462	
TylG	*Streptomyces fradiae*	AAB66506	45..469	
MonAI	*Streptomyces cinnamonensis*	AAO65796	19..426	
NidAI	*S. caelestis*	AAC46024	23..430	Type I KS^{Q}
OleAI	*Streptomyces antibioticus*	AAF82408	10..428	
TylG	*S. fradiae*	AAB66504	45..451	
ActI_α subunit	*Streptomyces coelicolor* A3(2)	CAC44200	1..467	Type II KS
DpsA	*Streptomyces peucetius*	AAA65206	1..419	
FrnL	*Streptomyces roseofulvus*	AAC18107	1..425	
OxyA	*Streptomyces rimosus*	AAZ78325	1..425	
TcmK	*Streptomyces glaucescens*	AAA67515	1..426	

WhiE_α subunit	*Streptomyces coelicolor*	P23155	1..423	
ZhuB	*Streptomyces* sp. R1128	AAG30189	1..417	
ActI_β subunit	*S. coelicolor* A3(2)	CAC44201	1..407	Type II CLF
DpsB	*S. peucetius*	AAA65207	1..425	
FrnM	*S. roseofulvus*	AAC18108	1..426	
OxyB	*S. rimosus*	AAZ78326	1..422	
TcmL	*S. glaucescens*	AAA67516	1..409	
WhiE_β subunit	*S. coelicolor*	P23156	1..424	
ZhuA	*Streptomyces* sp. R1128	AAG30188	1..415	
DpsC	*S. peucetius*	AAA65208	1..353	Type II KSIII
FrnI	*S. roseofulvus*	AAC18104	1..336	
ZhuH	*Streptomyces* sp. R1128	AAG30195	1.. 339	

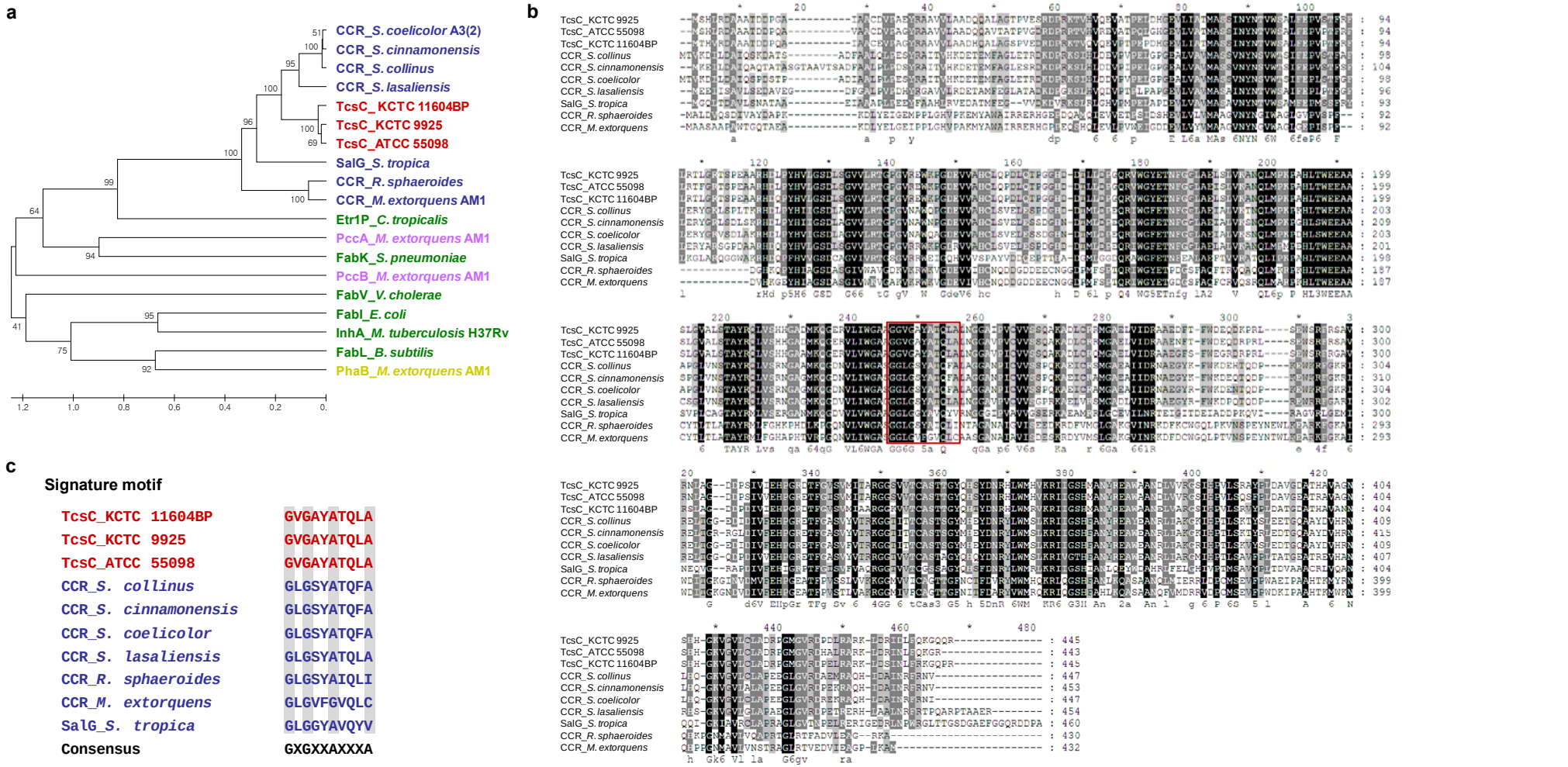

Figure S5. Phylogenetic analysis of TcsCs and their signature motif. (**a**) Color codes used in this figure are: blue, crotonyl-CoA carboxylase/reductase (CCR); purple, butyryl-CoA/propionyl-CoA carboxylase; green, enoyl-ACP reductase; yellow, acetoacetyl-CoA reductase. (**b**) Sequence alignment of TcsCs with a group of CCRs. The NADP(H) binding site is framed in red. (**c**) TcsC NADP(H) binding motif. A dominant motif, composed of 10 amino acid residues, is assigned with a group of CCRs as aligned, and the GXGXXAXXXA NADP(H) binding motif is conserved. See **Table S5**.

***Table S5*.** Sequences used in **Figure S5**

Protein	Organism	GenBank accession no	Residues	Function
TcsC	*Streptomyces* sp. KCTC 11604BP	HM116537	445	
TcsC	*Streptomyces kanamyceticus* KCTC 9225	HM116536	445	
TcsC	*Streptomyces* sp. ATCC 55098	HM116538	443	
CCR	*Streptomyces lasaliensis*	CAQ64684	454	Crotonyl CoA reductase
CCR	*Streptomyces collinus*	AAA92890	447	Crotonyl CoA reductase
CCR	*Streptomyces cinnamonensis*	AAD53915	453	Crotonyl CoA reductase
CCR	*Streptomyces coelicolor* A3(2)	CAA22721	447	Crotonyl-CoA carboxylase/reductase
CCR	*Rhodobacter sphaeroides*	ACJ71669	430	Crotonyl-CoA carboxylase/reductase
CCR	*Methylobacterium extorquens* AM1	ACS38140	432	Crotonyl-CoA carboxylase/reductase
SalG	*Salinispora tropica*	ABP73651	460	Crotonyl-CoA carboxylase/reductase
PccA	*M. extorquens* AM1	ACS40950	667	Butyryl-CoA/propionyl-CoA carboxylase
PccB	*M. extorquens* AM1	ACS38134	510	Butyryl-CoA/propionyl-CoA carboxylase
FabI	*Escherichia coli* str. K-12 substr. W3110	BAA14841	262	Enoyl-ACP reductase
FabL	*Bacillus subtilis* subsp. *subtilis* str. 168	CAB12693	250	Enoyl-ACP reductase
FabV	*Vibrio cholerae* bv. *albensis*	ABX38717	401	Enoyl-ACP reductase

InhA	*Mycobacterium tuberculosis* H37Rv	CAB02034	269	Enoyl-ACP reductase
FabK	*Streptococcus pneumoniae*	AAF98273	324	*Trans*-2-enoyl-ACP reductase
Etr1P	*Candida tropicalis*	Q8WZM3	386	Enoyl-ACP reductase
PhaB	*M. extorquens* AM1	AAK11537	242	Acetoacetyl-CoA reductase

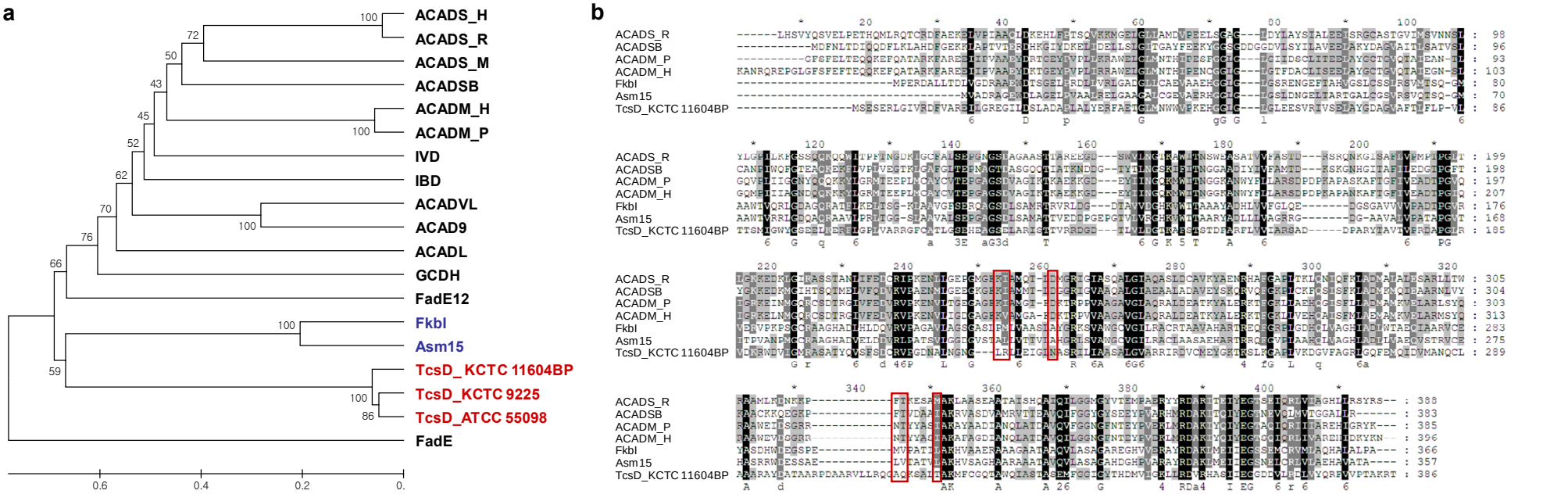

Figure S6. Phylogenetic analysis of TcsDs and their sequence alignment. (**a**) Phylogenetic tree of the acyl-ACP or acyl-CoA dehydrogenase (DH) obtained by comparing the amino acid sequence of each TcsD derived from three **1**-producing strains with those in the NCBI nr protein database. Acyl-ACP DHs are shown in blue and acyl-CoA DHs in black. (**b**) Sequence alignment of TcsDs along with acyl-ACP dehydrogenases (FabI and Asm15), as well as a group of acyl-coA DHs (ACADS_R, ACADSB, ACADM_P, and ACADM_H). Positions substituted with hydrophobic residues, which are commonly observed in acyl-ACP DHs (TcsD as well as FkbI and Asm15), are framed in red. See **Table S6**.

Table S6. Sequences used in **Figure S6**

Protein	Organism	GenBank accession no	Residues	Function
TcsD	*Streptomyces* sp. KCTC 11604BP	HM116537	386	
TcsD	*Streptomyces kanamyceticus* KCTC 9225	HM116536	386	
TcsD	*Streptomyces* sp. ATCC 55098	HM116538	386	
FkbI	*Streptomyces hygroscopicus* var. *ascomyceticus* ATCC 14891	AAF86388	366	Acyl-ACP dehydrogenase
Asm15	*Actinosynnema pretiosum* subsp. *auranticum*	AAM54093	357	Acyl-ACP dehydrogenase
ACADL	*Homo sapiens* (human)	P28330	430	Long chain-specific acyl-CoA dehydrogenase
ACADVL	*Homo sapiens*	P49748	655	Very long chain-specific acyl-CoA dehydrogenase
ACADM_H	*Homo sapiens*	P11310	421	Medium chain-specific acyl-CoA dehydrogenase
ACADM_P	*Sus scrofa* (pig)	AAW30430	421	Medium chain-specific acyl-coA dehydrogenase
ACADS_H	*Homo sapiens*	P16219	412	Short chain-specific acyl-CoA dehydrogenase
ACADS_M	*Megasphaera elsdenii*	AAA03594	383	Short chain-specific acyl-CoA dehydrogenase
ACADS_R	*Rattus norvegicus* (Norway rat)	AAA40669	414	Short chain-specific acyl-CoA dehydrogenase
ACADSB	*Homo sapiens*	P45954	432	Short/branched chain-specific acyl-CoA

				dehydrogenase
ACAD9	*Homo sapiens*	Q9H845	621	Acyl-CoA dehydrogenase family member 9
FadE	*Escherichia coli* K-12	Q47146	814	Acyl-CoA dehydrogenase
FadE12	*Mycobacterium tuberculosis*	P71539	388	Acyl-CoA dehydrogenase
GCDH	*Homo sapiens*	Q92947	438	Glutaryl-CoA dehydrogenase
IBD	*Homo sapiens*	Q9UKU7	415	Isobutyryl-CoA dehydrogenase
IVD	*Homo sapiens*	P26440	423	Isovaleryl-CoA dehydrogenase

Table S7. Bacterial strains and plasmids used in this study

Strain/vector	Relevant characteristics	Reference
Bacterial strains		
Escherichia coli		
DH5α	Host for general cloning	New England Biolabs
BL21(DE3)	Host for protein expression	Novagen
BL21(DE3)pLysS	Host for protein expression	Novagen
EPI300TM	Host for gene library construction	Epicentre Biotechnol.
ET12567/pUZ8002	Donor strain for intergeneric conjugation between *E. coli* and *Streptomyces*	MacNeil, D.J. *et al*.[1]
BL21 (DE3)pLysS/pTCSA-ACP	Strain for ACP_{tcsA} protein expression	This study
BL21(DE3)/pTCSC	Strain for TcsC protein expression	This study
BL21(DE3)pLysS/pSFP	Strain for Sfp (PPTase) protein expression	This study
Streptomyces		
ATCC 55098 (MA6858)	Wild-type FK506 (**1**)-producing strain	Motamedi, H. *et al*.[2]
KCTC 11604BP	Wild-type **1**-producing strain	This study
KCTC 9225	Wild-type **1**-producing strain	Muramatsu, H. *et al*.[3]
ATCC 14891	Wild-type FK520 (**2**)-producing strain	Wu, K. *et al*.[4]
ΔtcsA	Mutant of KCTC 11604BP with an in-frame deletion of *tcsA*, produces **2** & FK523 (**12**)	This study
ΔtcsB	Mutant of KCTC 11604BP with an in-frame deletion of *tcsB*, produces **2** & **12**	This study
ΔtcsC	Mutant of KCTC 11604BP with an in-frame deletion of *tcsC*, produces **2** & **12**	This study
ΔtcsD	Mutant of KCTC 11604BP with an in-frame deletion of *tcsD*, produces **2** & dihydro-FK506 (**18**)	This study

Δtcs1	Mutant of KCTC 11604BP with an in-frame deletion of *tcs1*, produces **1** & **2**	This study
Δtcs2	Mutant of KCTC 11604BP with an in-frame deletion of *tcs2*, produces **1** & **2**	This study
Δtcs3	Mutant of KCTC 11604BP with an in-frame deletion of *tcs3*, produces **1** & **2**	This study
Δtcs4	Mutant of KCTC 11604BP with an in-frame deletion of *tcs4*, produces **1** & **2**	This study
Δtcs5	Mutant of KCTC 11604BP with an in-frame deletion of *tcs5*, produces **1** & **2**	This study
ΔfkbA	Mutant of KCTC 11604BP with an in-frame deletion of *fkbA*, does not produce **1** or **2**	This study
S. lividans TK24	Host for protein expression	Walczak, R.J. *et al*[5]
S. lividans TK24/pTCSD	TK24 mutant, expresses heterologous *tcsD* using pTCSD	This study
Plasmids		
pCCFOS1 (fosmid)	Vector for genomic library construction	Epicentre Biotechnol.
Litmus 28	Multi-purpose *E. coli* cloning vector	New England Biolabs
pGEM-Teasy	PCR fragment cloning vector	Promega
pKC1139	High-copy-number temperature-sensitive *E. coli-Streptomyces* shuttle vector	Bierman, M. *et al*.[6]
pET15b, pET28a	*E. coli* protein expression vector	Novagen
pGF101	Sfp expression plasmid based on pET30a(+)	Zhou, P. *et al*.[7]
pSE34	pWHM3 with P_{ermE*} promoter	Yoon, Y.J. *et al*.[8]
pΔTCSA	Deletion plasmid with in-frame deletion of 1,287-bp internal *tcsA* fragment	This study
pΔTCSB	Deletion plasmid with in-frame deletion of 2,088-bp internal *tcsB* fragment	This study
pΔTCSC	Deletion plasmid with in-frame deletion of 1,041-bp internal *tcsC* fragment	This study
pΔTCSD	Deletion plasmid with in-frame deletion of 1,152-bp internal *tcsD* fragment	This study
pΔTCS1	Deletion plasmid with in-frame deletion of 1,110-bp internal *tcs1* fragment	This study

pΔTCS2	Deletion plasmid with in-frame deletion of 171-bp internal *tcs2* fragment	This study
pΔTCS3	Deletion plasmid with in-frame deletion of 1,209-bp internal *tcs3* fragment	This study
pΔTCS4	Deletion plasmid with in-frame deletion of 864-bp internal *tcs4* fragment	This study
pΔTCS5	Deletion plasmid with in-frame deletion of 666-bp internal *tcs5* fragment	This study
pΔFKBA	Deletion plasmid with in-frame deletion of 18,171-bp internal *fkbA* fragment	This study
pTCSC	N, C-terminal His_6-tagged TcsC expression plasmid based on pET28a(+)	This study
pTCSA-ACP	N-terminal His_6-tagged ACP_{tcsA} expression plasmid based on pET15b(+)	This study
pSFP	N-terminal His_6-tagged Sfp expression plasmid based on pET15b(+)	This study
pTCSD1	N-terminal His_6-tagged plasmid based on pET15b(+), contains *tcsD* ORF	This study
pTCSD	N-terminal His_6-tagged TcsD expression plasmid based on pSE34	This study
Fosmid clones		
From KCTC 11604BP		
fos1004F01	Fosmid clone, contains bases 1–40,366 of FK506 biosynthetic gene cluster	This study
fos1005D02	Fosmid clone, contains bases 39,116–80,661 of FK506 biosynthetic gene cluster	This study
fos1006D05	Fosmid clone, contains bases 58,172–97,743 of FK506 biosynthetic gene cluster	This study
From KCTC 9225		
fos1006G02	Fosmid clone, contains bases 1–35,521 of FK506 biosynthetic gene cluster	This study
fos1012A09	Fosmid clone, contains bases 31,026–67,758 of FK506 biosynthetic gene cluster	This study
fos1004E04	Fosmid clone, contains bases 41,430–85,253 of FK506 biosynthetic gene cluster	This study
fos1010E10	Fosmid clone, contains bases 76,978–111,990 of FK506 biosynthetic gene cluster	This study
From ATCC 55098		
fos1011B11	Fosmid clone, contains bases 1–41,779 of FK506 biosynthetic gene cluster	This study

fos1010H09	Fosmid clone, contains bases 9,843–44,811 of FK506 biosynthetic gene cluster	This study
fos1012B03	Fosmid clone, contains bases 27,398–72,806 of FK506 biosynthetic gene cluster	This study
fos1001F05	Fosmid clone, contains bases 59,900–95,979 of FK506 biosynthetic gene cluster	This study

Table S8. Primers used in this study

Primer	Sequence 5' to 3' (restriction site underlined)	Restriction enzyme
TcsALF	TTTAAGCTTCCGTCGGATCGGGGCGGCAG	*Hind*III
TcsALR	AAAGGATCCGAAGAGGAACGCCACCCCAC	*Bam*HI
TcsARF	TTTAGATCTTGATCCGGTCGTGATCTCCC	*Bgl*II
TcsARR	AAAGAATTCGTCGCCGGGCAGGTGCGC	*Eco*RI
TcsBLF	GACAAGCTTATGCTGGCGGTGAAGGCG	*Hind*III
TcsBLR	CCGTCTAGACCAGAAGGAATCGAGCCGGAA	*Xba*I
TcsBRF	CAGTCTAGAGTGATCCGTGCCCTGCACTCC	*Xba*I
TcsBRR	GCCGAATTCGATGACGATGTCCGGGTCG	*Eco*RI
TcsCLF	TTTAAGCTTAACAAGTCCCTGCTCGGTCA	*Hind*III
TcsCLR	AACGGATCCGTCTTCGACGGGGCTCCCGG	*Bam*HI
TcsCRF	AAAAGATCTTCCCGGGTCTACCCCCTCGA	*Bgl*II
TcsCRR	TTTGAATTCCTCACCCAGGCCCTGACGC	*Eco*RI
TcsDLF	GCTAAGCTTCTCAGGCGTCTGCGGATGC	*Hind*III
TcsDLR	ATCGGATCCTTCGCTCACCGGGGCTGCC	*Bam*HI
TcsDRF	AGCAGATCTGGCATGTTCTGGTCAGTCC	*Bgl*II
TcsDRR	GTCGAATTCCATGCCACGAACGGGTCGA	*Eco*RI
Tcs1LF	TATAAGCTTACTCGTCGCACGCGGCAGC	*Hind*III
Tcs1LR	ATATCTAGACTCACCCAGGCCCTGACGC	*Xba*I
Tcs1RF	ATATCTAGACCAGTGATGCGAAGGCATG	*Xba*I
Tcs1RR	GACGAATTCCAGGAGGTTGACGGTGGTT	*Eco*RI
Tcs2LF	ATTAAGCTTGGGCGAACTCCTCGTTCG	*Hind*III
Tcs2LR	ATTTTTGGATCCCGCACGAGTCTCGGG	*Bam*HI
Tcs2RF	GACGGATCCTCTGAATCGGAGATTCGT	*Bam*HI

Tcs2RR	TTAGAATTCGTGGCCGTTGGAGATGAA	*Eco*RI
Tcs3LF	AGCAAGCTTAGTCCTCTGAGGAGCTGGTAG	*Hind*III
Tcs3LR	TCGAGATCTCACGAGGTCTCCTTGGAGACA	*Bgl*II
Tcs3RF	AAAGGATCCGTCATCATCGACCCGTAG	*Bam*HI
Tcs3RR	TTTGAATTCTCCTTGCTGGTCTGGACG	*Eco*RI
Tcs4LF	TTTAAGCTTCGGCGTGGAGGCGTGGTCG	*Hind*III
Tcs4LR	AAAGGATCCCGTGAGGCCCTCGGCGACA	*Bam*HI
Tcs4RF	AAAGGATCCGACGAGGTGGACTCCCACG	*Bam*HI
Tcs4RR	TTTGAATTCCCAGCACCCTGTCGTCCCG	*Eco*RI
Tcs5LF	CCGAAGCTTACAGCACGGGGATACTCTG	*Hind*III
Tcs5LR	GGATCTAGACAGCCGTTCGGCGATCGCG	*Xba*I
Tcs5RF	AAATCTAGAATGCGCTGACGCGGCCCCG	*Xba*I
Tcs5RR	TTTGGATCCACGGTCGACTCACGCCGCC	*Bam*HI
FkbDF	GAGCGGCACGGTS(C/G)GGY(C/T)TCG	For fosmid selection
FkbDR	CGGGCAGCATCTCGGACGG	For fosmid selection
FkbOF	TGGGCCCGCACCGN(A/C/G/T)CGACCTGTT	For fosmid selection
FkbOR	GGCGATGTTGTCCAGGGCGACN(A/C/G/T)TCGC	For fosmid selection
FkbALF	GTTACCAAGCTTGTACCGAGGACCACGTAC	*Hind*III
FkbALR	GAATCCGGATCCGACCGT TTTGTCCTGTTC	*Bam*HI
FkbARF	TTTACCGGATTCTTCACCGGCTCCACCGAT	*Bam*HI
FkbARR	GGGTCCTCTAGAAGAGAGTGTCGAGGAGATCG	*Xba*I
TcsCF	ATTAGGATCCATGACCCACGTTCGCGA	*Bam*HI
TcsCR	TATATACTCGAGCCGGGGCTGCCCCTT	*Xho*I
TcsAF	CATATGACCAGTGGGGTGGCGTTC	*Nde*I
TcsAR	GGATCCTCACCGCCGCCCGGA	*Bam*HI

SfpF	ATACATATGAAGATTTACGGAATTTATATGGACC	*Nde*I
SfpR	ATAGGA TCCTTATAAAAGCTCTTCGTACGA	*Bam*HI
TcsDF	TTAACCCATATGAGCGAATCCGAACGCC	*Nde*I
TcsDR	TATTCTCGAGCTAGGTACGTTTCGCGGT	*Xho*I

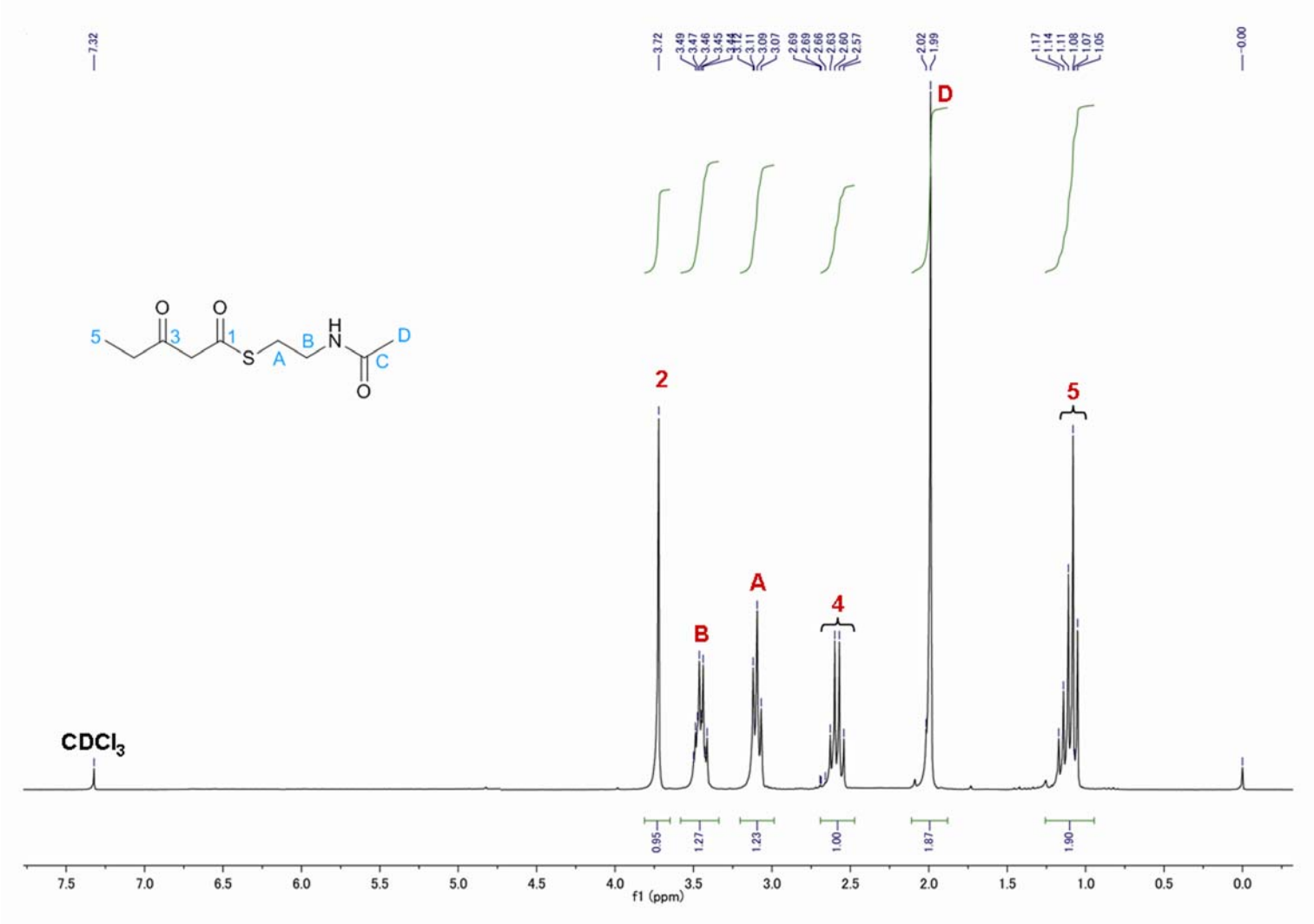

Figure S7. ^{1}H NMR (250 MHz, $CDCl_3$) spectrum of the synthetic 3-oxopentanoyl-SNAC (**13**) thioester. See **Supporting Methods** for the detailed synthesis.

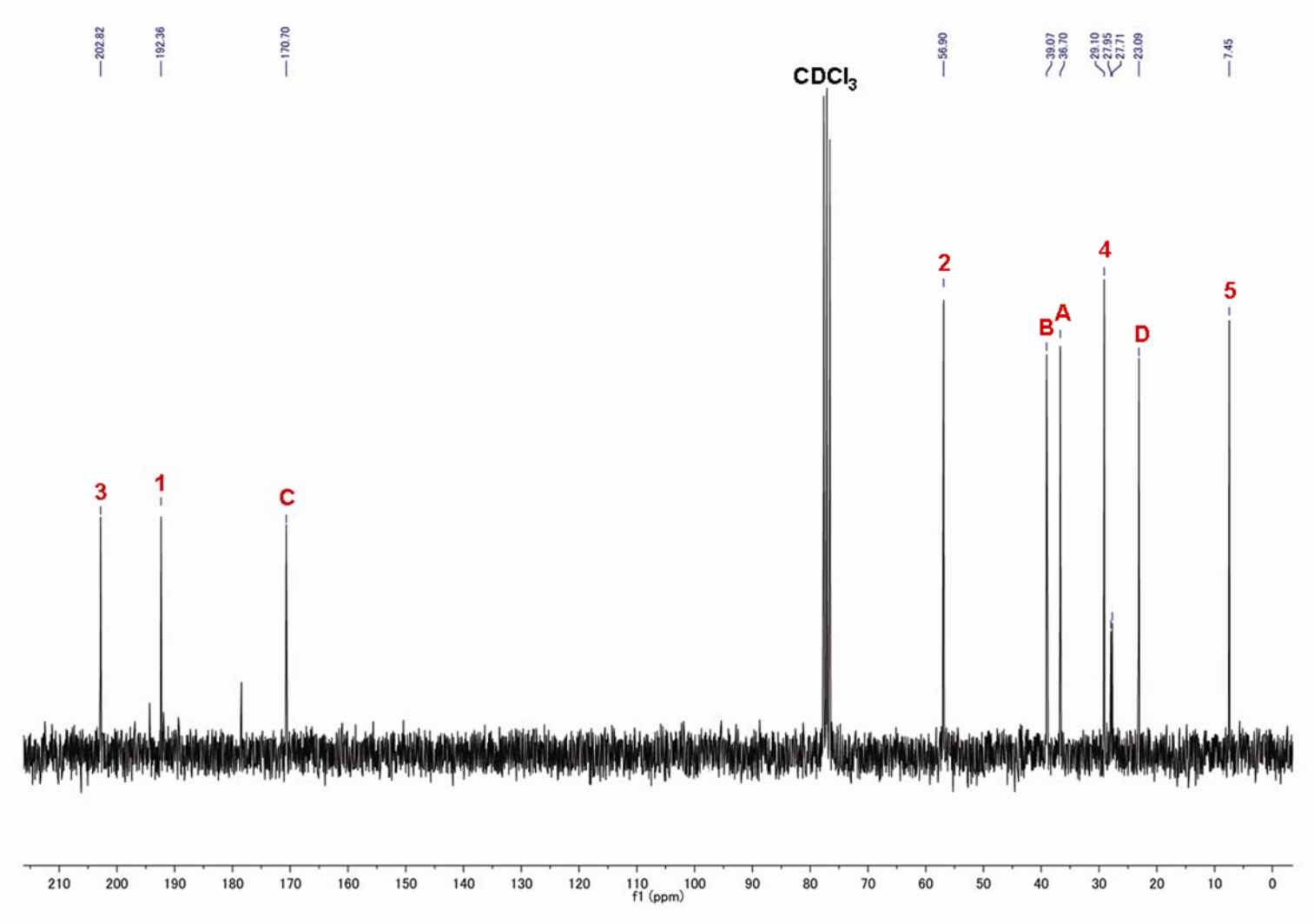

Figure S8. ^{13}C NMR (62.5 MHz, $CDCl_3$) spectrum of the synthetic 3-oxopentanoyl-SNAC (**13**) thioester. See **Supporting Methods** for the detailed synthesis.

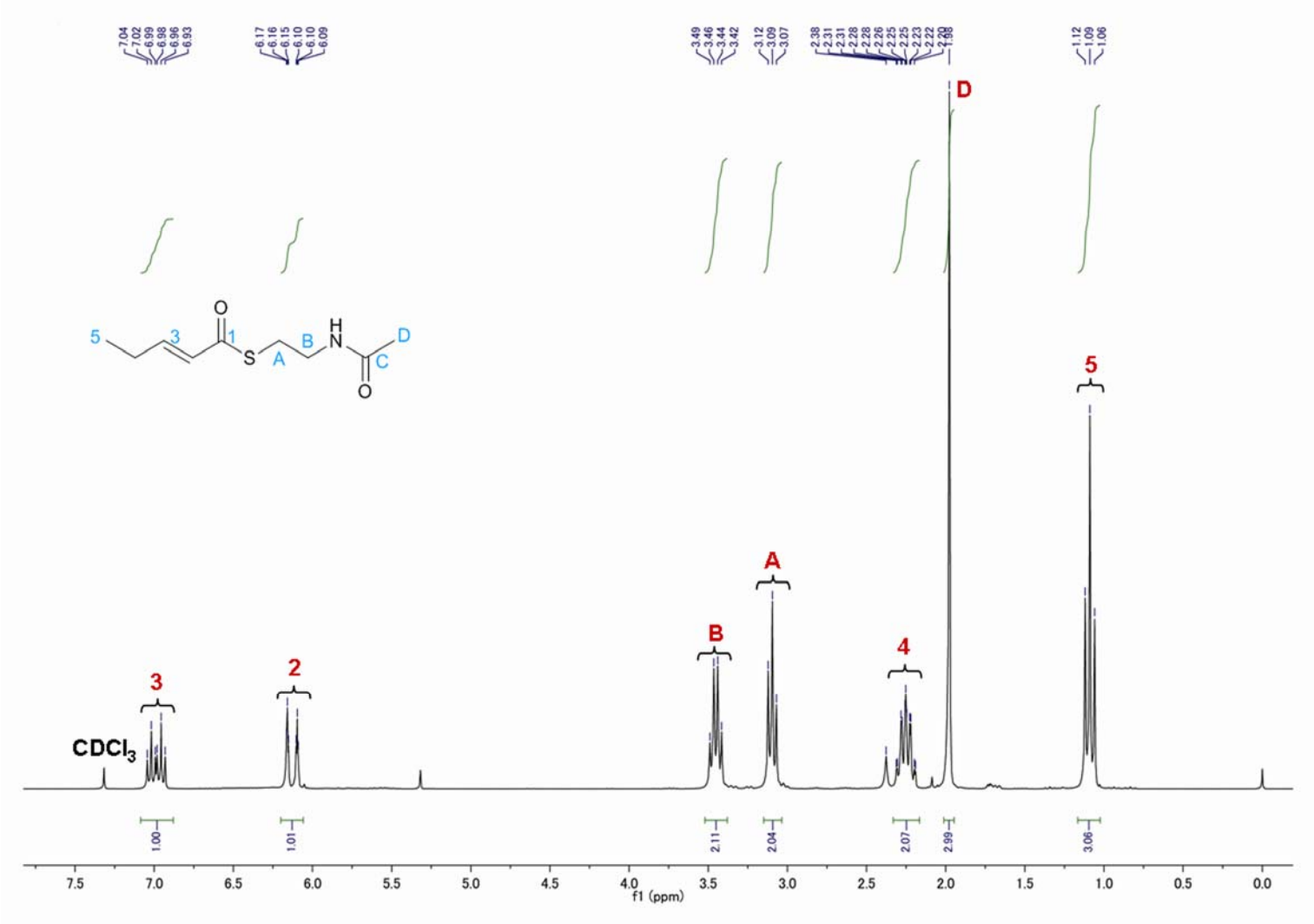

Figure S9. ^{1}H NMR (250 MHz, $CDCl_3$) spectrum of the synthetic *trans*-2-pentenyl-SNAC (**14**) thioester. See **Supporting Methods** for the detailed synthesis.

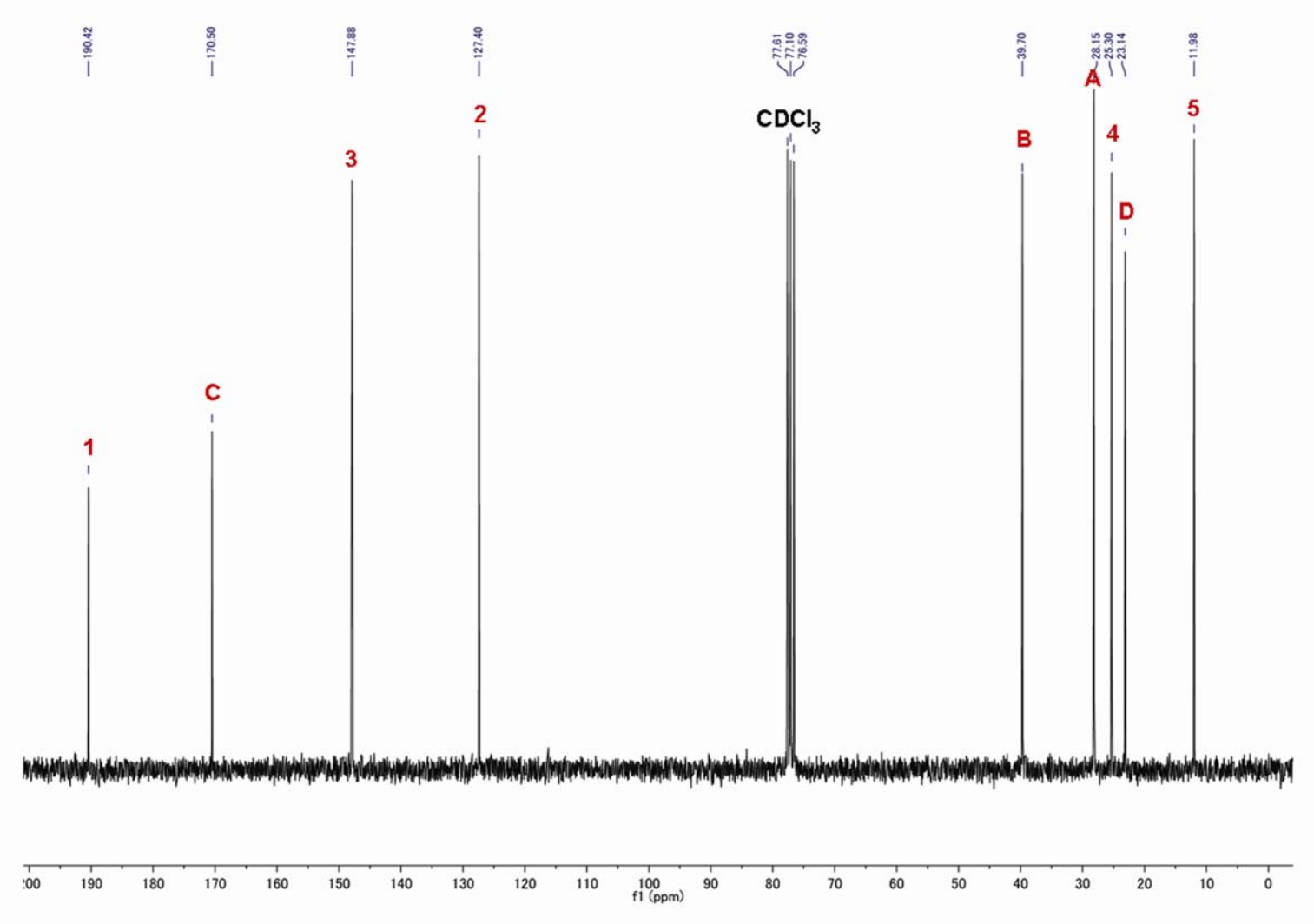

Figure S10. ^{13}C NMR (62.5 MHz, $CDCl_3$) spectrum of the synthetic *trans*-2-pentenyl-SNAC (**14**) thioester. See **Supporting Methods** for the detailed synthesis.

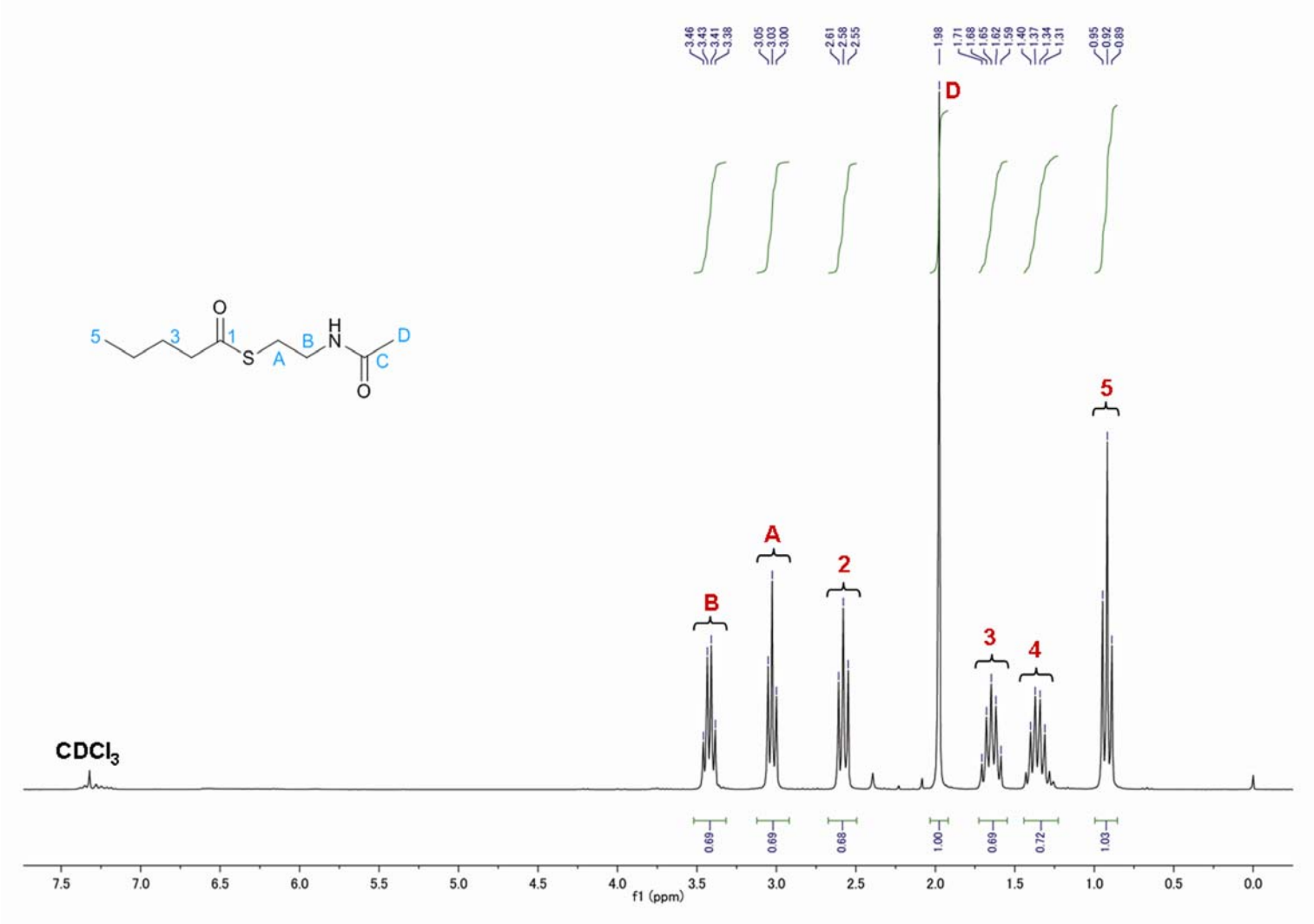

Figure S11. ^{1}H NMR (250 MHz, $CDCl_3$) spectrum of the synthetic pentanoyl-SNAC (**15**) thioester. See **Supporting Methods** for the detailed synthesis.

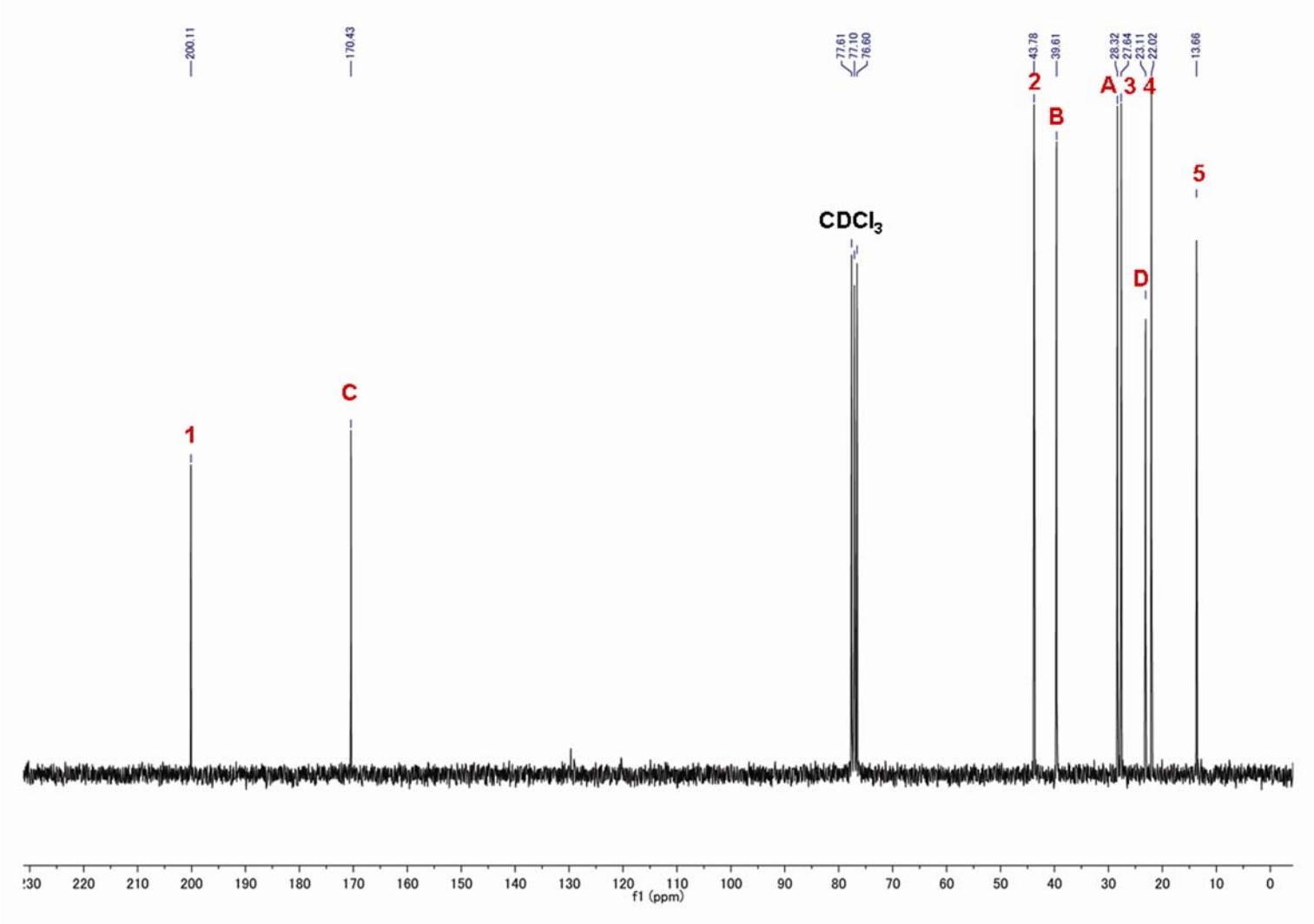

Figure S12. ^{13}C NMR (62.5 MHz, $CDCl_3$) spectrum of the synthetic pentanoyl-SNAC (**15**) thioester. See **Supporting Methods** for the detailed synthesis.

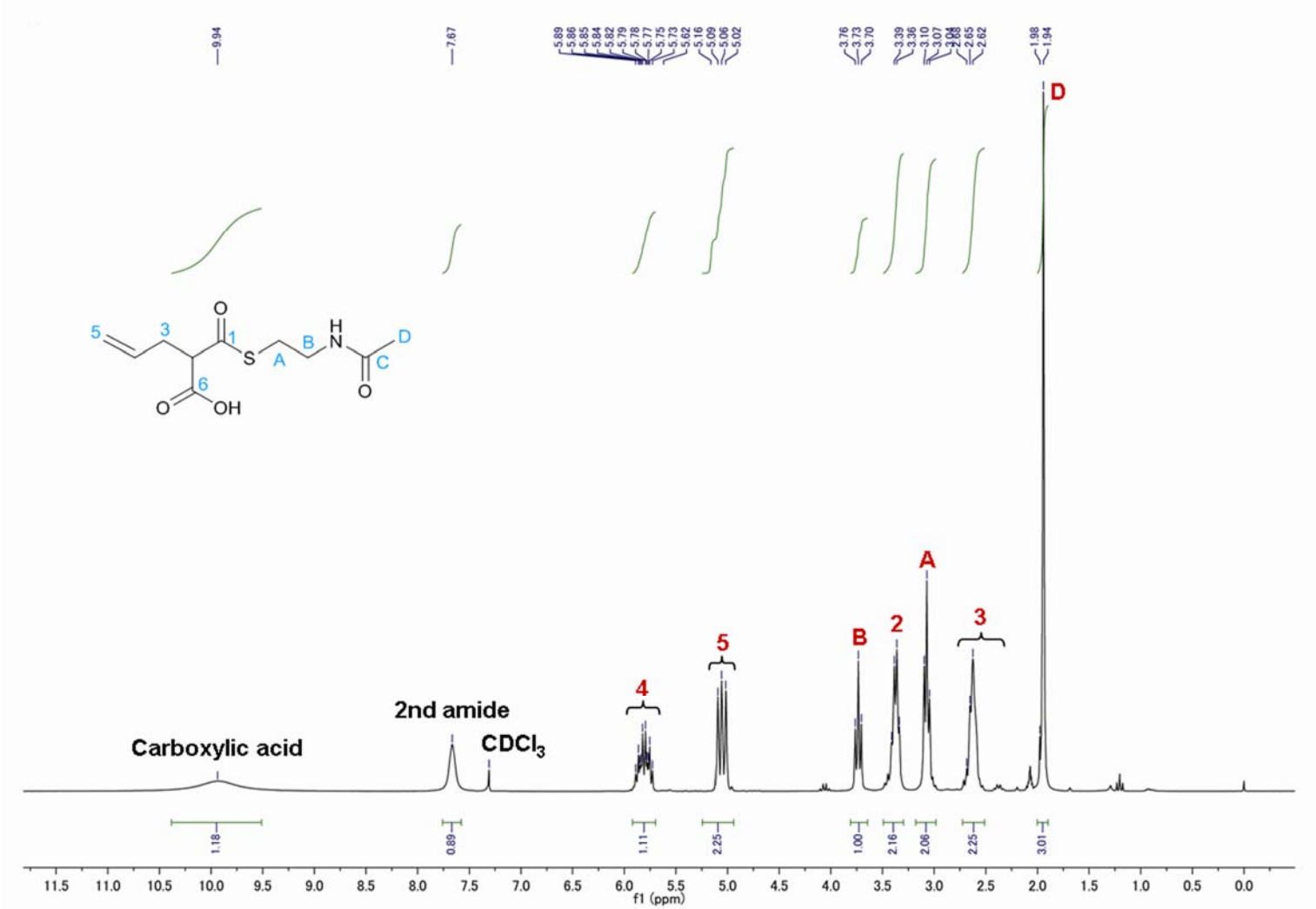

Figure S13. ^{1}H NMR (250 MHz, $CDCl_3$) spectrum of the synthetic allylmalonyl-SNAC (**16**) thioester. See **Supporting Methods** for the detailed synthesis.

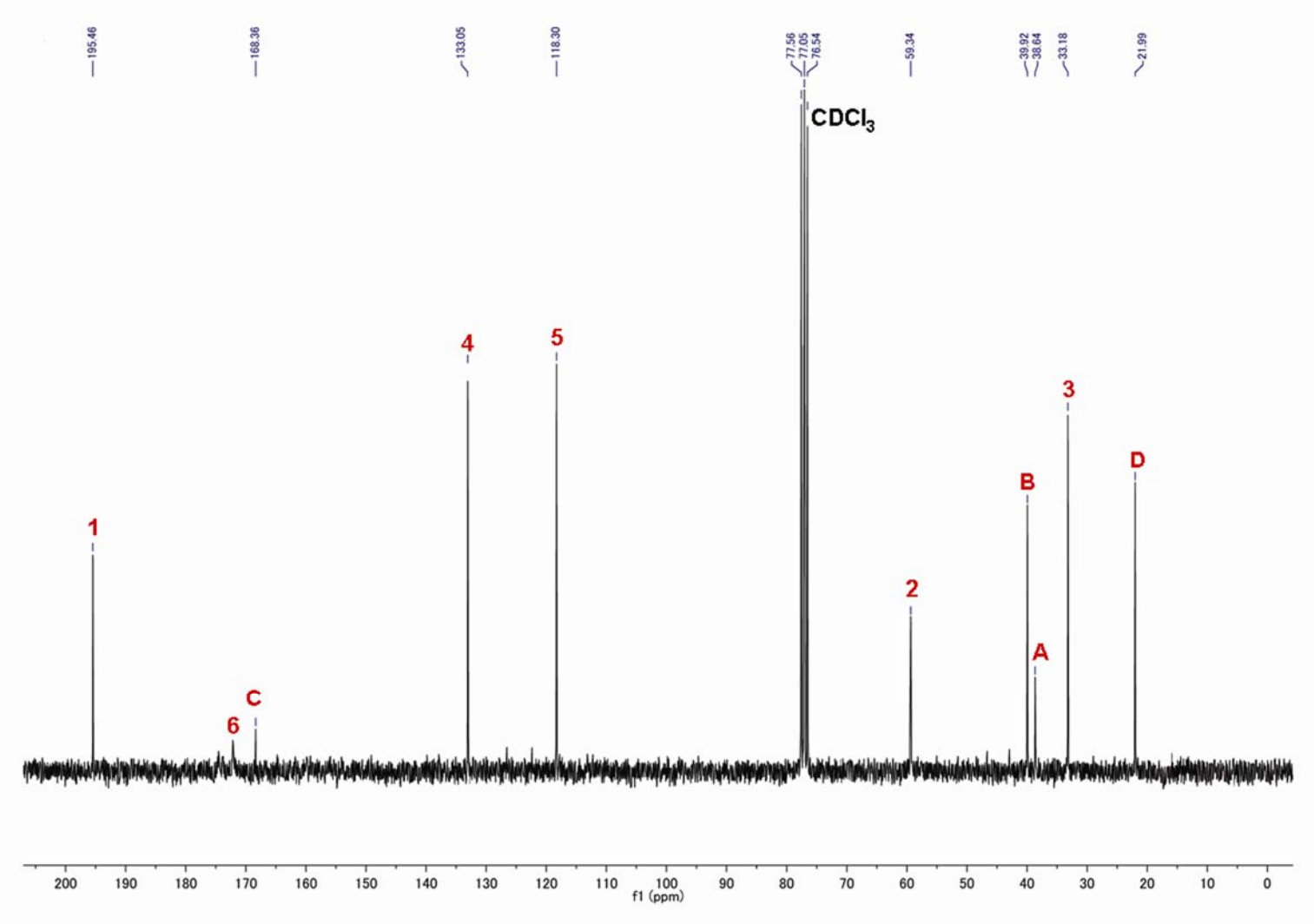

Figure S14. ^{13}C NMR (62.5 MHz, $CDCl_3$) spectrum of the synthetic allylmalonyl-SNAC (**16**) thioester. See **Supporting Methods** for the detailed synthesis.

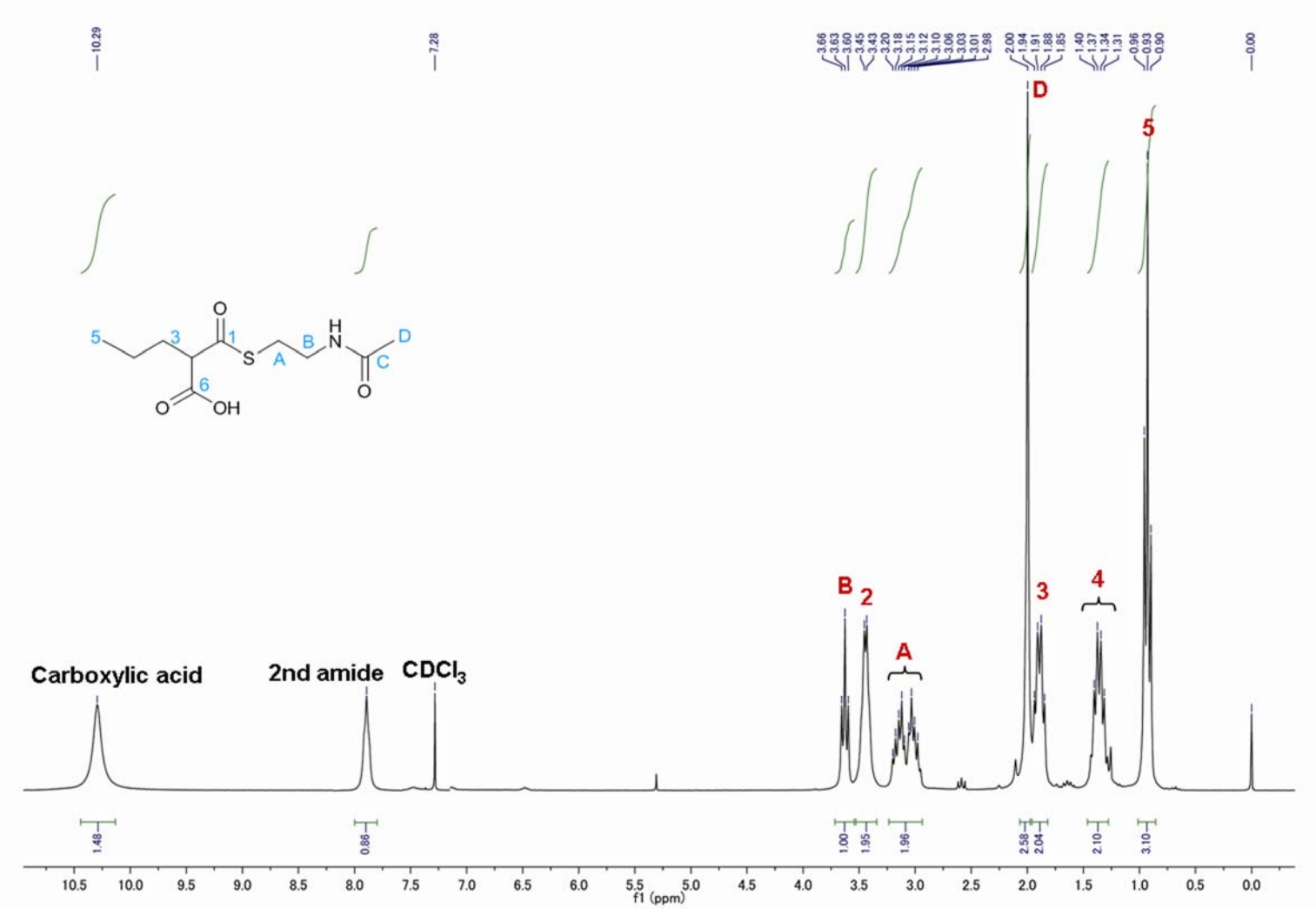

Figure S15. ^{1}H NMR (250 MHz, $CDCl_3$) spectrum of the synthetic propylmalonyl-SNAC (**17**) thioester. See **Supporting Methods** for the detailed synthesis.

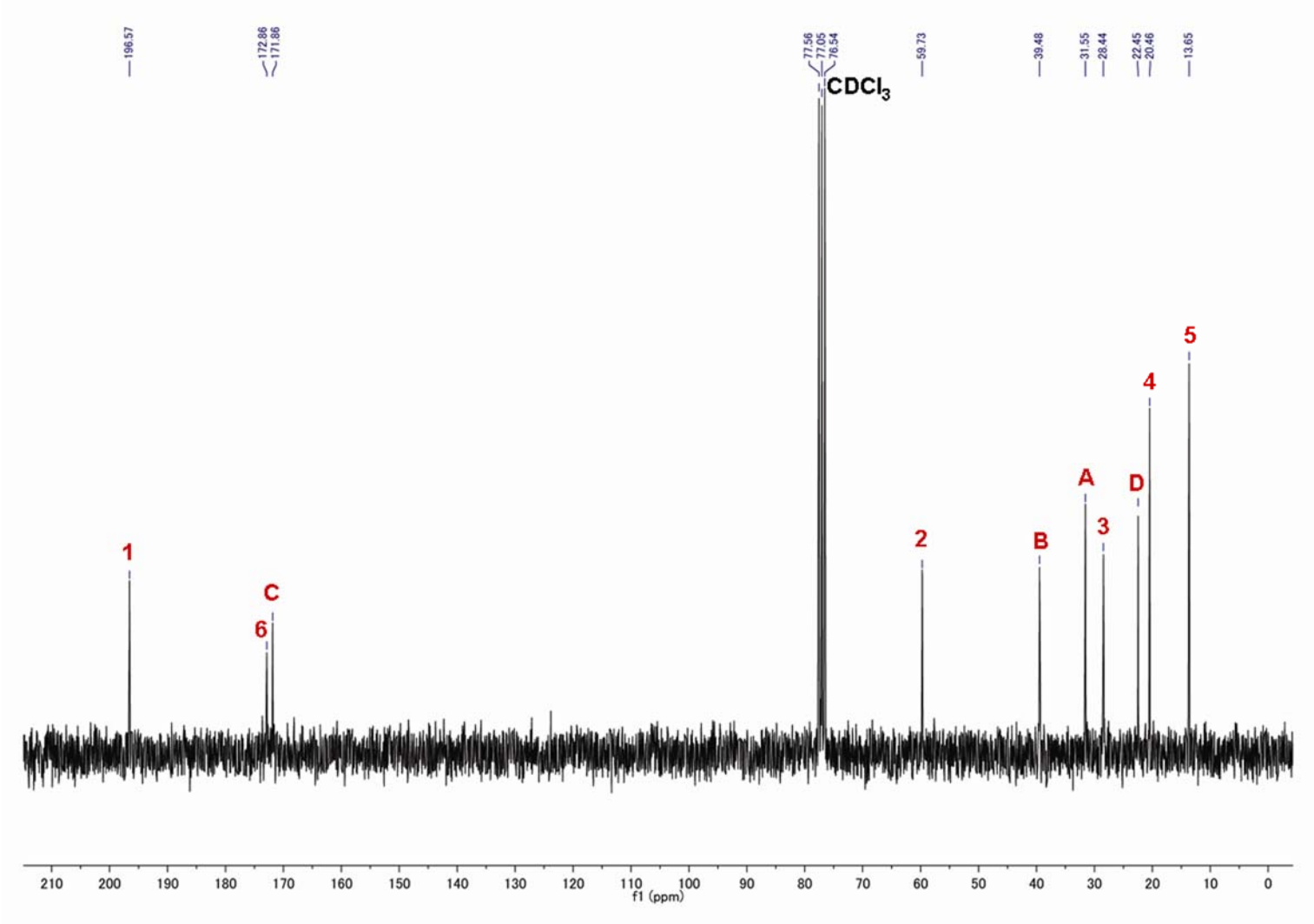

Figure S16. ^{13}C NMR (62.5 MHz, $CDCl_3$) spectrum of the synthetic propylmalonyl-SNAC (**17**) thioester. See **Supporting Methods** for the detailed synthesis.

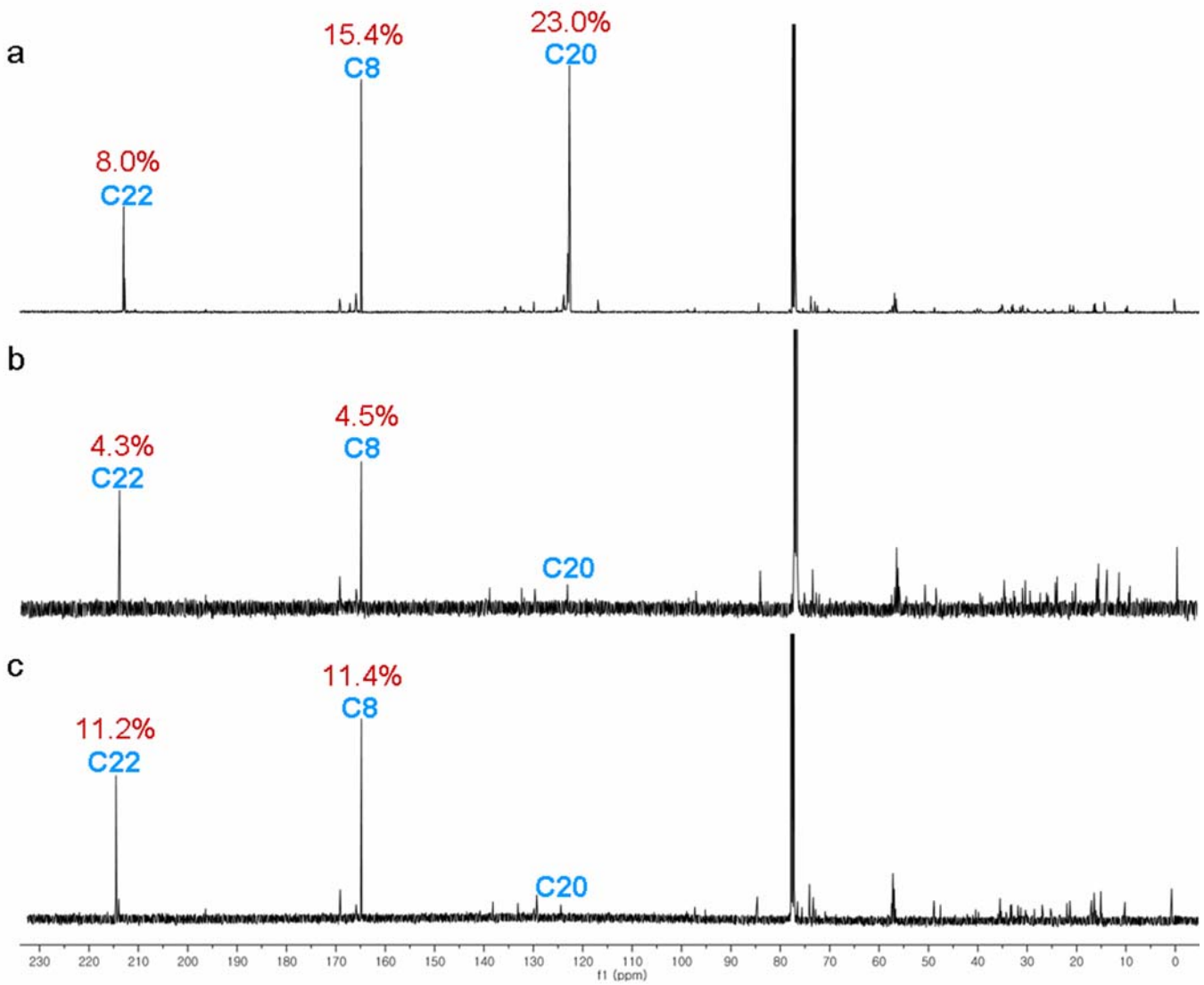

Figure S17. ^{13}C enrichment of FK506 (**1**), FK520 (**2**), and FK523 (**12**). ^{13}C NMR (125MHz, $CDCl_3$) spectra of **1** (**a**), **2** (**b**), and **12** (**c**). % incorporation = (A-B)/B where A = intensity of enriched carbon and B = intensity of natural abundance carbon (see **Supporting Methods**).

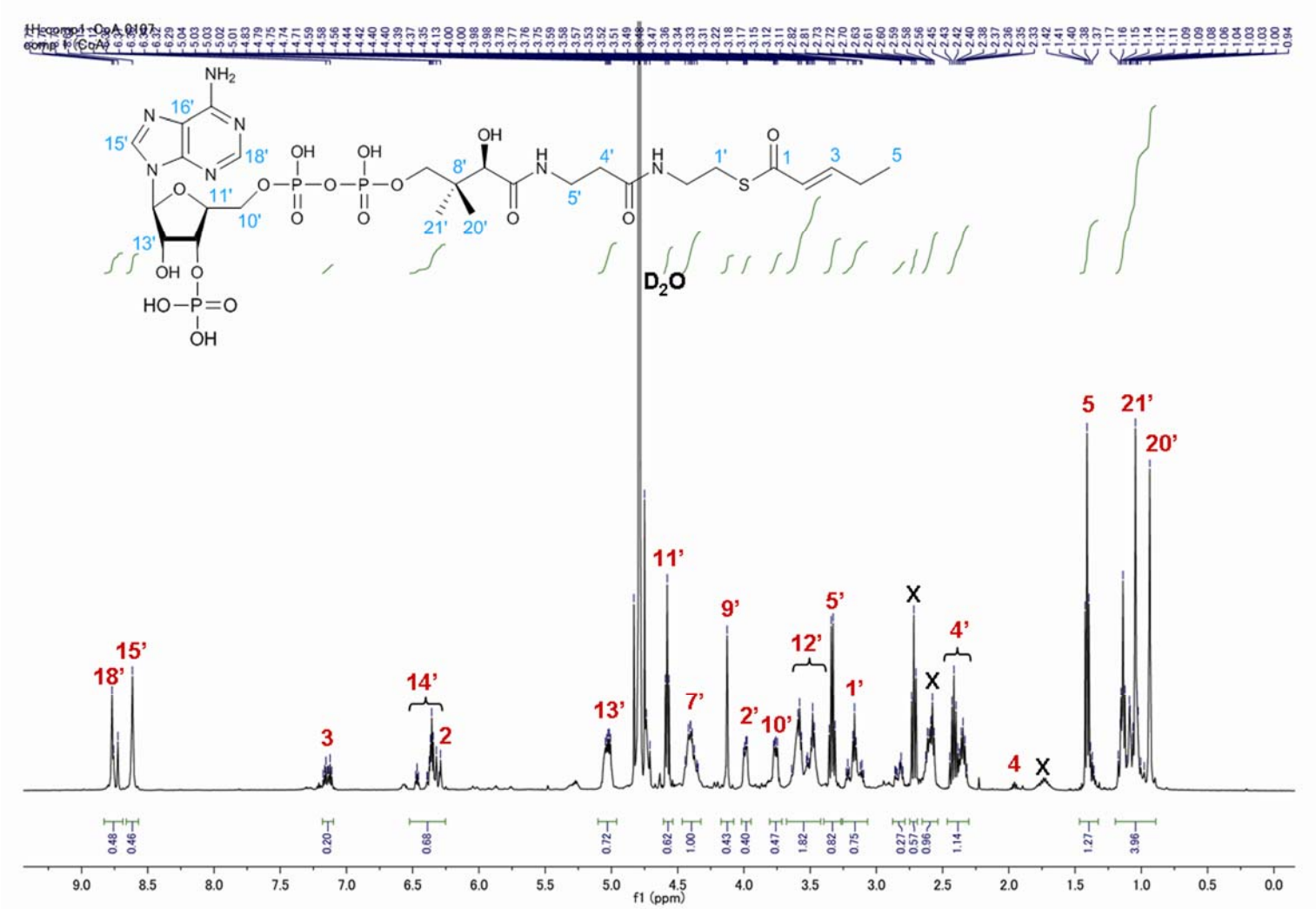

Figure S18. ^{1}H NMR (500 MHz, D_2O) spectrum of the synthetic *trans*-2-pentenyl-CoA (**11**). See **Supporting Methods** for the detailed synthesis. "X" indicates the presence of impurities.

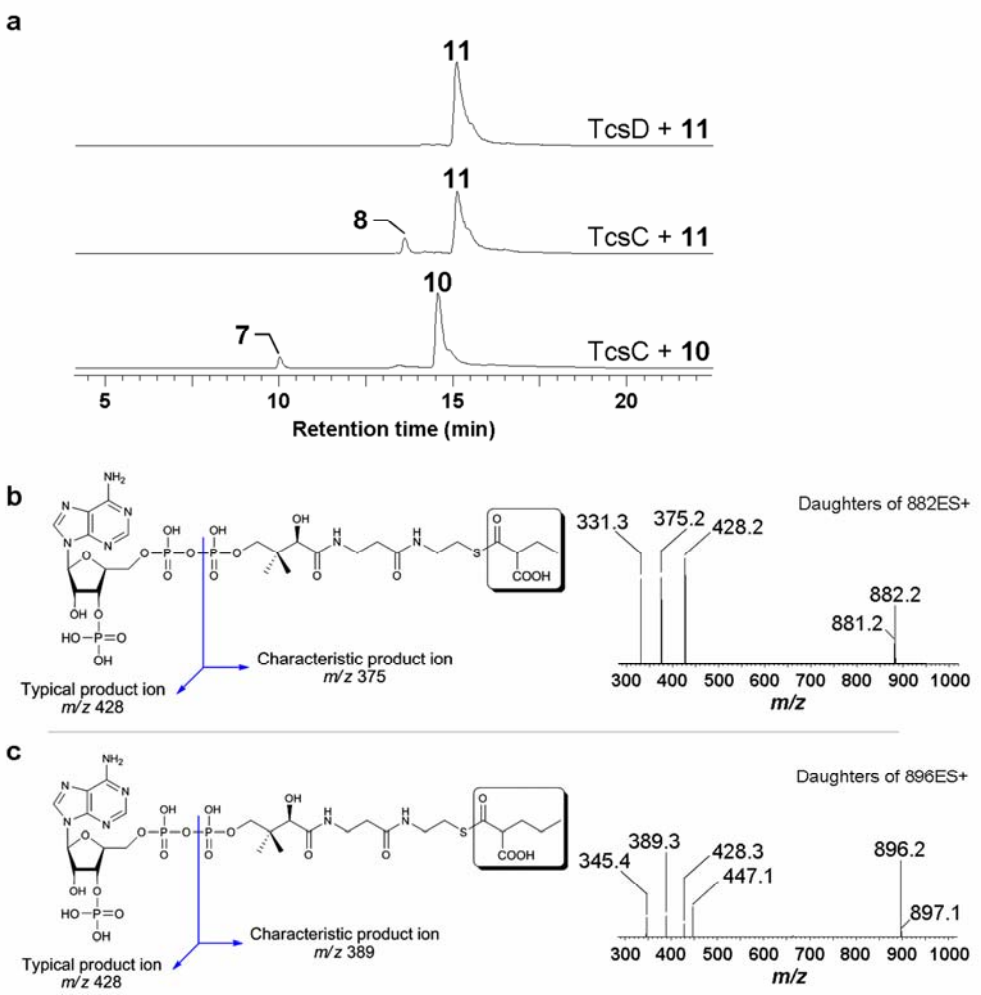

Figure S19. HPLC-ESI-MS/MS analysis of CoA-esters obtained from *in vitro* reactions using recombinant TcsC and TcsD. (**a**) Chromatograms of TcsC-catalyzed production of ethylmalonyl-CoA (**7**) and propylmalonyl-CoA (**8**), supplemented with crotonyl-CoA (**10**) and *trans*-2-pentenyl-CoA (**11**), respectively. No product was detected when TcsD was incubated with **11** (upper chromatogram). Tracing of CoA-esters was done in multiple reactions monitoring mode by selecting mass transit from the protonated molecular ion to the specific fragmented product ion: 882 > 375 for **7**; 896 > 389 for **8**; 836 > 329 for **10**; and 850 > 343 for **11**, as previously described[9]. (**b**) ESI-MS/MS fragmentation pattern of **7** and its MS/MS spectra obtained from the TcsC reactions with **10**. (**c**) ESI-MS/MS fragmentation pattern of **8** and its MS/MS spectra obtained from the reactions of TcsC with **11**.

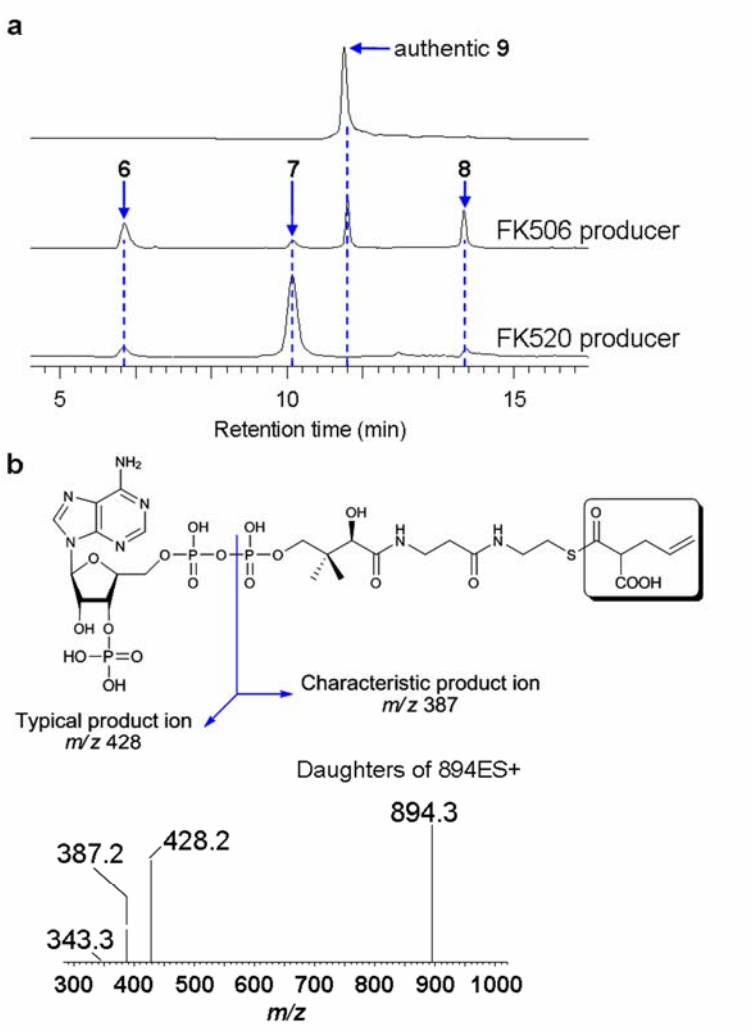

Figure S20. HPLC-ESI-MS/MS analysis of intracellular CoA-esters obtained from 3-day cultures of wild-type FK506-producing *Streptomyces* sp. KCTC 11604BP and FK520-producing S. *hygroscopicus* var. *ascomyceticus* ATCC 14891 strains. (**a**) Chromatograms of intracellular CoA-esters extracted from both strains and the authentic synthesized allylmalonyl-CoA (**9**). Tracing of CoA-esters was done in multiple reactions monitoring mode by selecting mass transit from the protonated molecular ion to the specific fragmented product ion: 868 > 361 for methylmalonyl-CoA (**6**); 882 > 375 for ethylmalonyl-CoA (**7**); 896 > 389 for propylmalonyl-CoA (**8**); and 836 > 329 for **9**, as previously described[9]. (**b**) ESI-MS/MS fragmentation pattern of **9** and its MS/MS spectra obtained from KCTC 11604BP.

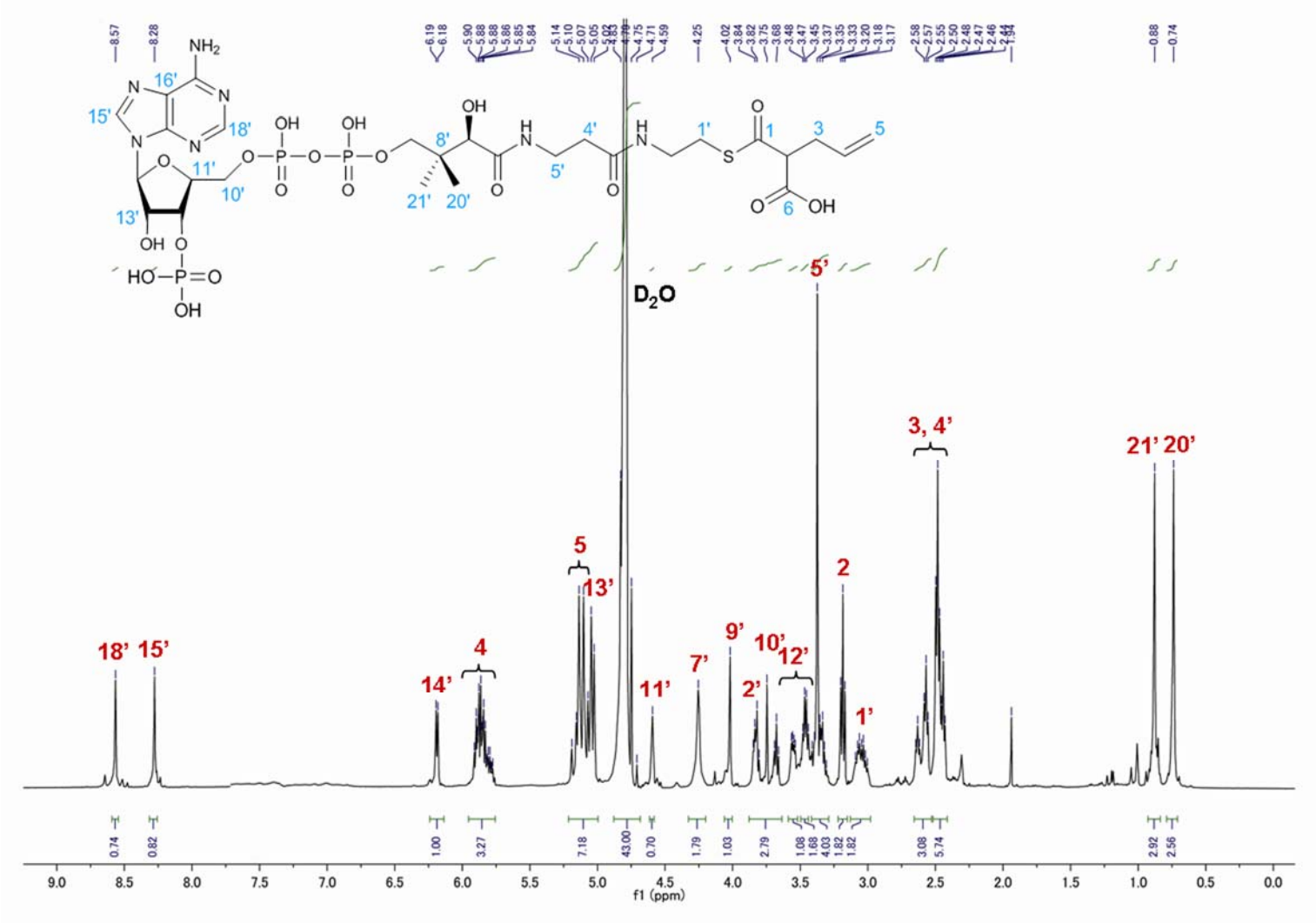

Figure S21. ^{1}H NMR (500 MHz, D_2O) spectrum of the synthetic allylmalonyl-CoA (**9**). See **Supporting Methods** for the detailed synthesis.

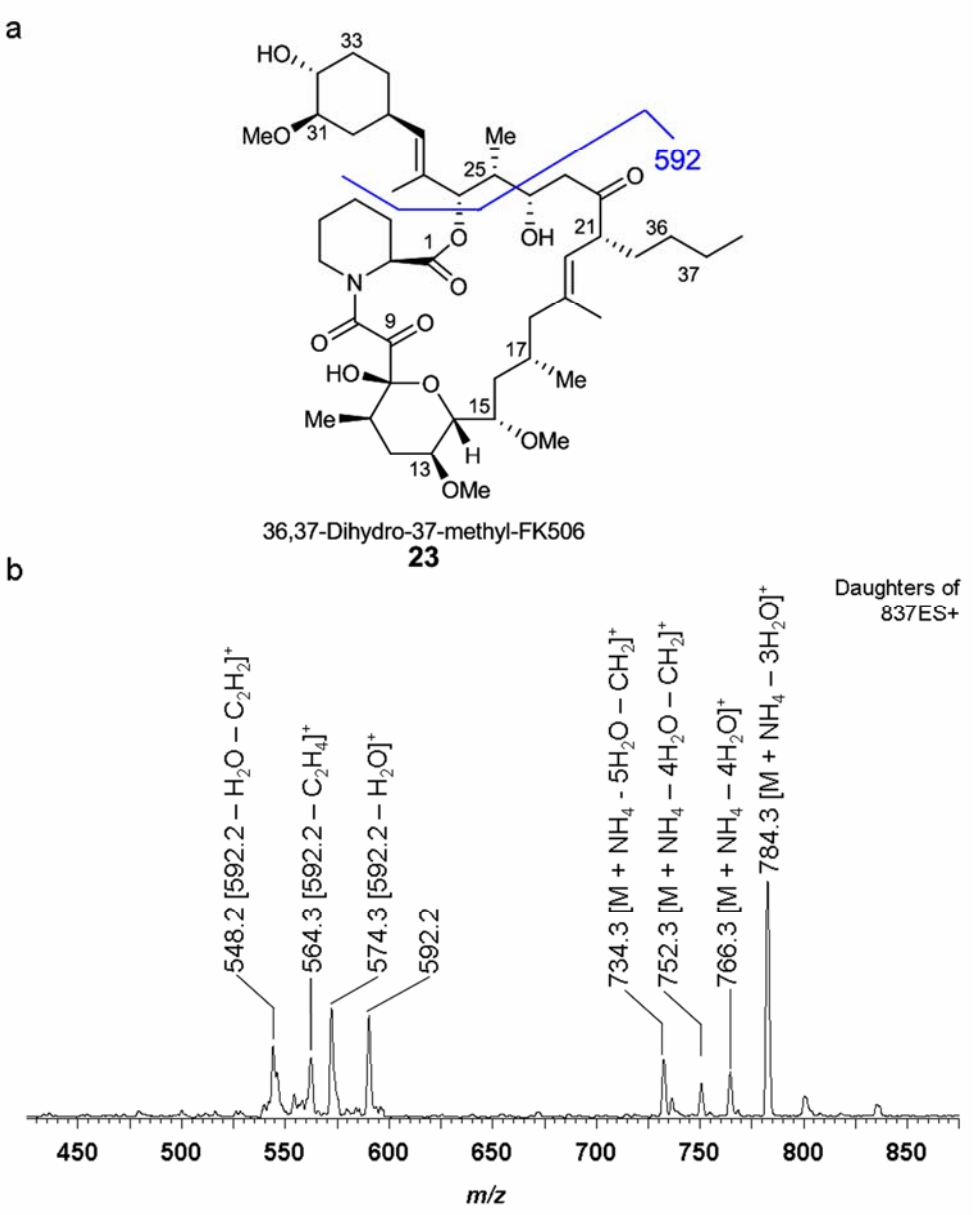

Figure S22. ESI-MS/MS analysis of 36,37-dihydro-37-methyl-FK506 (**23**) obtained from the *tcsB* deletion mutant of *Streptomyces* sp. KCTC 11604BP (ΔtcsB strain) supplemented with *trans*-2-hexenoic acid (**20**). (**a**) ESI-MS/MS fragmentation pattern of **23**. (**b**) MS/MS spectra of **23**. Structural estimation of FK506 congeners produced by the same strain was carried out as previously described[10].

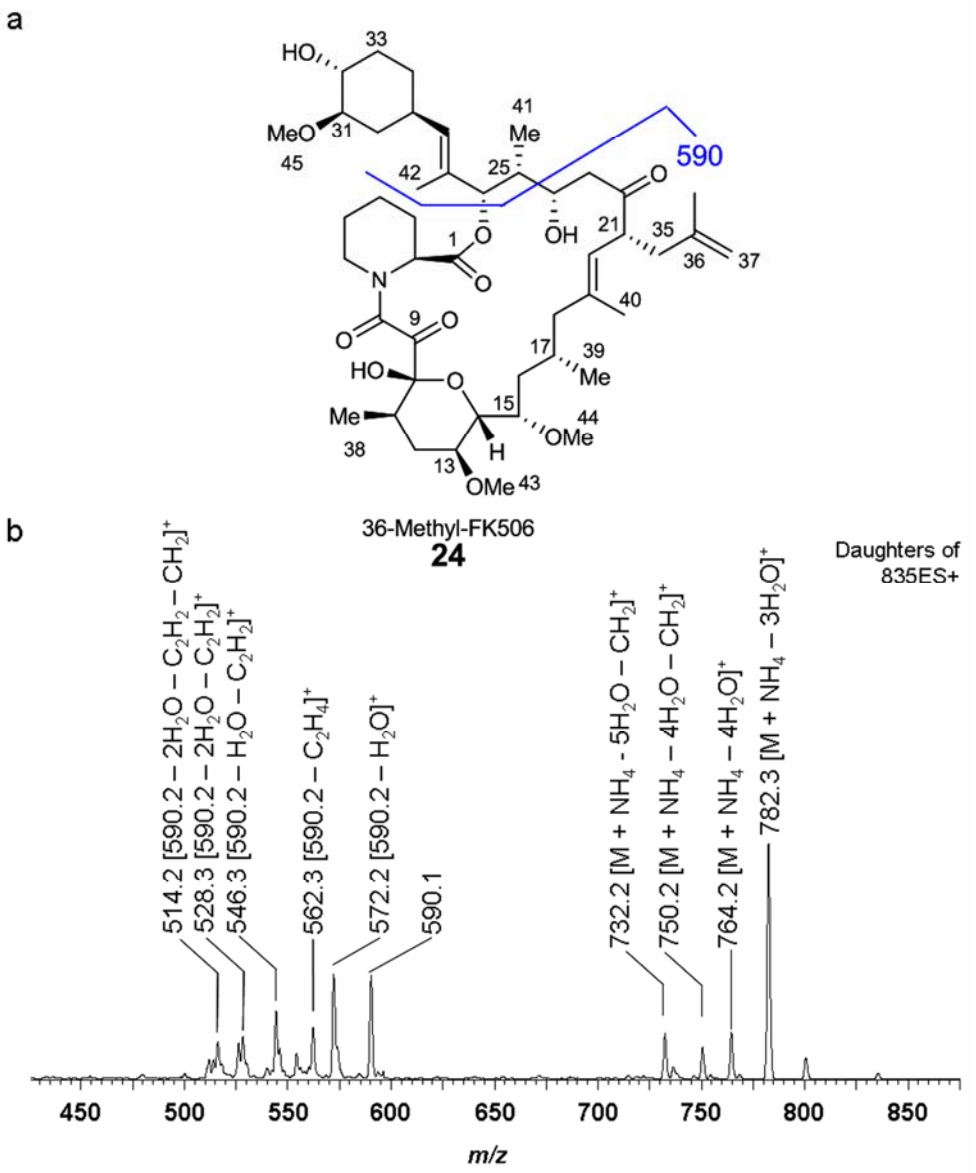

Figure S23. ESI-MS/MS analysis of a novel FK506 analog, 36-methyl-FK506 (**24**) obtained from the *tcsB* deletion mutant of *Streptomyces* sp. KCTC 11604BP (ΔtcsB strain) supplemented with 4-methylpentanoic acid (**21**). (**a**) ESI-MS/MS fragmentation pattern of **24**. (**b**) MS/MS spectra of **24**. Structural estimation of FK506 congeners produced by the same strain was carried out as previously described[10].

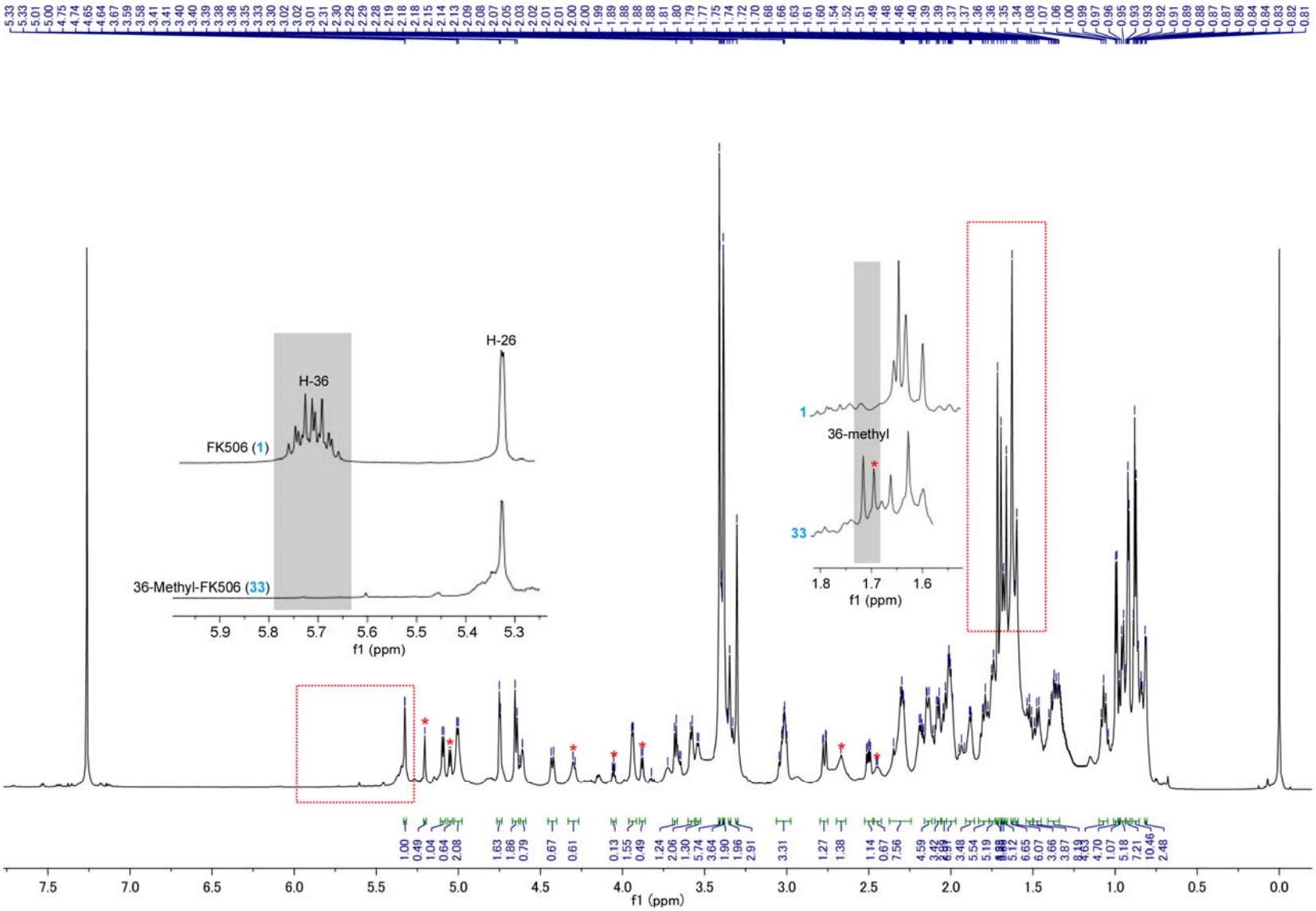

Figure S24. ^{1}H NMR (900 MHz, $CDCl_3$) spectrum of 36-methyl-FK506 (**24**). "*" indicates the coexistence of tautomer.

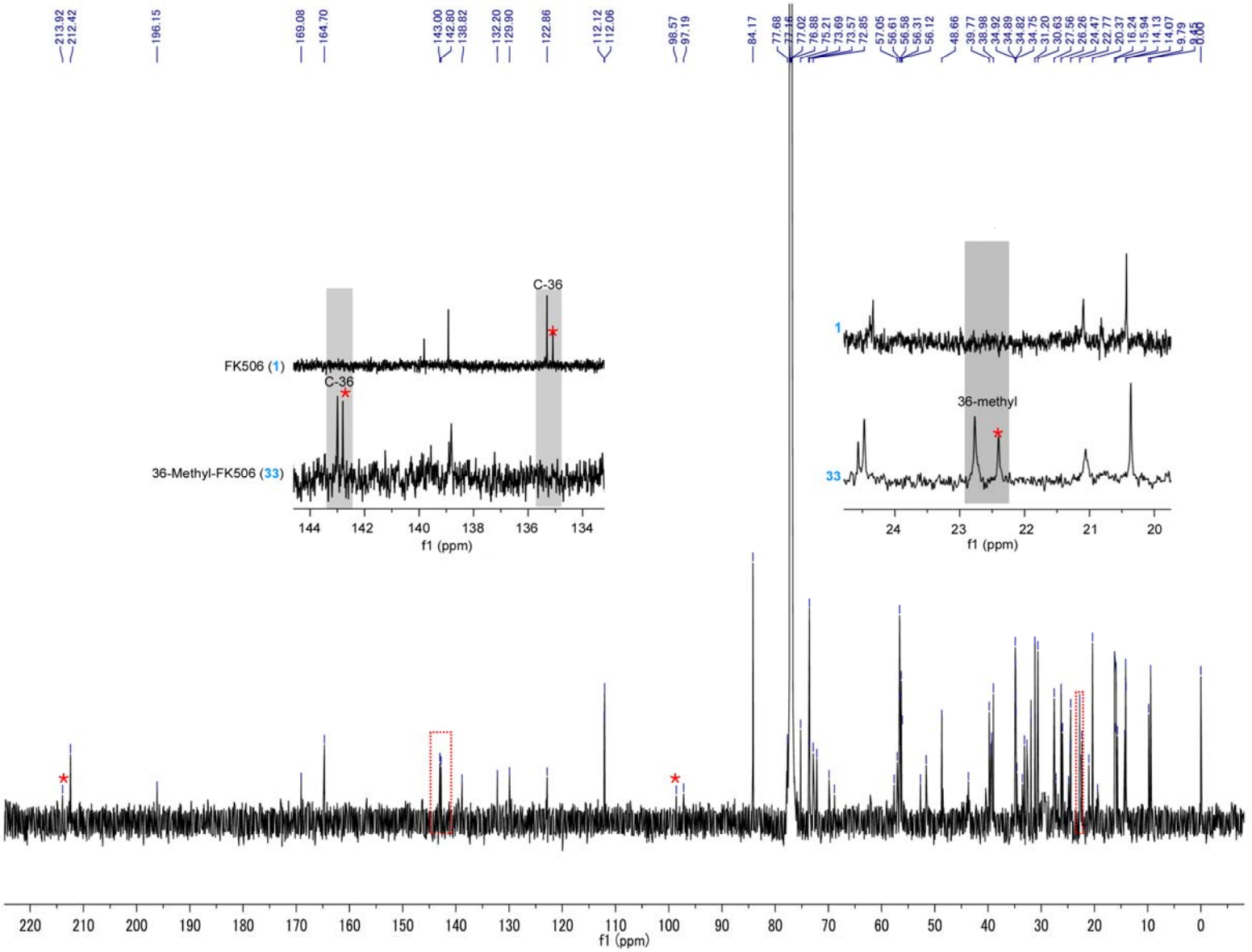

Figure S25. ^{13}C NMR (225 MHz, $CDCl_3$) spectrum of 36-methyl-FK506 (**24**). "*" indicates the coexistence of tautomer.

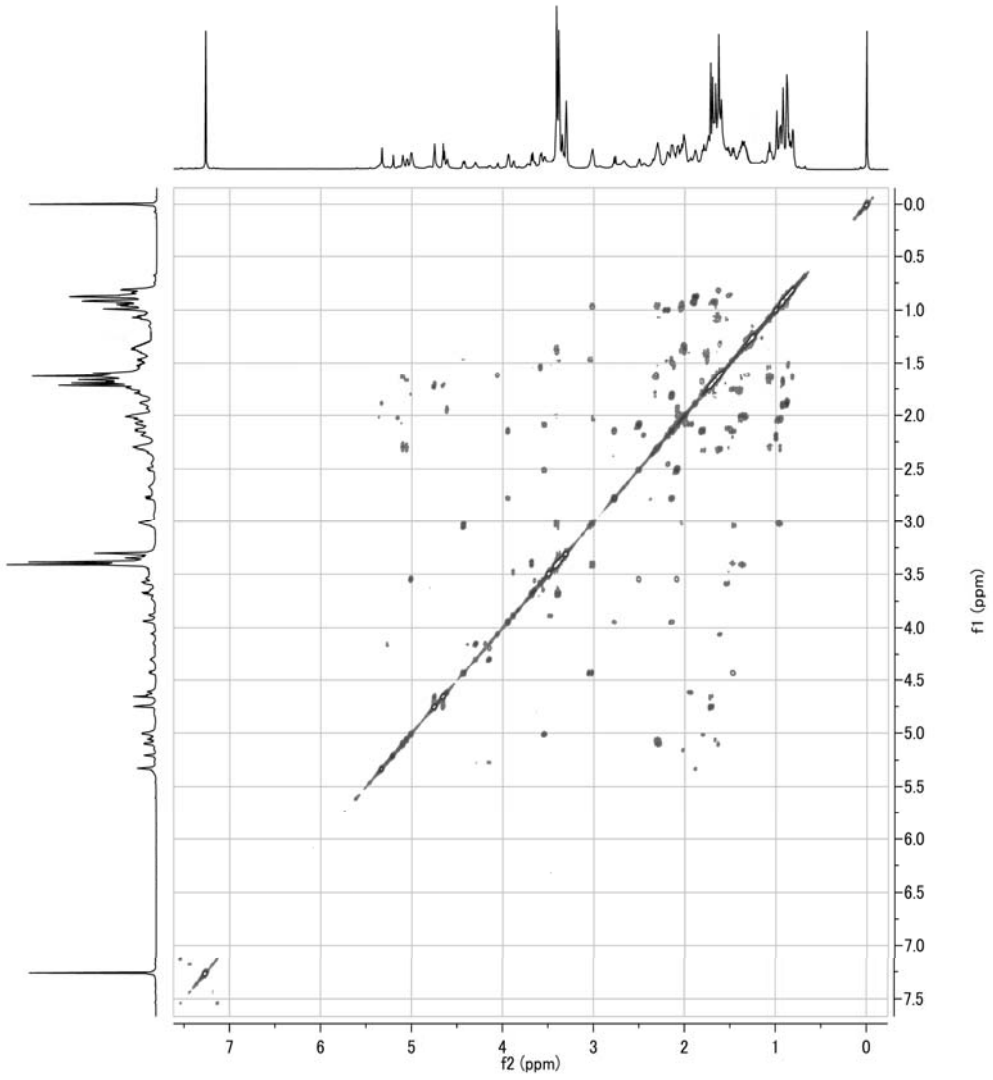

Figure S26. 2D ^{1}H-^{1}H COSY NMR spectrum of 36-methyl-FK506 (**24**).

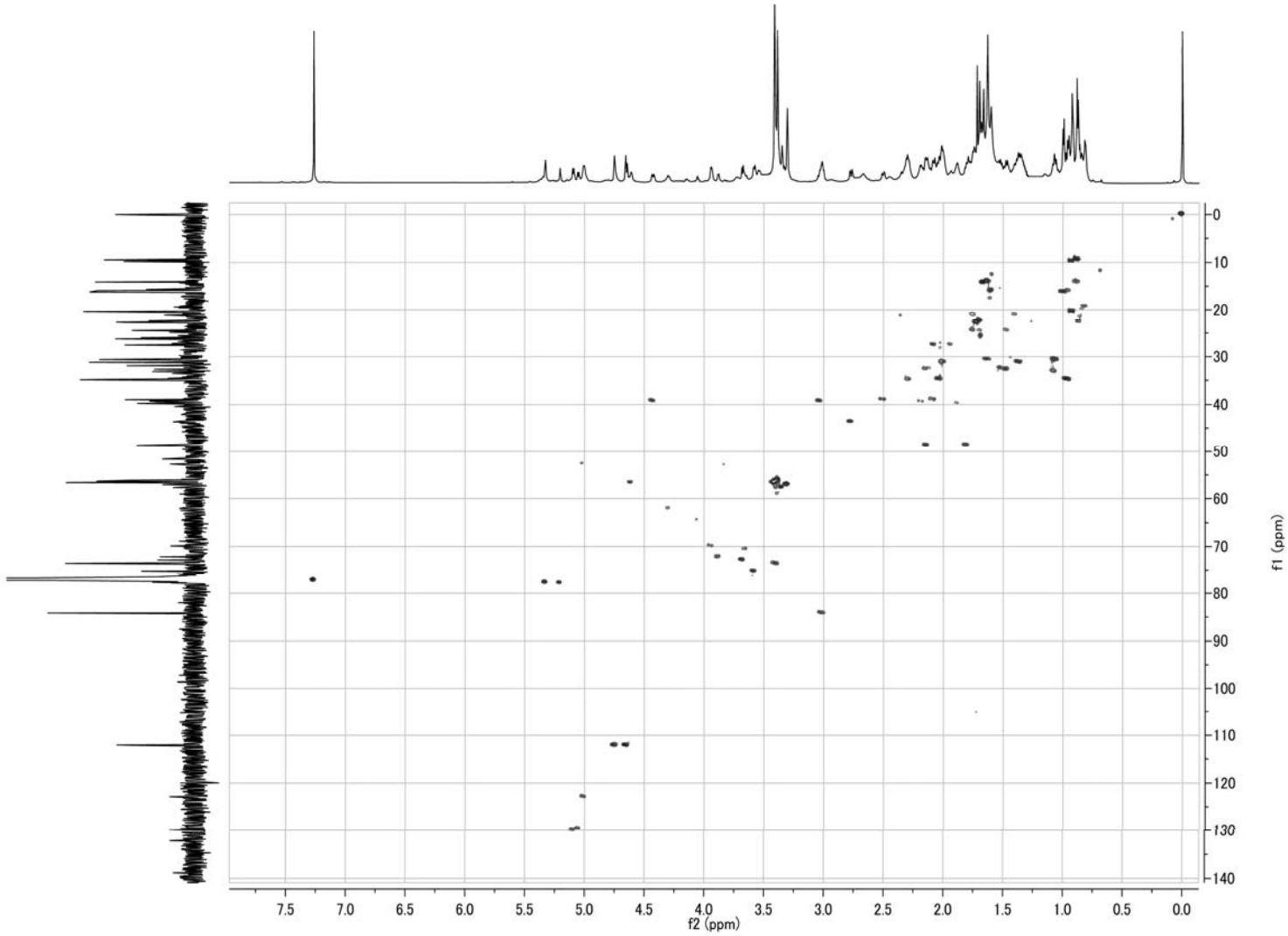

Figure S27. 2D HMQC NMR spectrum of 36-methyl-FK506 (**24**).

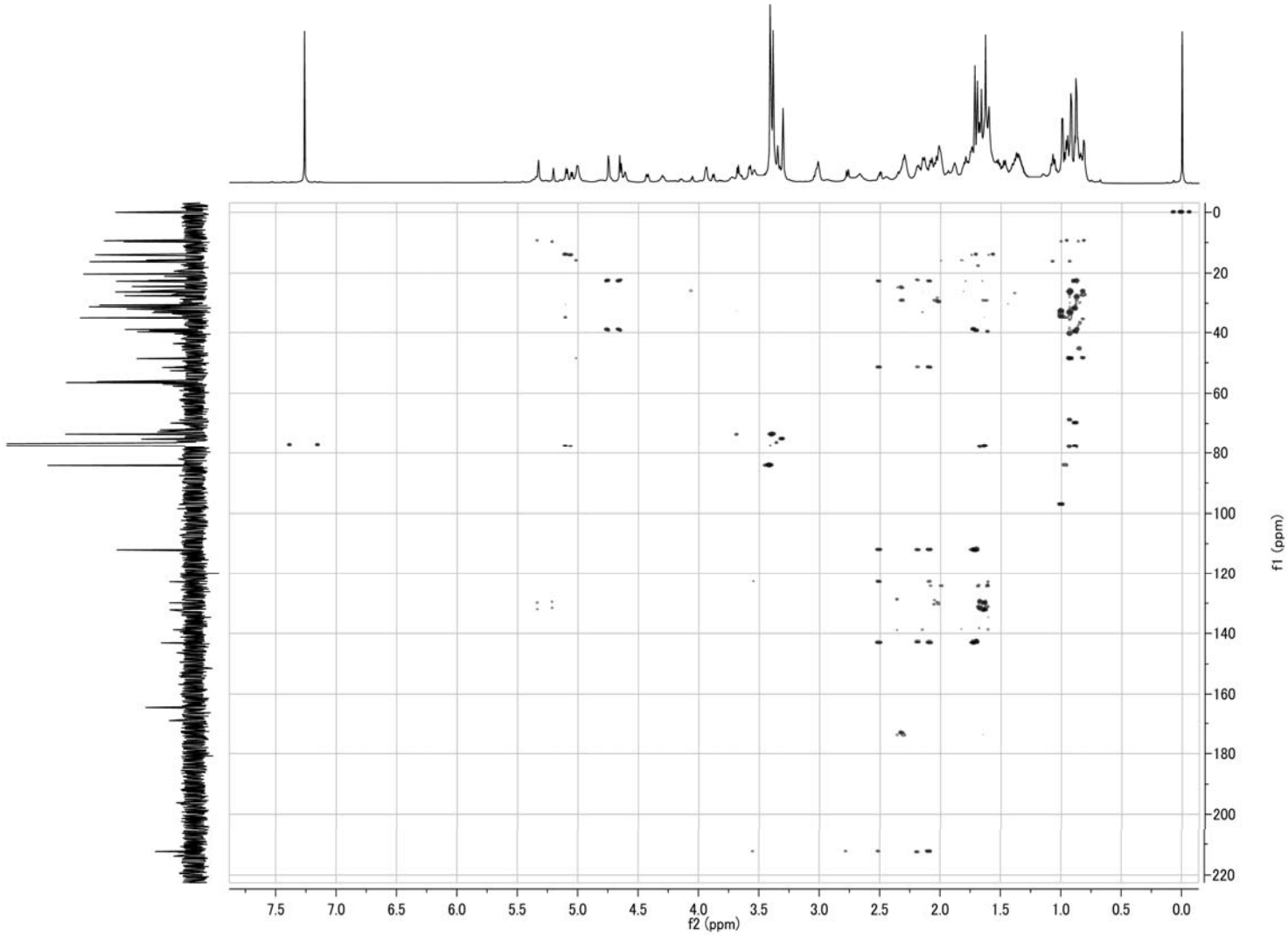

Figure S28. 2D HMBC NMR spectrum of 36-methyl-FK506 (**24**).

Table S9. NMR data for the novel FK506 analog 36-methyl-FK506 (**24**)

Position	C	H	COSY correlations	HMBC correlations
1	169.08	-		
2	56.62	4.61	H-3b	C-1, 3, 4
3	27.56	2.08	H-3b	
		1.94	H-4b	
4	21.06	1.75	H-4b	C-3, 6
		1.39		
5	24.47	1.75	H-5b	C-3, 6
		1.47	H-4b	
6	39.30	4.43	H-5a/b, H-6b	C-2, 4, 5, 8
		3.03	H-5a/b	C-2, 8
7	-	-		
8	164.70	-		
9	196.14	-		
10	97.19	-		
11	34.60	2.19	H-12b, 38	
12	32.68	2.14		C-13
		1.47		C-11, 13
13	73.57	3.40	H-12a/b	
14	72.85	3.68	H-13, 15	C-10, 12, 13, 15
15	75.21	3.58	H-16a/b	
16	33.15	1.53	H-16b	
		1.07		
17	26.00	1.68	H-16a/b, 39	C-19
18	48.66	2.14	H-17, 18b	C-16, 17, 19, 20, 39, 40
		1.80		C-16, 17, 19, 20, 39, 40
19	138.82	-		
20	122.86	5.02	H-21	C-18, 21, 35, 40
21	51.61	3.55	H-35a/b	C-19, 20, 22, 35, 36

22	212.42	-		
23	43.69	2.78	H-23b	C-22, 24, 25
		2.16		C-21, 22
24	69.89	3.95	H-23a/b, 25	C-26
25	39.77	1.89	H-41	C-24, 41
26	77.68	5.33	H-25	C-24, 25, 27, 28, 41, 42
27	132.19	-		
28	129.90	5.10	H-29	C-26, 29, 30, 34, 42
29	34.89	2.31	H-30b, 34a	
30	34.82	2.02		C-28, 31
		0.96		C-28, 29, 31, 32, 34
31	84.17	3.02	H-30a/b	C-32, 45
32	73.69	3.42	H-31, 33b	C-31, 33
33	31.20	2.02	H-33b, 34a	
		1.37	H-34b	C-32
34	30.63	1.64		C-28, 29, 30
		1.08		
35	38.98	2.50		C-36methyl, 20, 21, 22, 36, 37
		2.09		C-36methyl, 20, 21, 22, 36, 37
36	143.00	-		
37	112.06	4.76		C-36
		4.66		
38	16.24	1.00		C-10, 12
39	20.37	0.93		C-16, 17, 18
40	15.94	1.61		C-18, 19, 20
41	9.45	0.88		C-24, 25, 26
42	14.13	1.64		C-26, 27, 28
43	56.31	3.42		C-13
44	57.06	3.31		C-15
45	56.58	3.42		C-31
36-methyl	22.77	1.72		C-36

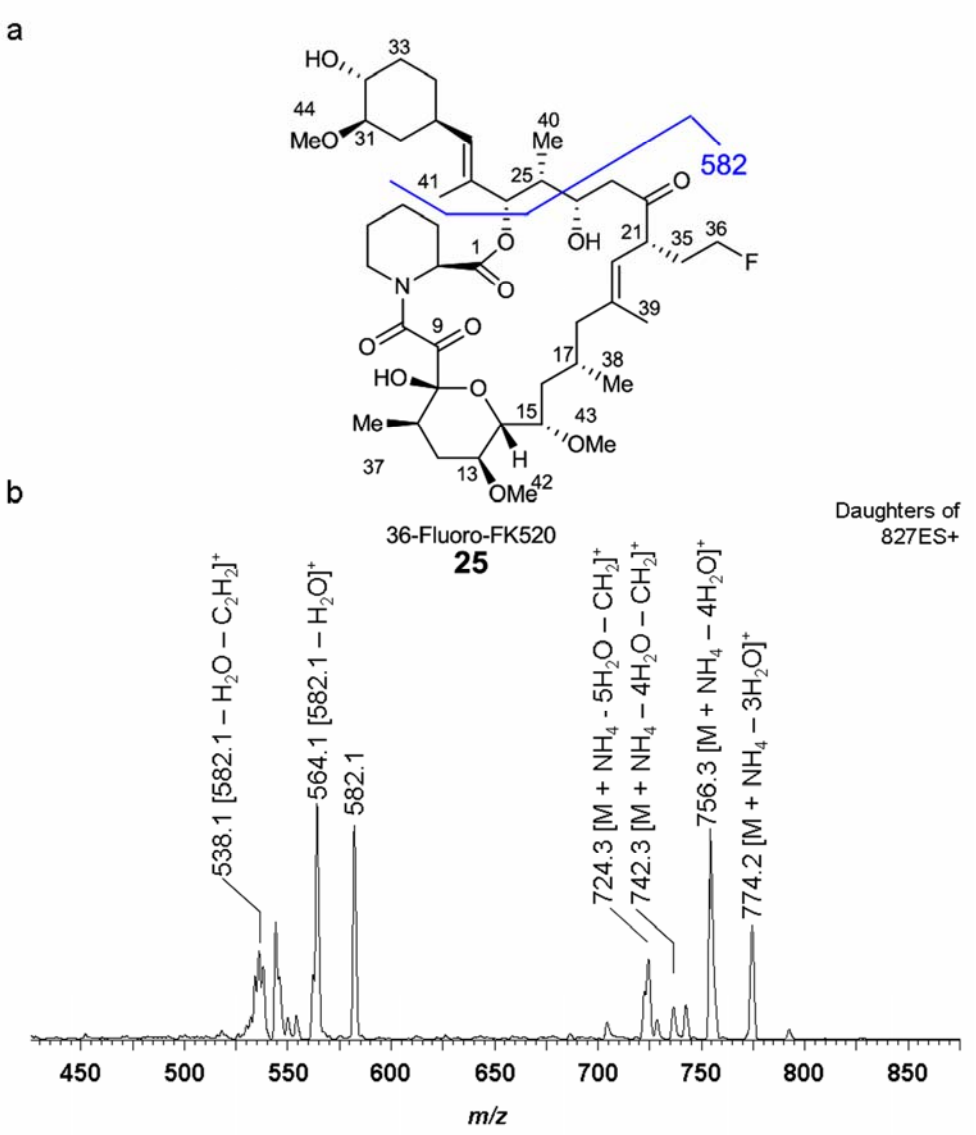

Figure S29. ESI-MS/MS analysis of a novel FK506 analog, 36-fluoro-FK520 (**25**) obtained from the *tcsB* deletion mutant of *Streptomyces* sp. KCTC 11604BP (ΔtcsB strain) supplemented with 4-fluorocrotonic acid (**22**). (**a**) ESI-MS/MS fragmentation pattern of **25**. (**b**) MS/MS spectra of **25**. Structural estimation of FK506 congeners produced by the same strain was carried out as previously described[10].

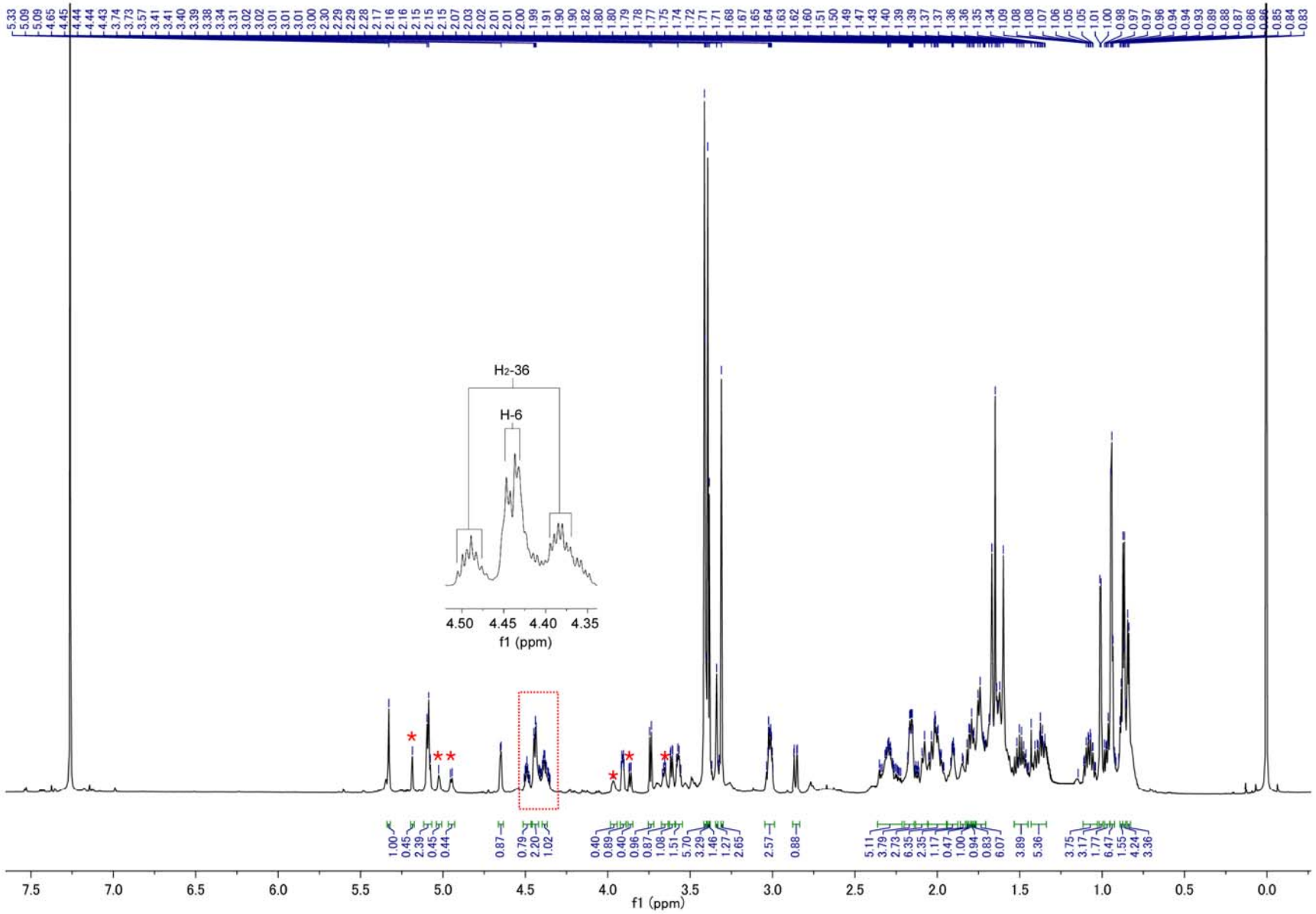

Figure S30. ^{1}H NMR (900 MHz, $CDCl_3$) spectrum of 36-fluoro-FK520 (**25**). "*" indicates the coexistence of tautomer.

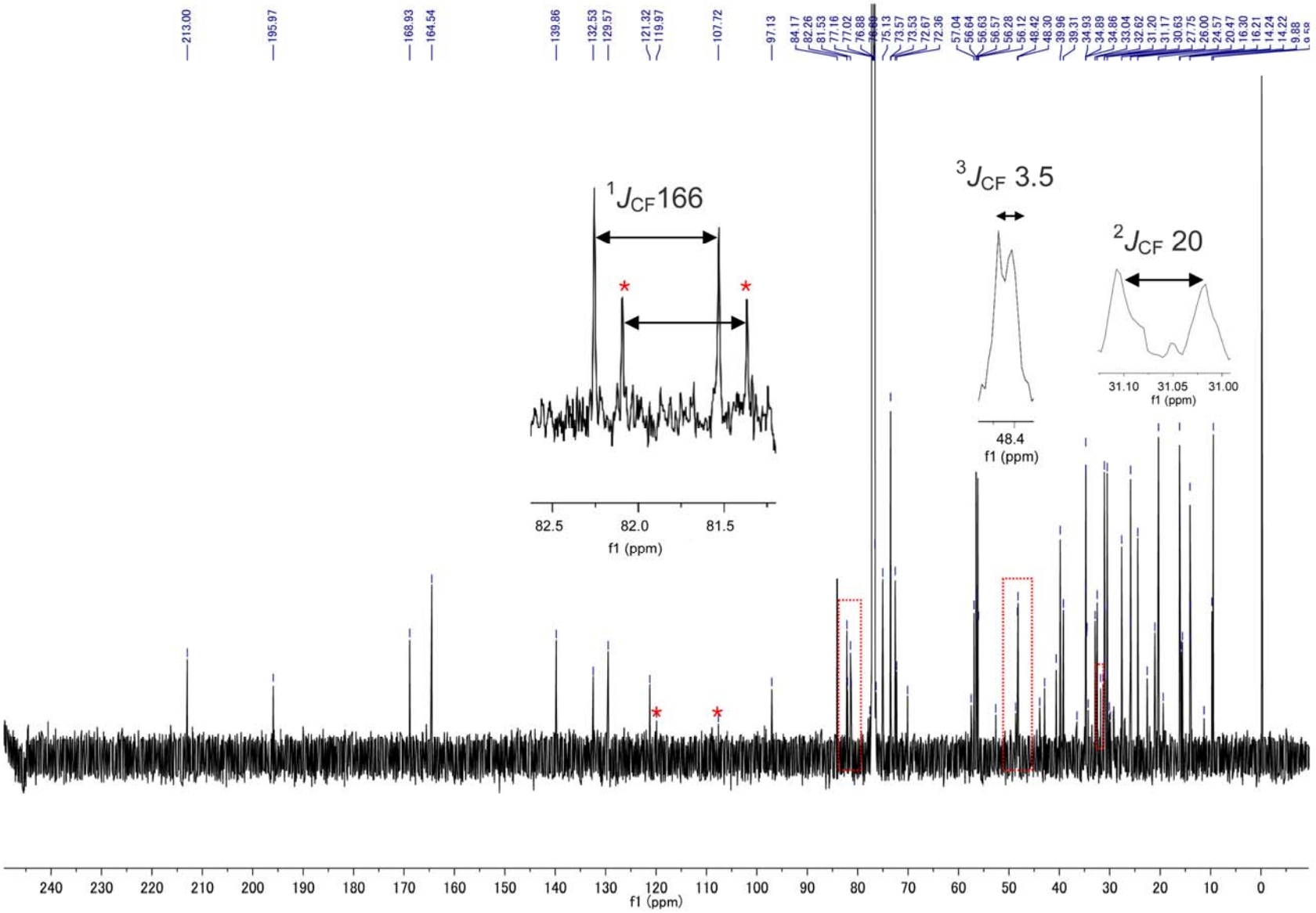

Figure S31. ^{13}C NMR (225 MHz, $CDCl_3$) spectrum of 36-fluoro-FK520 (**25**).

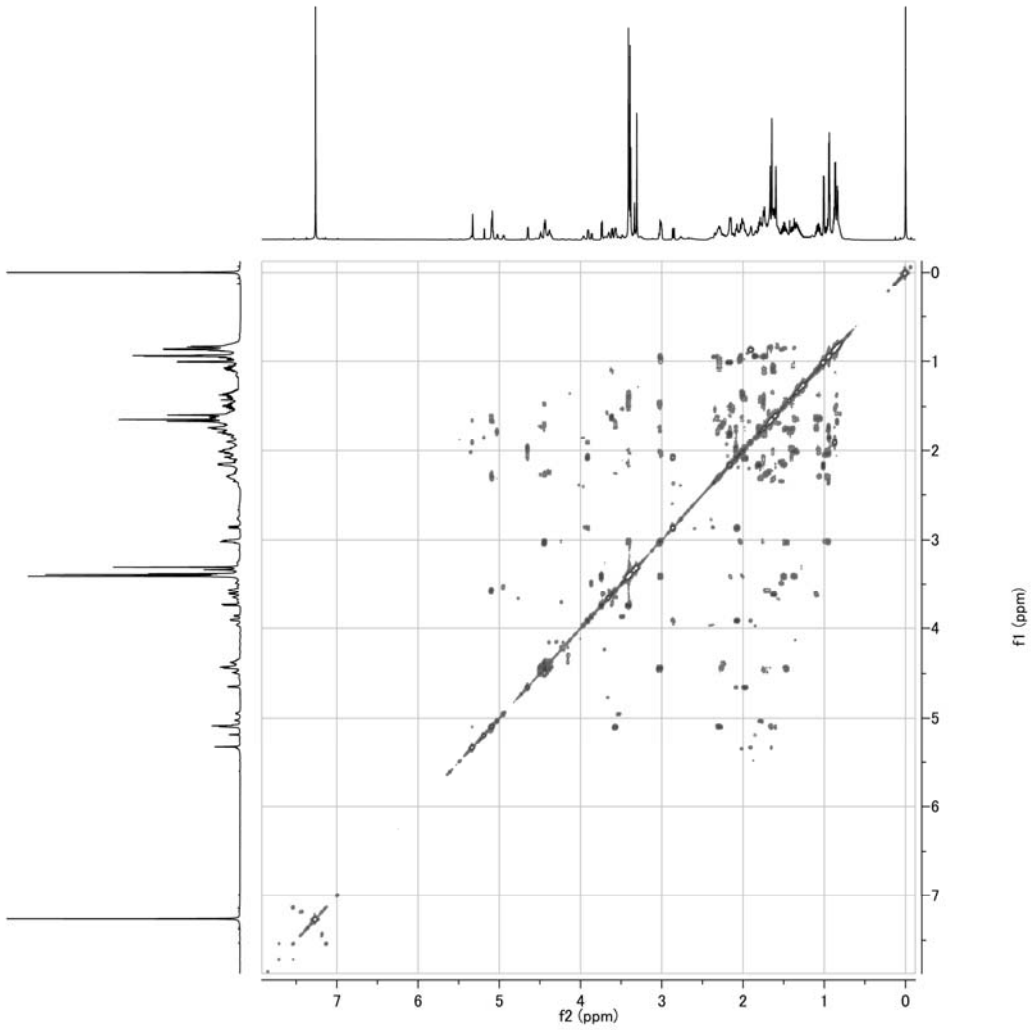

Figure S32. 2D ^{1}H-^{1}H COSY NMR spectrum of 36-fluoro-FK520 (**25**).

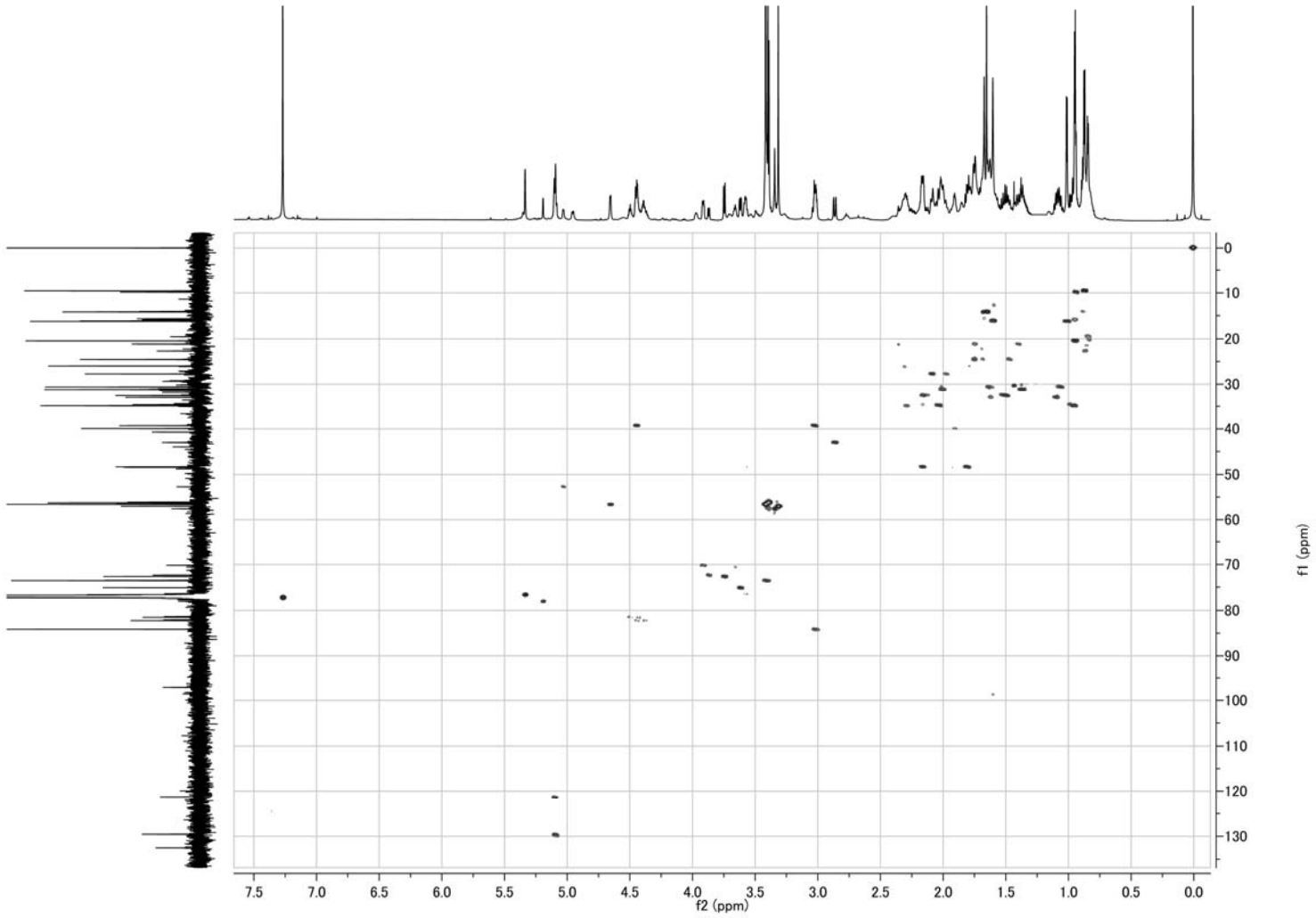

Figure S33. 2D HMQC NMR spectrum of 36-fluoro-FK520 (**25**).

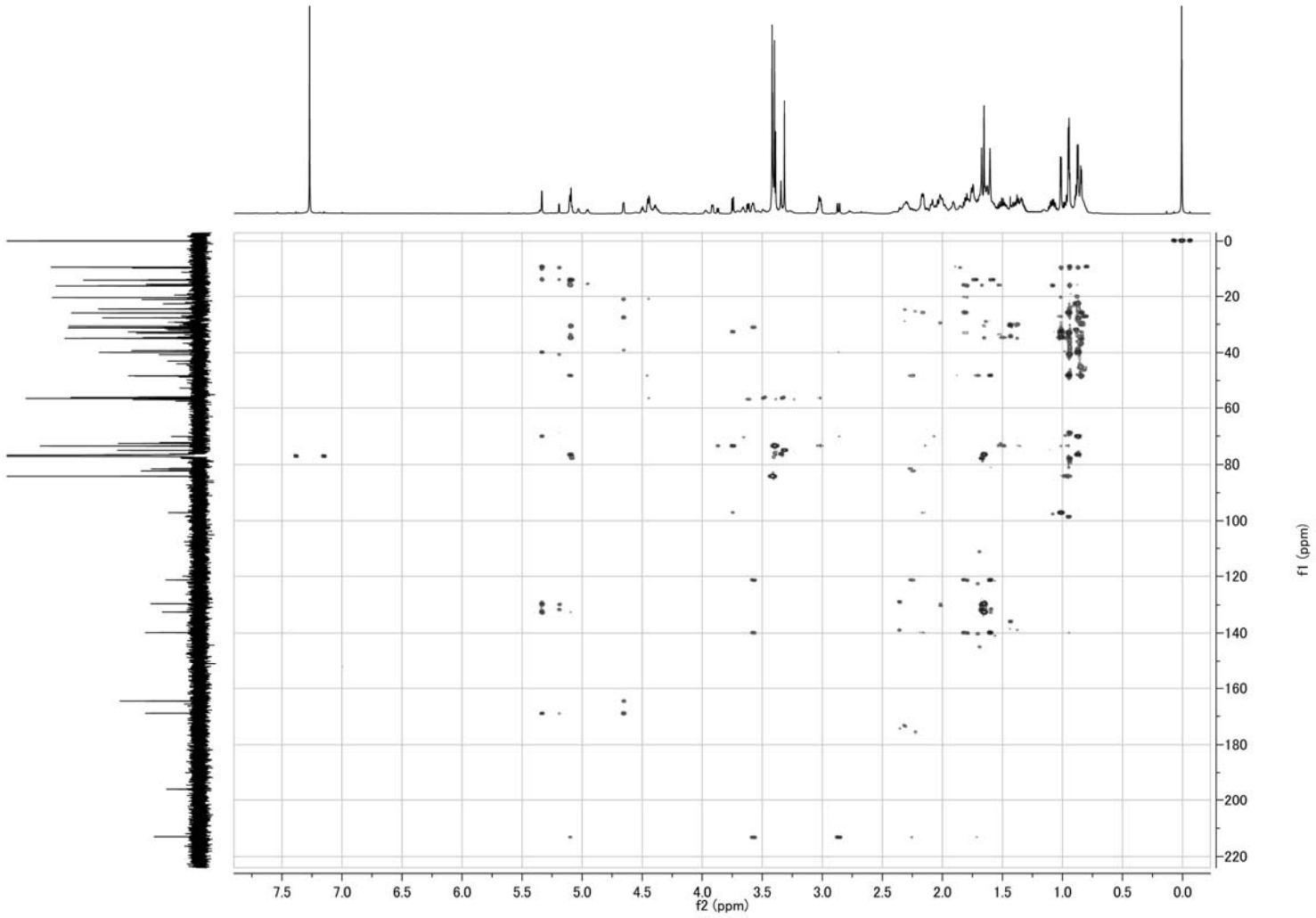

Figure S34. 2D HMBC NMR spectrum of 36-fluoro-FK520 (**25**).

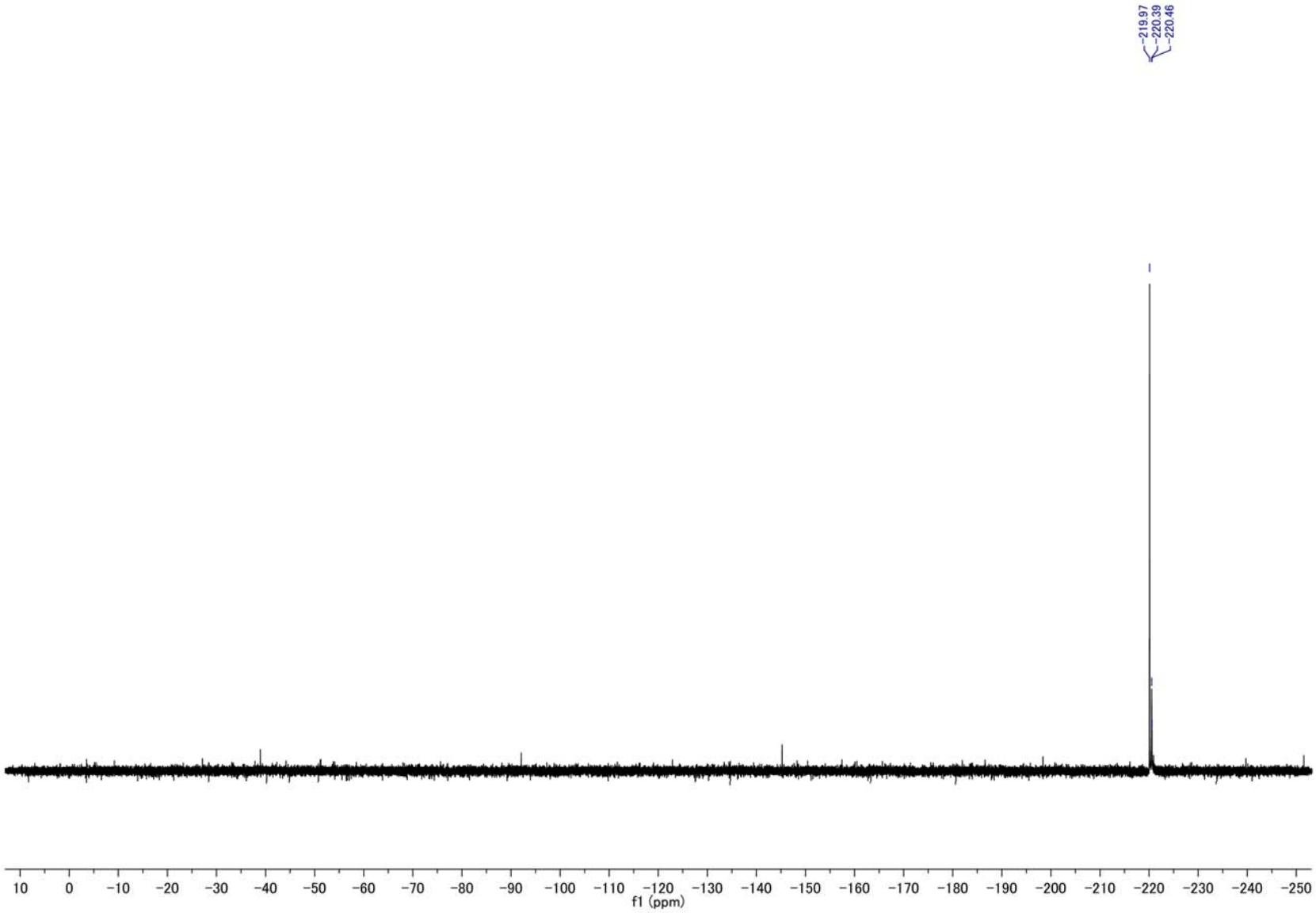

Figure S35. ^{19}F NMR spectrum of 36-fluoro-FK520 (**25**).

Table S10. NMR data for the novel FK506 analog 36-fluoro-FK520 (**25**)

Position	C	H	COSY correlations	HMBC correlations
1	168.84	-	-	
2	56.61	4.65	H-3a/b	C-1, 3, 4, 6, 8
3	27.71	2.09	H-2, 3b, 4a	
		1.98	H-2, 4a/b	C-1, 2
4	21.15	1.75	H-3a, 4b, 5b	C-2, 3, 6
		1.40	H-3a/b, 4a, 5a/b	
5	24.55	1.75	H-4b, 5b, 6a/b	C-3, 6
		1.47	H-4a, 5a, 6a/b	
6	39.29	4.45	H-5a/b	C-2, 8, 4, 5
		3.02	H-5a/b	C-2, 8
7	-	-		
8	164.45	-		
9	195.88	-		
10	97.04	-		
11	34.63	2.16	H-12b	C-10
12	32.60	2.16		C-13
		1.50		C-11, 13
13	73.55	3.41	H-12a/b	
14	72.65	3.75	H-13, 15	C-10, 12, 13, 15
15	75.12	3.62	H-16a/b	C-16
16	33.02	1.63	H-16b	C-14
		1.10		C-14, 15, 17
17	25.98	1.79		C-16, 19, 38
18	48.23	2.16	H-17	C-17,19
		1.81		C-16, 17, 19, 20, 39, 38
19	139.77	-		
20	121.23	5.10	H-21	C-18, 21, 22, 35, 39
21	48.40	3.58	H-20, 35	C-19, 20, 22, 35, 36

22	212.91	-		
23	43.02	2.86	H-23b, 24	C-22, 24, 25
		2.08	H-23a, 24	C-22, 24
24	70.19	3.91	H-23a/b, 25	C-26
25	39.94	1.90	H-24, 26	C-24, 40
26	76.67	5.34	H-25	C-24, 25, 27, 28, 40, 41
27	132.44	-		
28	129.48	5.10	H-29	C-26, 27, 29, 30, 34, 41
29	34.87	2.29	H-30a/b, 34a/b	
30	34.84	2.04	H-29, 31	
		0.97	H-29, 30a, 31	C-28, 29, 31, 32, 34
31	84.15	3.02	H-30a/b, 32	C-32, 44
32	73.51	3.41	H-31, 33a/b	C-31
33	31.18	2.00	H-32, 33b, 34a	
		1.38	H-32, 33a, 34a/b	C-29, 32, 34
34	30.62	1.64	H-29, 33a/b, 34b	C-28, 29, 30
		1.06	H-29, 33a/b	
35	31.05	2.25	H-36	C-20, 21, 22, 36
36	81.57	4.42	H-35	C-21
37	16.28	1.01	H-11	C-10, 11, 12
38	20.45	0.95	H-17	C-16, 17, 18
39	15.95	1.60		C-18, 19, 20
40	9.56	0.87	H-25	C-24, 25, 26
41	14.20	1.65		C-26, 27, 28
42	56.27	3.40		C-13
43	56.61	3.32		C-15
44	56.60	3.42		C-31

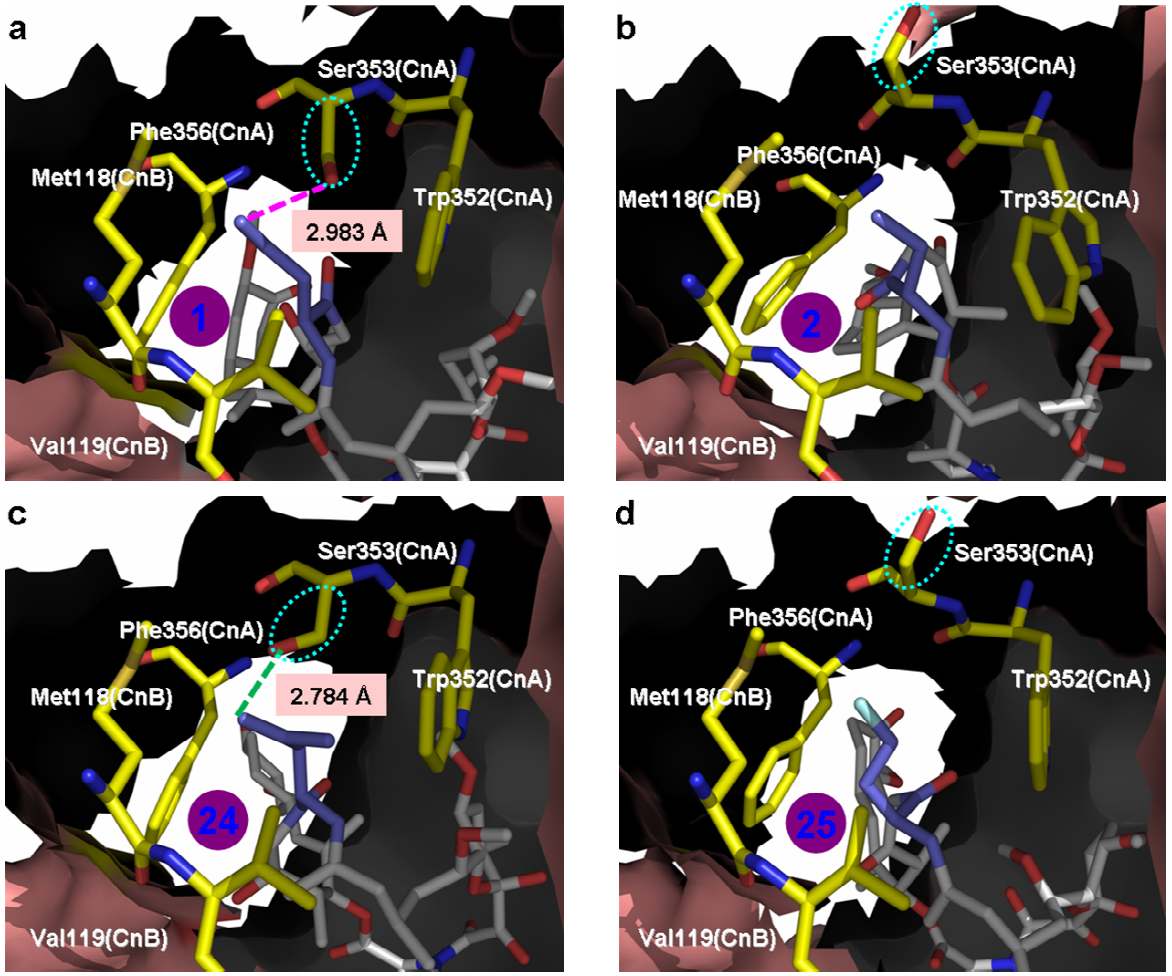

Figure S36. Snapshots of the average structure of the binding sites in 3-dimensional docking models. (**a**) Calcineurin A (CnA)-Calcineurin B (CnB)-FK506 (**1**), (**b**) CnA-CnB-FK520 (**2**), (**c**) CnA-CnB-36-methyl-FK506 (**24**), and (**d**) CnA-CnB-36-fluoro-FK520 (**25**) during 10-ns molecular dynamics simulation. The average distances between the oxygen atom of Ser353 in CnA and C-37 of **1** (purple dash) and **24** (green dash) in the simulated complex were 2.983 and 2.784 Å, respectively. The side chains of **1** and its analogs are shown in dark slate blue and the fluorine atom in **25** is shown in cyan. The dotted circles represent the orientation of Ser353 in CnA.

Table S11. Binding free energies of calcineurin-FKBP12 complex with **1** and its analog

Compound	ΔG_{elec}	ΔG_{vdw}	$\Delta G_{nonpol,\ sol}$	$\Delta G_{elec,sol}$	$-T\Delta S$	ΔG_{bind}
1	-11.83±0.12	-25.08±0.09	-2.93±0.01	21.53±0.09	12.61±0.41	-6.42±0.05
2	-14.36±0.13	-23.53±0.10	-3.03±0.01	23.13±0.06	11.76±0.56	-6.03±0.05
24	-12.20±0.12	-25.45±0.09	-2.90±0.01	20.40±0.08	12.37±0.54	-7.78±0.04
25	-11.75±0.07	-24.78±0.09	-3.05±0.01	21.45±0.08	12.31±0.56	-5.82±0.09

1: FK506, **2**: FK520, **24**: 36-methyl-FK506, **25**: 36-fluoro-FK520. The binding free energies were based on molecular dynamics simulation. All energies are given in units of kcal/mol. ΔG_{elec}, ΔG_{vdw}, $\Delta G_{nonp/sol}$, $\Delta G_{elec/sol}$, ΔG_{bind} represent electrostatic, van der Waals, nonpolar solvation, electrostatic solvation, and binding free energies, respectively. The uncertainties are the standard error of the mean calculated with 200 snapshots (50 snapshots for entropic calculations).

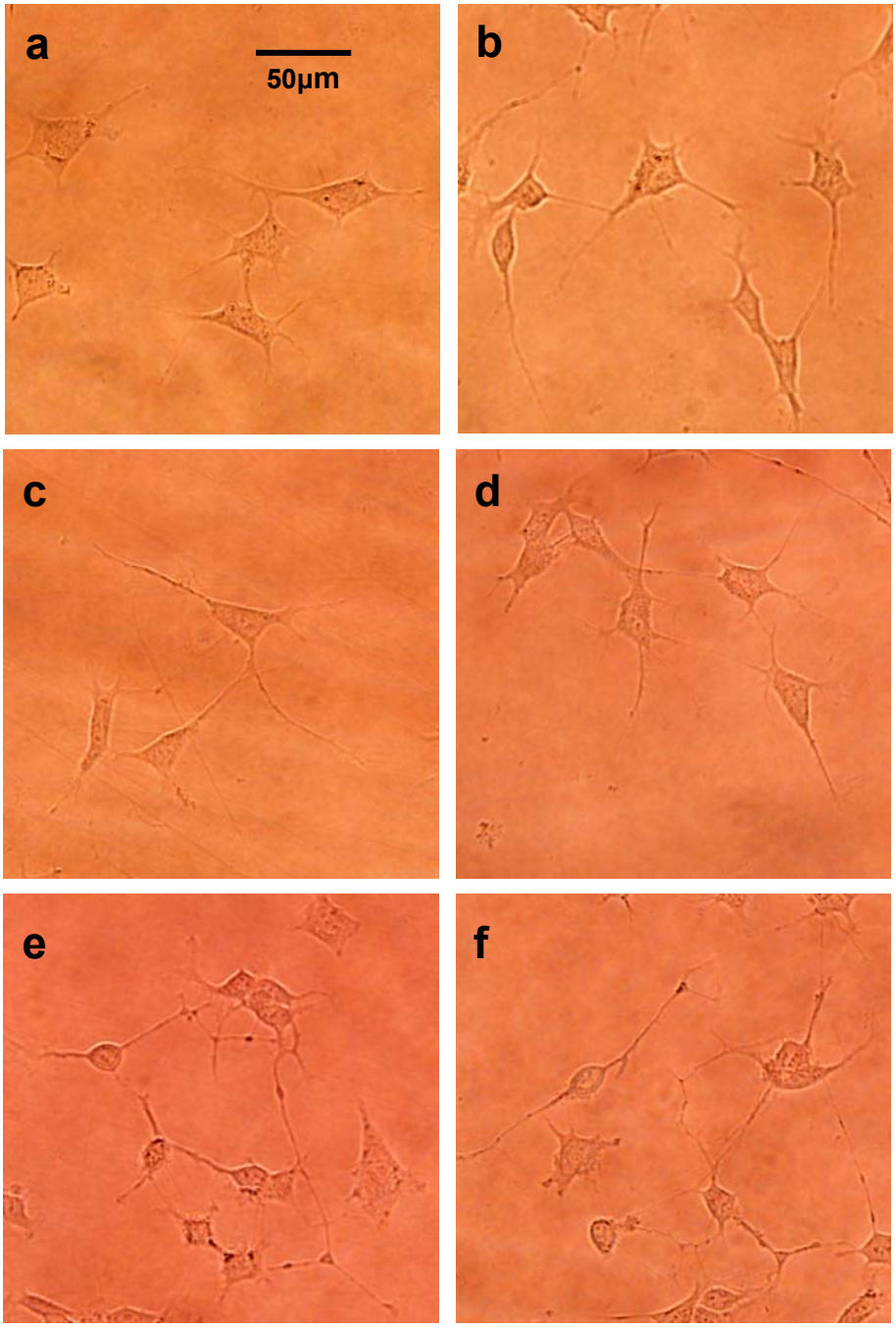

Figure S37. Representative micrographs of SH-SY5Y neuroblastoma cells. Untreated cells (**a**), cells treated with NGF alone (**b**), and cells treated with NGF in the presence of **1** (**c**), **2** (**d**), **24** (**e**) and **25** (**f**) at a concentration of 1 nM after 96 h of cultivation. Neurite processes are longer in treated cells, with the exception of those treated with **2** (**d**), compared with those treated with NGF alone (**b**) (see **Supporting Methods**).

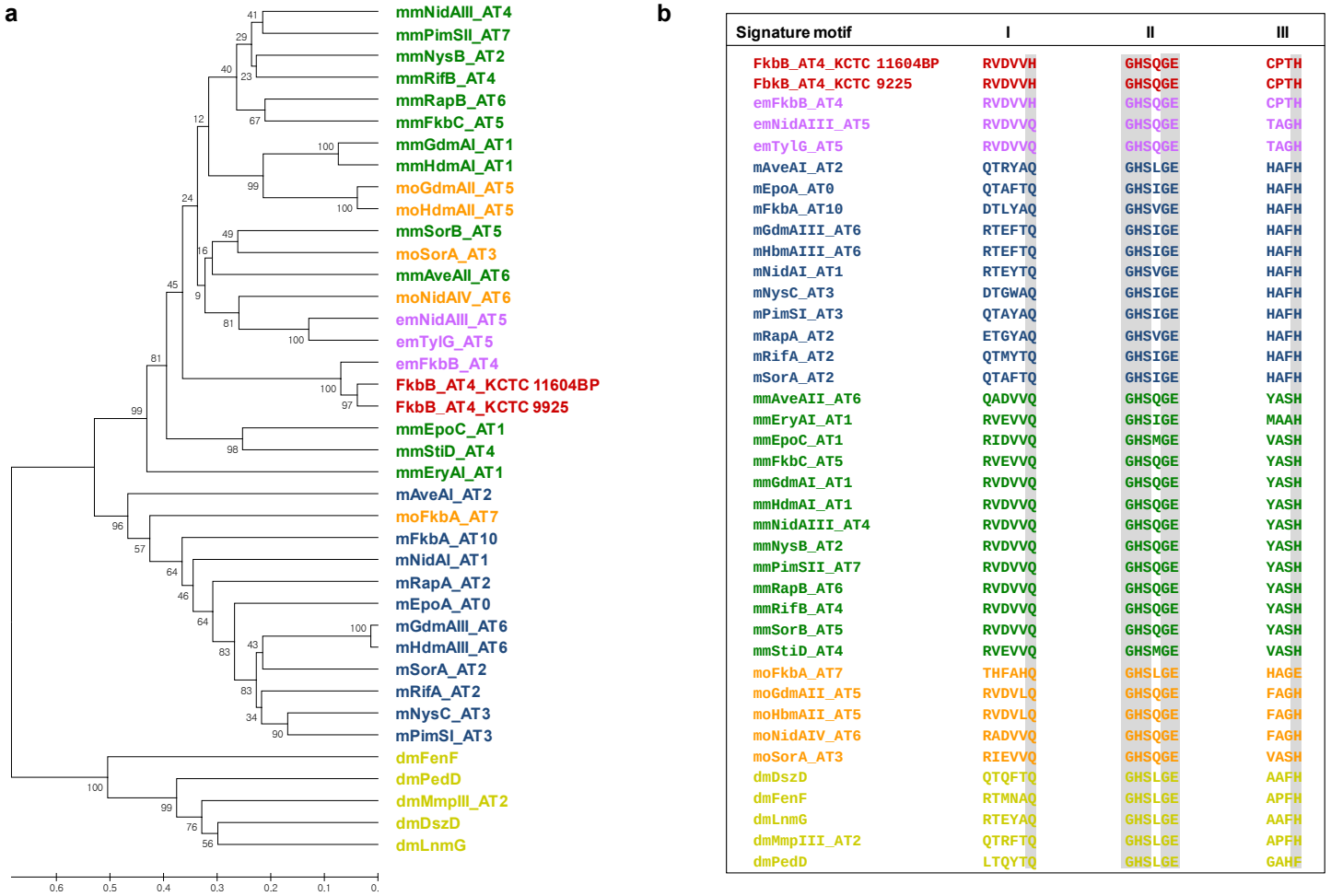

Figure S38. Phylogenetic analysis of module4 AT domains and their signature motifs. (**a**) Phylogenetic tree of the acyl transferase (AT) domains obtained by comparing the amino acid sequence of each module 4 AT domain derived from two **1**-producing strains with those in the NCBI nr protein database. (**b**) Module4 AT domain signature motifs. Three dominant motifs, containing of 6, 6, and 4 amino acid residues, are assigned with a group of ATs. Color codes used in this figure are: purple, ethylmalonyl (em)-specific AT domain; blue, malonyl (m)-specific AT domain; green, methylmalonyl (mm)-specific AT domain; orange, methoxylmalonyl (mo)-specific AT domain; and yellow, discrete malonyl (dm)-specific AT domain.

Supporting Methods

Materials, bacterial strains, and culture conditions. FK506 (**1**), FK520 (**2**), ethylmalonyl-CoA (**7**), propylmalonyl-CoA (**8**), crotonyl-CoA (**10**), [1-^{13}C]pentanoic acid (**19**), *trans*-2-hexenoic acid (**20**), 4-methylpentanoic acid (**21**), *trans*-2-pentenoic acid, diethyl propylmalonic acid, nicotinamide adenine dinucleotide phosphate (NADPH), ampicillin, apramycin, chloramphenicol, kanamycin, and nalidixic acid were purchased from Sigma. Ammonium acetate and allylmalonic acid were purchased from Fluka, and HPLC-grade acetonitrile, methanol, glacial acetic acid, and water were supplied by J.T. Baker. 4-Fluorocrotonic acid (**22**) was chemically synthesized as previously described[11]. A Copy Control Fosmid construction kit was purchased from Epicentre Biotechnologies. His-Bind nickel chelate chromatography resin was obtained from Novagen. Restriction endonucleases and T4 DNA ligase were purchased from New England Biolabs. Polymerase chain reactions were carried out using Taq DNA polymerase from Stratagene. All other chemicals were of the highest purity available. For NMR characterization of FK506 congeners and their analogs obtained from the culture media, samples purified via reversed-phase HPLC were prepared by dissolving each compound in 250 μl of $CDCl_3$ (Sigma) and placing the solution in a 5-mm Shigemi advanced NMR microtube (Sigma) matched to the solvent. ^{1}H, ^{13}C, ^{19}F, and 2D NMR spectra were acquired using a Bruker 9503DPX, Bruker DRX 300, Varian INOVA 500 and Bruker Avance II 900 spectrometer at 298K. Chemical shifts are given in ppm using tetramethylsilane (TMS) as an internal reference. All NMR data processing was done using the Mnova (Mestrelab Research S.L.) software.

Bacterial strains used in this study are listed in **Table S7**. The **1**-producing strains *Streptomyces* sp. KCTC 11604BP and *Streptomyces kanamyceticus* KCTC 9225 were obtained from GenoTech (Daejeon, Republic of Korea) and the Korean Collection for Type Cultures (Republic of Korea), respectively. The **2**-producing *Streptomyces hygroscopicus* var. *ascomyceticus* ATCC 14891 and **1**-producing *Streptomyces* sp. ATCC 55098 were obtained from the American Type Culture Collection (USA). Spores of *Streptomyces* sp. KCTC 11604BP, its gene deletion mutants, and *S. kanamyceticus*

KCTC 9225 were generated on ISP4 agar plates[12] and a seed culture was prepared in R2YE broth[13]. Fifty miligrams of vegetative cells grown in the seed culture were inoculated into a 250-ml baffled flask containing 50 ml of R2YE medium and cultivated on an orbital shaker (set at 180 rpm) for 6 d at 28 °C. *S. hygroscopicus* var. *ascomyceticus* ATCC 14891 was incubated in a baffled 250-ml flask containing 50 ml of SY medium[14] and grown on an orbital shaker for 6 d at 30 °C. *Streptomyces lividans* TK24, which was used as a heterologous host for preparing recombinant TcsD, was grown in YEME liquid medium[13]. *Escherichia coli* DH5α[15] was used for routine subcloning, while *E. coli* BL21(DE3) and *E. coli* BL21(DE3)pLysS (Novagen) were used as heterologous hosts for expression of recombinant TcsC and ACP_{tcsA}. *E. coli* ET12567/pUZ8002 was the nonmethylating plasmid donor strain[1] for intergeneric conjugation with *Streptomyces* sp. KCTC 11604BP. The *E. coli* strains were grown in LB, SOB or SOC liquid medium[15]. Ampicillin (100 μg/ml), apramycin (50 μg/ml), chloramphenicol (25 μg/ml), kanamycin (50 μg/ml), thiostrepton (25 μg/ml), and nalidixic acid (25 μg/ml) were selectively added to the growth media as required.

Identification and sequencing of the FK506 gene cluster. The genomic DNAs of *Streptomyces* sp. KCTC 11604BP, *S. kanamyceticus* KCTC 9225, and *Streptomyces* sp. ACTC 55098 were isolated using standard procedures[13] and size-fractionated through an agarose gel by pulsed field gel electrophoresis. Fragments approximately 40 kb in size were excised, recovered from the gel, and then cloned into the pCCFOS1 fosmid vector using the Copy Control Fosmid construction kit according to the manufacturer's protocols. The fosmid library was screened by end sequencing with pCC1/pEpiFOS forward and reverse primers, then the sequences of selected fosmids were determined by PCR analysis using FK506-specific primers. The PCR primer pairs (FkbDF/FkbDR and FkbOF/FkbOR) were designed based on the conserved sequences found in *Streptomyces* sp. ATCC 53770 (GenBank accession no. U65940.1) and *S. hygroscopicus* var. *ascomyceticus* ATCC 14891 (GenBank accession no. AF235504.1) (see **Table S3**).The PCR products were analyzed on an ABI PRISM 3700 automated sequencer (Applied Biosystems). The raw sequence data were processed and assembled with Management and Analysis for

Polyketide Synthase Type I (MAPSI) software[16]. Annotation analysis of the sequence data was performed through database comparison with the Basic Local Alignment Search Tool (BLAST) server of the National Center for Biotechnology Information (NCBI)[17].

Chemical synthesis of 3-oxopentanoyl-SNAC thioester (13). Pyridine (4.88 ml, 60 mmol) was added to a solution of Meldrum's acid (**13a**; 4.33 g, 30 mmol) in dichloromethane (MC; 30 ml) at 0 °C. A solution of propionyl chloride (CH_3CH_2COCl; 2.78 g, 30 mmol) in MC (30 ml) was then added dropwise to this solution. The reaction mixture was stirred at 0 °C for 1 h and warmed to room temperature, then stirred for 20 h. The reaction mixture was washed with 2 N HCl (3 × 40 ml), dried over $MgSO_4$ and concentrated *in vacuo* to give 2,2-dimethyl-5-propionyl-1,3-dioxane-4,6-dione (**13b**; 5.53 g, 92%) as a red solid. ^{1}H NMR (250 MHz, $CDCl_3$): δ 5.36 (s, 1H), 3.12 (q, J = 7.5 Hz, 2H), 1.74 (s, 6H), 1.26 (t, J = 7.5 Hz, 3H); ^{13}C NMR (62.5 MHz, $CDCl_3$): δ 198.6, 170.5, 159.9, 104.6, 90.8, 53.5, 29.3, 26.5, 9.5.

A solution of *N*-acetylcysteamine (HSNAC; 0.4 g, 3.33 mmol) in benzene (C_6H_6; 7 ml) was added to a stirred solution of **13b** (1.0 g, 5 mmol) in C_6H_6 (27.8 ml). The reaction mixture was heated to reflux under a nitrogen atmosphere for 7 h. After evaporation of the solvent, the residue was purified by chromatography to give the product 3-oxopentanoyl-SNAC thioester (**13**) as a yellow crystalline solid (0.47 g, 64%). ^{1}H NMR (250 MHz, $CDCl_3$): δ 3.72 (s, 2H), 3.49-3.44 (m, 2H), 3.12-3.07 (m, 2H), 2.69-2.57 (m, 2H), 1.99 (s, 3H), 1.07 (t, 3H). ^{13}C NMR (62.5 MHz, $CDCl_3$): δ 202.82, 192.36, 170.70, 56.90, 39.07, 36.70, 29.10, 23.09, 7.45 (see **Figures S7,S8**). Overall synthetic schemes for **13** are illustrated below.

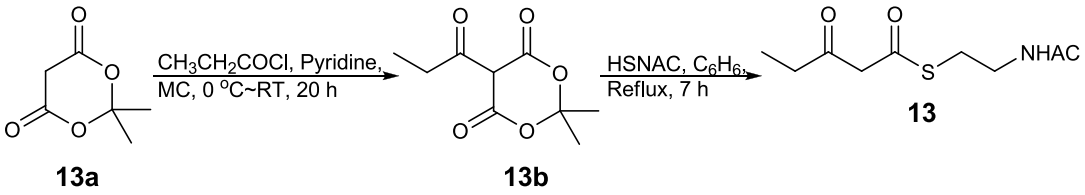

Chemical synthesis of *trans*-2-pentenyl-SNAC thioester (14). To an oven-dried, nitrogen-purged 100-

ml round bottom flask equipped with a stir bar was added *trans*-2-pentenoic acid (0.79 g, 7.92 mmol) and 50 ml of MC. After cooling to 0 °C, 1-(3-dimethylaminopropyl)-3-ethylcarbodiimide·HCl (EDCl; 1.66 g, 8.71 mmol) and 4-(*N*,*N*-dimethylamino)pyridine (DMAP; 50.2 mg, 0.42 mmol) were added to the mixture. After stirring at 0 °C for 15 min, HSNAC (0.94 g, 7.92 mmol) was added, and the mixture was allowed to warm to room temperature and was stirred for 4 h. After concentration *in vacuo*, the residue was dissolved in 50 ml of chloroform, washed successively with 0.01 N HCl (3 x 20 ml) and saturated aqueous NaCl, then dried over $MgSO_4$. After concentration *in vacuo*, the clear oil residue was purified by silica gel chromatography eluted with ethyl acetate:hexane (6:4) to yield 1.3 g of **14** (6.47 mmol, 82%). ^{1}H NMR (250 MHz, $CDCl_3$): δ 7.04-6.93 (m, 1H), 6.12 (d, 1H), 3.45 (q, 2H), 3.09 (t, 2H), 2.31-2.20 (m, 2H), 1.98 (s, 3H), 1.09 (t, 3H); ^{13}C NMR (62.5 MHz, $CDCl_3$): δ 190.42, 170.50, 147.88, 127.40, 39.70, 28.15, 25.30, 23.14, 11.98 (see **Figures S9,S10**). The synthetic scheme for **14** is illustrated below.

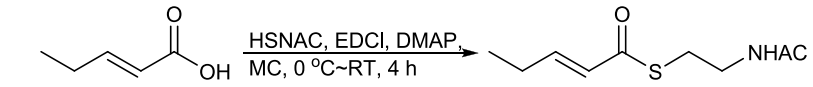

Trans-2-pentenoic acid **14**

Chemical synthesis of pentanoyl-SNAC thioester (15). To a 50-ml two-necked round-bottom flask containing diethyl propylmalonic acid (2.0 g, 10.0 mmol) and ethanol (EtOH, 5.0 ml) was added aqueous NaOH solution (6 M, 5.0 ml). The reaction was refluxed for 6 h, then neutralized with concentrated HCl (6 M, 8.25 ml). The organic phase was extracted with diethyl ether and washed with water and brine. The combined organic phase was dried over $MgSO_4$ and the volatile fraction was evaporated to afford propylmalonic acid as a white solid (1.26 g, 87%), which was used directly for the next step. ^{1}H NMR (250 MHz, $(CD_3)_2CO$): δ 3.37 (t, 1H), 1.89-1.80 (m, 2H), 1.45-1.39 (m, 2H), 0.94 (t, 3H); ^{13}C NMR (62.5 MHz, $(CD_3)_2CO$): δ 171.01, 52.32, 31.55, 21.17, 14.03.

Propylmalonic acid (0.73 g, 5.0 mmol) was dissolved in dimethylformamide (DMF, 50 ml) at 0 °C, treated with diphenylphosphoryl azide ($Ph_2P(O)_3N_3$; 1.63 ml, 7.5 mmol) and triethylamine (Et_3N; 1.39 ml, 10.0 mmol), then stirred for 2 h. HSNAC (0.54 ml, 5.0 mmol) was added and the mixture was

stirred at room temperature for an additional 3 h. The reaction was quenched by adding water (100 ml) and then extracted twice with ethyl acetate. The organic layer was evaporated, dried with anhydrous $MgSO_4$, and purified by silica gel chromatography eluted with MC: methanol (20:1) to give **15** (0.87 g, 85%) as a colorless oil. ^{1}H NMR (250 MHz, $CDCl_3$): δ 3.42 (q, 2H), 3.03 (t, 2H), 2.58 (t, 2H), 1.98 (s, 3H), 1.71-1.59 (m, 2H), 1.40-1.31 (m, 2H), 0.92 (t, 3H); ^{13}C NMR (62.5 MHz, $CDCl_3$): δ 200.11, 170.43, 43.78, 39.61, 28.32, 27.64, 23.11, 22.02, 13.66 (see **Figures S11,S12**). The overall synthetic schemes for **15** are illustrated below.

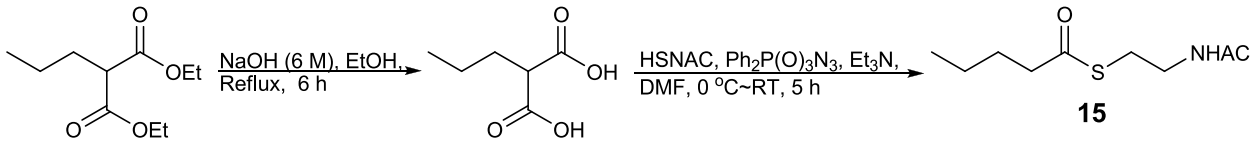

Propylmalonic acid

Chemical synthesis of allylmalonyl-SNAC thioester (16). Allylmalonic acid (0.2 g, 1.38 mmol) was dissolved in dry tetrahydrofuran (THF; 0.84 ml). To this solution, pyridine (0.24 ml) and *tert*-butanol (0.24 ml, 2.51 mmol) were added with stirring. The mixture was cooled to 0 °C, and methanesulfonyl chloride (0.11 ml, 1.42 mmol) was added over 10 min. The mixture was stirred at room temperature for 3 h and then filtered to remove the pyridine hydrochloride salt. The filtrate was diluted in water (10 ml). This solution was brought to pH ~11 using 4 N NaOH, then washed with MC (3 x 5 ml). The aqueous layer was acidified to pH~3 with concentrated HCl and extracted with MC (4 x 5 ml). Evaporation of MC afforded **16a** as a colorless oil (0.2 g, 71%). ^{1}H NMR (250 MHz, $CDCl_3$): δ 11.52 (s, 1H), 5.85-5.74 (m, 1H), 5.18-5.01 (m, 2H), 3.39 (t, J = 7.4 Hz, 1H), 2.63 (t, J = 7.1 Hz, 2H), 1.47 (s, 9H); ^{13}C NMR (62.5 MHz, $CDCl_3$): δ 176.0, 171.0, 136.3, 114.1, 72.3, 51.0, 28.0, 27.1.

To an oven-dried, nitrogen-purged 15-ml round-bottom flask equipped with a stir bar was added **16a** (0.15 g, 0.75 mmol) and 5 ml of MC. After cooling to 0 °C, EDCl (0.16 g, 0.82 mmol) and DMAP (4.75 mg, 0.04 mmol) were added successively to the mixture. The reaction mixture was stirred at 0 °C for 15 min and then HSNAC (0.12 ml, 1.12 mmol) was added. The reaction mixture was stirred overnight at room temperature, then concentrated *in vacuo*. The residue was dissolved in 25 ml of chloroform, washed

with 0.01 N HCl (3 x 10 ml) and then brine, then dried over $MgSO_4$. Concentration *in vacuo* gave a clear oil, which was purified by silica gel chromatography eluted with ethyl acetate:hexane (6:4), to yield **16b** (0.19 g, 0.63 mmol, 84%). ^{1}H NMR (250 MHz, $CDCl_3$): δ 5.97 (s, 1H), 5.83-5.16 (m, 1H), 5.16-5.05 (m, 2H), 3.58 (t, J = 7.5 Hz, 1H), 3.49-3.40 (m, 2H), 3.11-3.05 (m, 2H), 2.66-2.60 (m, 2H), 1.97 (s, 3H), 1.46 (s, 9H); ^{13}C NMR (62.5 MHz, $CDCl_3$): δ 195.3, 170.4, 167.2, 133.7, 117.7, 82.5, 60.3, 39.4, 33.3, 28.7, 27.8, 23.1.

A solution of **16b** (0.9 g, 3.0 mmol) in trifluoroacetic acid (TFA; 25 ml) was stirred for 12 h at 0 °C. The TFA was removed *in vacuo*, and the residue was repeatedly dissolved in benzene and concentrated *in vacuo* to afford 0.67 g of **16** (2.72 mmol, 91%). ^{1}H NMR (250 MHz, $CDCl_3$): δ 5.89-5.62 (m, 1H), 5.16-5.02 (m, 2H), 3.73 (t, 2H), 3.39-3.34 (m, 1H), 3.10-3.04 (m, 2H), 2.68-2.32 (m, 2H), 1.94 (s, 3H); ^{13}C NMR (62.5 MHz, $CDCl_3$): δ 195.46, 172.23, 168.36, 133.05, 118.30, 59.34, 39.92, 38.64, 33.18, 21.99 (see **Figures S13,S14**). The overall synthetic schemes for **16** are illustrated below.

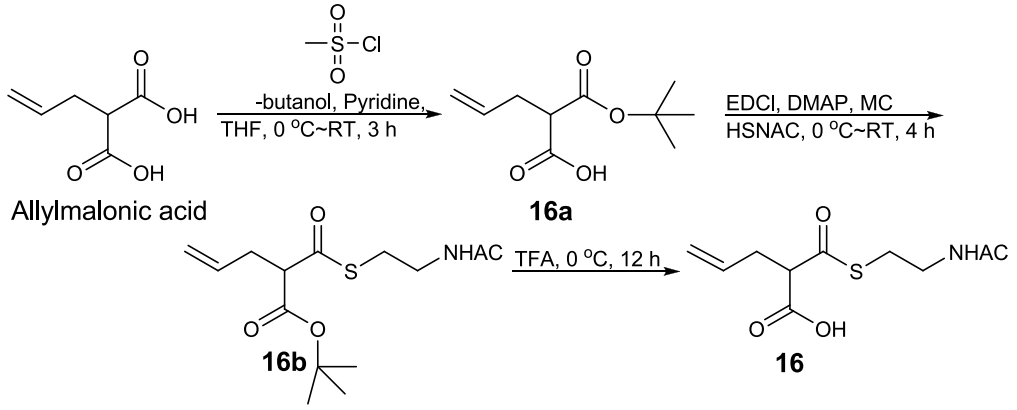

Chemical synthesis of propylmalonyl-SNAC thioester (17). Propylmalonic acid (0.2 g, 1.37 mmol) was dissolved in dry THF (0.84 ml). Pyridine (0.24 ml) and *tert*-butanol (0.24 ml, 2.51mmol) were added with stirring. After cooling to 0 °C, methanesulfonyl chloride (0.11 ml, 1.42 mmol) was added over 10 min. The mixture was stirred at room temperature for 3 h and then filtered to remove the pyridine hydrochloride salt. The filtrate was diluted in water (10 ml). This solution was brought to pH ~11 using 4 N NaOH and then washed with MC (3 x 5 ml). The aqueous layer was acidified to pH ~3 with concentrated HCl and

extracted with MC (4 x 5 ml). Evaporation of the solvent afforded **17a** as a colorless oil (0.19 g, 70%). ^{1}H NMR (250 MHz, $CDCl_3$): δ 11.51 (s, 1H), 3.30 (t, J = 7.5 Hz, 1H), 1.91-1.82 (m, 2H), 1.47 (s, 9H), 1.45-1.33 (m, 2H), 0.93 (t, J = 7.3 Hz, 3H); ^{13}C NMR (62.5 MHz, $CDCl_3$): δ 177.0, 172.0, 73.2, 52.0, 29.0, 27.1, 19.7, 13.7.

To a solution of **17a** (0.15 g, 0.75 mmol) in MC (5 ml) were successively added EDCl (0.16 g, 0.82 mmol) and DMAP (4.75 mg, 0.04 mmol). The mixture was stirred at 0 °C for 15 min and then HSNAC (0.12 ml, 1.12 mmol) was added. The reaction mixture was stirred overnight at room temperature, then concentrated *in vacuo*. The residue was dissolved in 20 ml of chloroform and washed successively with 0.01 N HCl (3 x 10 ml) and brine, then dried over $MgSO_4$. After concentration *in vacuo*, the clear oil residue was purified by silica gel chromatography eluted with ethyl acetate:hexane (6:4) to yield **17b** (0.2 g, 0.64 mmol, 87%). ^{1}H NMR (250 MHz, $CDCl_3$): δ 6.23 (s, 1H), 3.53-3.42 (m, 3H), 3.11-3.04 (m, 2H), 1.97 (s, 3H), 1.88-1.84 (m, 2H), 1.46 (s, 9H), 1.39-1.30 (m, 2H), 0.93 (t, J = 7.3 Hz, 3H); ^{13}C NMR (62.5 MHz, $CDCl_3$): δ 196.0, 170.5, 167.9, 82.2, 60.8, 39.4, 31.4, 28.6, 27.8, 23.1, 20.4, 13.7.

In an oven-dried, nitrogen-purged 50-ml round-bottom flask equipped with a stir bar, compound **17b** (0.91 g, 3.0 mmol) was cooled to 0 °C, then 25 ml of TFA was added and the mixture was stirred for 24 h at 0 °C. After evaporation of TFA *in vacuo*, the residue was repeatedly dissolved in benzene and concentrated *in vacuo* to afford 0.67 g of **17** (2.70 mmol, 90%). ^{1}H NMR (250 MHz, $CDCl_3$): δ 3.63 (t, 2H), 3.46-3.43 (m, 1H), 3.20-2.98 (m, 2H), 2.00 (s, 3H), 1.94-1.85 (m, 2H), 1.40-1.31 (m, 2H), 0.93 (t, 3H); ^{13}C NMR (62.5 MHz, $CDCl_3$): δ 196.57, 172.86, 171.86, 59.73, 39.48, 31.55, 28.44, 22.45, 20.46, 13.65 (see **Figures S15,S16**). The overall synthetic schemes for **17** are illustrated below.

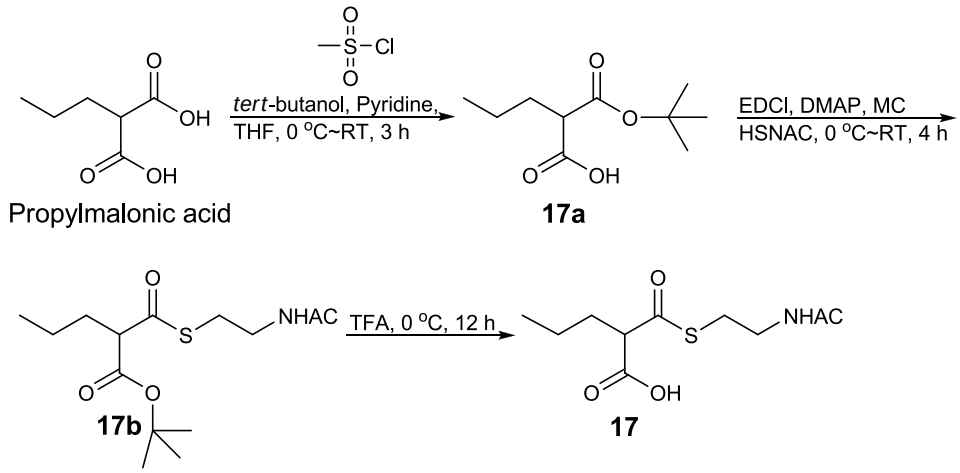

Chemical synthesis of allylmalonyl-CoA (9). To a solution of allylmalonic acid (0.5 g, 3.47 mmol) and thiophenol (0.35 ml, 3.42 mmol) in DMF (35 ml), a solution of dicyclohexylcarbodiimide (DCC, 0.87 g, 0.61 mmol) in dimethylformamide (50 ml) was added over 2 h at 0 °C. Stirring was continued for an additional 3 h at 0 °C, then the reaction was quenched by adding 10 ml of water. The precipitated dicyclohexyl urea was filtered, and the filtrate was acidified with 1 N HCl to pH 2.5. The monothiophenyl ester present in the filtrate was extracted with ether (4 × 100 ml). The combined organic extracts were washed with 0.1 N HCl and then concentrated *in vacuo* until the volume of the solution was ~50 ml. The monothiophenyl ester present in the ether was extracted with 0.2 N sodium bicarbonate ($NaHCO_3$). The aqueous phase was extracted with 50 ml of ether to remove traces of thiophenol and dithiophenyl ester. Then, the pH was adjusted with cold 1 N HCl to ~2. The monothiophenyl ester was extracted again with ether (2 × 100 ml). The combined organic extracts were washed with brine (50 ml) and dried over anhydrous sodium sulfate, then filtered and concentrated *in vacuo* to give **9a** (0.65 g) as a white solid (yield = 81%). ^{1}H NMR (250 MHz, $CDCl_3$): δ 10.01 (s, 1H), 7.45 (s, 5H), 5.87-5.79 (m, 1H), 5.26-5.15 (m, 2H), 3.84 (t, J = 7.5 Hz, 1H), 2.80-2.74 (m, 2H); ^{13}C NMR (62.5 MHz, $CDCl_3$): δ 192.7, 173.6, 134.5, 133.1, 129.9, 129.4, 126.6, 118.5, 58.8, 33.4 ppm.

To 10 mg of CoA ester (CoA; 12 μmol) dissolved in 167 μl of 0.1M $NaHCO_3$ (pH 8.0) was added monothiophenyl ester **9a** (15.44 mg, 65.3μmol) in 100 μl of 0.1 M $NaHCO_3$ at 0 °C. The solution pH was

adjusted by addition of a cold 0.2 N NaOH solution to ~8, then stirring was continued for 6 h at 0 °C. The reaction was quenched by acidification to pH 4 with 0.5 N HCl, then the mixture was extracted with ether (4 × 10 ml) to remove traces of monothiophenyl ester and thiophenol. The aqueous phase was extracted with ethyl acetate (5 × 10 ml) to remove the allylmalonic acid and then lyophilized to give 11.5 mg of allylmalonyl-CoA (**9**; yield = 98%). ^{1}H NMR (500 MHz, D_2O): δ 8.57 (s, 1H), 8.26 (s, 1H), 6.18 (d, 1H), 5.90-5.84 (m, 1H), 5.12 (d, 2H), 5.07-5.02 (m, 1H), 4.69-4.59 (m, 1H), 4.25 (s, 1H), 4.02 (s, 2H), 3.84-3.80 (m, 2H), 3.75-3.68 (m, 2H), 3.43-3.49 (m, 1H), 3.38-3.31 (m, 2H), 3.18 (t, 1H), 3.08-3.01 (m, 2H), 2.57 (t, 2H), 2.59-2.44 (m, 2H), 0.88 (s, 3H), 0.74 (s, 3H) (see **Figure S21**). The overall synthetic schemes for **9** are illustrated below.

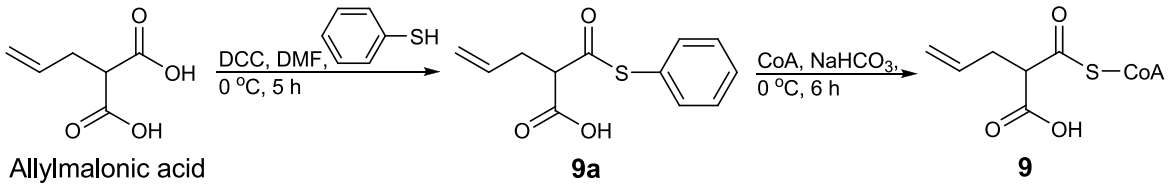

Chemical synthesis of *trans*-2-pentenyl-CoA (11). To a solution of *trans*-2-pentenoic acid (18.62 mg, 0.186 mmol, 6 equiv.) in anhydrous THF (8 ml), cooled to 0 °C and under nitrogen, was added Et_3N (26 µl, 0.186 mmol, 6 equiv.) followed by ethyl chloroformate (18 µl, 0.188 mmol, 6 equiv.), and the mixture was stirred at 0 °C for 45 min. The stirring was then stopped to allow the resulting solid to precipitate. The clear THF supernatant was added slowly to a solution of hydrated CoA (24 mg, 0.031 mmol, 1 equiv.) and $NaHCO_3$ (15 mg, 0.18 mmol) in double distilled water (3 ml). The reaction mixture was stirred at room temperature for 4 h after which the THF was removed under vacuum. The aqueous solution was acidified to pH 3 using 1 N HCl and then extracted with ethyl acetate (3 × 3 ml) to remove excess *trans*-2-pentenoic acid. The aqueous solution was then lyophilized and the resulting solid was washed with methanol to afford *trans*-2-pentenyl-CoA (**11**) as a white solid. ^{1}H NMR (500 MHz, D_2O): δ 8.79 (s, 1H), 8.68 (s, 1H), 7.20-7.13 (m, 1H), 6.42-6.35 (m, 1H), 6.30 (d, 1H), 5.11-5.01 (m, 1H), 4.65-4.60 (m, 1H), 4.42 (s, 1H), 4.16 (s, 1H), 4.04-3.98 (m, 2H), 3.79-3.73 (m, 2H), 3.68-3.47 (m, 1H), 3.32 (t,

2H), 3.19 (t, 2H), 2.49-2.33 (m, 2H), 1.99-1.93 (m, 2H), 1.38 (t, 3H), 1.07 (s, 3H), 0.96 (s, 3H) (see **Figure S18**). The synthetic scheme for **11** is illustrated below.

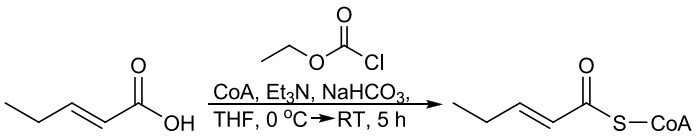

Trans-2-pentenoic acid **11**

Construction of in-frame gene deletion plasmids. pGEM-T Easy Vector (Promega) and Litmus28 (New England Biolabs) were used for routine subcloning. *E. coli–Streptomyces* shuttle vector pKC1139[6] was used for in-frame gene deletion. To delete nine *tcs* genes (*tcsA*, *tcsB*, *tcsC*, *tcsD*, *tcs1*, *tcs2*, *tcs3*, *tcs4*, and *tcs5*) and *fkbA* in *Streptomyces* sp. KCTC 11604BP, the construction of recombinant plasmids was carried out by PCR amplification of the left- and right-flanking fragments from fosmid (fos1004F01) DNA derived from *Streptomyces* sp. KCTC 11604BP. One gene was targeted in each reaction. The primer pairs TcsALF/TcsALR, TcsBLF/TcsBLR, TcsCLF/TcsCLR, TcsDLF/TcsDLR, Tcs1LF/Tcs1LR, Tcs2LF/Tcs2LR, Tcs3LF/Tcs3LR, Tcs4LF/Tcs4LR, Tcs5LR/Tcs5LF, and FkbALF/FkbALR were designed for the amplification of left-flanking fragments of target genes, whereas TcsARF/TcsARR, TcsBRF/TcsBRR, TcsCRF/TcsCRR, TcsDRF/TcsDRR, Tcs1RF/Tcs1RR, Tcs2RF/Tcs2RR, Tcs3RF/Tcs3RR, Tcs4RF/Tcs4RR, Tcs5RR/Tcs5RF, and FkbARF/FkbARR were for right-flanking fragments (**Table S8**). A total of 20 PCR fragments were separately cloned in pGEM-T Easy vector and sequenced. After digestion with appropriate restriction enzymes, the fragments were cloned into pKC1139 digested with *Hind*III-*Eco*RI or *Hind*III-*Xba*I, to construct 10 different in-frame deletion plasmids: pΔTCSA, pΔTCSB, pΔTCSC, pΔTCSD, pΔTCS1, pΔTCS2, pΔTCS3, pΔTCS4, pΔTCS5 and pΔFKBA (**Table S7**).

Construction of protein expression plasmids. pET15b (Novagen) containing an N-terminal His_6-tag was used for the expression of recombinant ACP_{tcsA} and Sfp (PPTase), whereas N, C-terminal His_6-tagged

pET28a (Novagen) was used for TcsC. Amplification of *tcsC* was accomplished with the primers TcsCF and TcsCR. The PCR product was cloned into pET28a to generate pTCSC with an N, C-terminal His_6-tag (**Tables S7,S8**). Amplification of the DNA fragments containing ACP_{tcsA} domain in *tcsA* was accomplished with the primers TcsAF and TcsAR. The PCR product was cloned into pET15b to produce pTCSA-ACP with an N-terminal His_6-tag (**Tables S7,S8**). The gene *sfp* encoding 4'-phosphopantetheinyl transferase (PPTase) from *Bacillus subtilis* was amplified by PCR from pGF101[7] using primers SfpF and SfpR. The PCR product was cloned into pET15b to generate pSFP with an N-terminal His_6-tag (**Tables S7, S8**). Amplication of *tcsD* was performed using primers TcsDF and TcsDR. The PCR product was cloned into pET15b to generate pTCSD1 with an N-terminal His_6-tag. This plasmid was digested with *Xba*I and *Hind*III and then cloned into pSE34, yielding pTCSD.

Gene deletion. The plasmids used for in-frame gene deletion are summarized in **Table S7**. They were introduced into *Streptomyces* sp. KCTC 11604BP by conjugation from ET12567/pUZ8002[1] and then target genes were deleted by homologous recombination. A strain in which a single crossover between deletion plasmid and the KCTC 11604BP chromosome had occurred was selected by cultivation of an apramycin-resistant transconjugant at 37 °C (the non-permissive temperature for the pSG5-based replicon) in the presence of apramycin. One such colony was then subjected to three rounds of propagation in the absence of selection at 30 °C to allow for the second crossover. The ten desired double crossover mutants, ΔtcsA, ΔtcsB, ΔtcsC, ΔtcsD, Δtcs1, Δtcs2, Δtcs3, Δtcs4, Δtcs5, and ΔfkbA, were selected by their apramycin-sensitive phenotype, then verified by PCR and selectively confirmed by Southern blot analysis (see **Table S7**).

Chemical complementation of the four *tcs* deletion mutants with acyl-SNAC thioesters. Seed cultures of the mutant strains were grown in R2YE medium for 2 d at 28 °C and then used as 50-mg (wet weight) inocula for 50-ml liquid cultures of the same medium as described above. 3-Oxopentanoyl- (**13**), *trans*-2-pentenyl- (**14**), pentanonyl- (**15**), allylmalonyl- (**16**), and propylmalonyl- (**17**) SNAC thioesters

were added to separate culture of mutants of *Streptomyces* sp. KCTC 11604BP (strains ΔtcsA, ΔtcsB, ΔtcsC, and ΔtcsD) at a final concentration of 10 mM on 3 d. The production cultures were grown for 5 d at 28 °C as described above. The culture broth was collected by vacuum filtration, and then extracted twice with an equal volume of ethyl acetate[18]. The organic extract was evaporated to dryness under reduced pressure and then dissolved in 0.2 ml methanol for HPLC–ESI–MS/MS analysis (**Figure 4**; see **Methods**). Independent experiments were carried out in triplicate.

Measurement of labeled precursor incorporation rate using [1-^{13}C]pentanoic acid (19). Following the general feeding procedure as described above, [1-^{13}C]**19** (1.03 g/l) was added to the *tcsB* in-frame deletion mutant (ΔtcsB strain). [8-^{13}C, 20-^{13}C, 22-^{13}C] FK506 (**1**; 4.32 mg), [8-^{13}C, 22-^{13}C] FK520 (**2**; 1.91 mg), and [8-^{13}C, 22-^{13}C] FK523 (**12**; 1.54 mg) were purified via reversed-phase HPLC (Watchers C_{18}, 5 μm, 250 × 4.6 mm, flow rate 1.0 ml/min, detection at 205 nm, 50 °C) using an isocratic gradient of 60% (v/v) aqueous acetonitrile. **1**, **2**, and **12** were eluted at 27.5, 26.0, and 20.0 min, respectively (see **Figure S17**).

Production of FK506 analogs. The ΔtcsB mutant of *Streptomyces* sp. KCTC 11604BP was grown as described above. *Trans*-2-hexenoic acid (**20**), 4-methylpentanoic acid (**21**), and 4-fluorocrotonic acid (**22**) were supplemented as described above in 50-ml cultures at a final concentration of 10 mM.

36,37-Dihydro-37-methyl-FK506 (23). The broth (300 ml) to which 343 mg of **20** had been added was harvested, and the cell-free broth was extracted with ethyl acetate as described above. Evaporation of the ethyl acetate under reduced pressure left approximately 0.1 g of reddish foam. HPLC purification of this material gave a trace amount of **23**; HR-ESI-MS: m/z $[M+NH_4]^+$ 837.0682 (calculated for $C_{45}H_{73}NO_{12}$, 837.0606); fragmented product ions: 784.3 $[M+NH_4\text{-}3H_2O]^+$, 766.3 $[M+NH_4\text{-}4H_2O]^+$, 752.3 $[M+NH_4\text{-}4H_2O\text{-}CH_2]^+$, 734.3 $[M+NH_4\text{-}5H_2O\text{-}CH_2]^+$, 592.2, 574.3 $[592.2\text{-}H_2O]^+$, 564.3 $[592.2\text{-}C_2H_4]^+$, 548.2 $[592.2\text{-}H_2O\text{-}C_2H_2]^+$ (see **Figure S22** for ESI-MS/MS spectrum of **23**).

36-Methyl-FK506 (24). The broth (18.0 liters) to which 20.9 g of **21** had been added was harvested, and the cell-free broth was extracted with ethyl acetate as described above. Evaporation of the ethyl acetate under reduced pressure left approximately 1.5 g of reddish foam. HPLC purification of this material gave **24** (1.2 mg); HR-ESI-MS: m/z $[M+NH_4]^+$ 835.0499 (calculated for $C_{45}H_{71}NO_{12}$, 835.0447); fragmented product ions: 782.3 $[M+NH_4\text{-}3H_2O]^+$, 764.2 $[M+NH_4\text{-}4H_2O]^+$, 750.2 $[M+NH_4\text{-}4H_2O\text{-}CH_2]^+$, 732.2 $[M+NH_4\text{-}5H_2O\text{-}CH_2]^+$, 590.1, 572.2 $[590.2\text{-}H_2O]^+$, 562.3 $[590.2\text{-}C_2H_4]^+$, 546.3 $[590.2\text{-}H_2O\text{-}C_2H_2]^+$, 528.3 $[590.2\text{-}2H_2O\text{-}C_2H_2]^+$, 514.2 $[590.2\text{-}2H_2O\text{-}CH_2]^+$. The ESI-MS/MS and NMR spectra of **24** are illustrated in **Figures S23** to **S28** and **Table S9**.

36-Fluoro-FK520 (25). The broth (1.6 liters) to which 200 mg of **22** had been added was harvested, and the cell-free broth was extracted with ethyl acetate as described above. Evaporation of the ethyl acetate under reduced pressure left approximately 0.3 g of reddish foam. HPLC purification of this material gave **25** (0.7 mg); HR-ESI-MS: m/z $[M+NH_4]^+$ 827.0050 (calculated for $C_{43}H_{68}FNO_{12}$, 827.0012); fragmented product ions: 774.2 $[M+NH_4\text{-}3H_2O]^+$, 756.3 $[M+NH_4\text{-}4H_2O]^+$, 742.3 $[M+NH_4\text{-}4H_2O\text{-}CH_2]^+$, 724.3 $[M+NH_4\text{-}5H_2O\text{-}CH_2]^+$, 582.1, 564.1 $[582.1\text{-}H_2O]^+$, 538.1 $[582.1\text{-}H_2O\text{-}C_2H_2]^+$. The ESI-MS/MS and NMR spectra of **25** are illustrated in **Figures S29** to **S35** and **Table S10**.

Phylogenetic analysis and sequence alignment of *tcsA* through *tcsD*, and the AT4 domain in *fkbB*. Gene sequences obtained from GenBank were manually edited and aligned based on their protein sequence using the ClustalX[19] and MEGA 4[20] programs. Deduced amino acid sequences of the AT domain in TcsA, the ACP domain in TcsA, as well as the TcsB, TcsC, TcsD, and the AT domain of module 4, were used as queries to search for related proteins in the nr protein database at NCBI using the BLASTP algorithm with default parameters. Distances were calculated with the Dayhoff-PAM matrix using PROTDIST and then a neighbor-joining tree was produced using NEIGHBOUR in the PHYLogeny Interface Package v3.65 (PHYLIP)[21]. One hundred bootstrap resamplings were performed using

SEQBOOT and CONSENSE in the PHYLIP package.

Preparation and purification of a recombinant ACP_{tcsA}, TcsC, Sfp and TcsD. For the expression and purification of the ACP domain of TcsA (ACP_{tcsA}), the expression plasmid pTCSA-ACP was introduced into *E.coli* BL21(DE3)pLysS and the BL21(DE3)pLysS/pTCSA-ACP strain was grown in LB medium supplemented with 50 μg/ml ampicillin, and 25 μg/ml chloramphenicol. Each liter of culture was inoculated with 10 ml of overnight starter culture. The culture was grown at 37 °C to an optical density (OD_{600}) of 0.6, then expression was induced with 0.1 mM isopropyl-β-D-thiogalactopyranoside (IPTG). At the same time, the incubation temperature was shifted from 37 to 18 °C and the culture was grown for another 15 to 16 h. Cells were harvested by centrifugation (10 min at 6,000 × *g*), re-suspended in lysis buffer (50 mM sodium phosphate buffer, pH 8.0, containing 300 mM NaCl and 10 mM imidazole), and then lysed by sonication. The lysate was clarified by centrifugation (30 min at 15,000 × *g*). Recombinant ACP_{tcsA} was purified by Ni-affinity chromatography according to the manufacturer's recommendations (Qiagen). The purified protein was subjected to 13% SDS-PAGE and visualized with Coomassie blue staining. The resultant protein was dialyzed against 50 mM phosphate buffer (pH 7.2) containing 1 mM EDTA, 1 mM dithiothreitol (DTT) and 10% glycerol, and then stored at -80 °C before use in the *in vitro* reaction.

For the expression and purification of TcsC, the expression plasmid pTCSC was introduced into *E.coli* BL21(DE3), and the BL21(DE3)/pTCSC strain was grown in LB medium supplemented with 50 μg/ml kanamycin. Each liter of culture was inoculated with 10 ml of overnight starter culture. The culture was grown at 37 °C to an OD_{600} of 0.6, then expression was induced with 0.1 mM IPTG. At the same time, the incubation temperature was shifted from 37 to 28 °C and the culture was grown for another 15 to 16 h. Recombinant TcsC was purified as described above.

For the expression and purification of Sfp (PPTase), the expression plasmid pSFP was introduced into *E.coli* BL21(DE3) pLysS, and the BL21(DE3)pLysS/pSFP strain was grown in LB medium

supplemented with 50 μg/ml ampicillin and 25 μg/ml chloramphenicol. Each liter of culture was inoculated with 10 ml of overnight starter culture. The culture was grown at 37 °C to an OD_{600} of 0.6, then expression was induced with 0.1 mM IPTG. The culture was grown for another 4 h. Recombinant Sfp was also purified as described above.

For the expression and purification of TcsD, pTCSD was introduced into another heterologous host *S. lividans* TK24, by transformation via a standard method[13]. The resulting *S. lividans* TK24/pTCSD was grown in YEME medium with 25 μg/ml of thiostrepton according to a previous method[22]. Recombinant TcsD was also purified as described above.

Protein concentrations were determined with a commercial Bio-Rad protein assay kit, and then corrected for the *in vitro* reactions as described below.

***In vitro* characterization of TcsC as 2-pentenyl-ACP carboxylase/reductase and TcsD as acyl-ACP dehydrogenase.** As a substrate for TcsC and TcsD reactions, 2-pentenyl-ACP_{tcsA} was prepared by phosphopantetheinylation of apo-ACP_{tcsA} using recombinant Sfp from *B. subtilis*[23]. The reaction mixture (50 μl), which contained 340 μM recombinant apo-ACP_{tcsA}, 100 mM sodium phosphate buffer (pH 7.2), 100 mM $MgCl_2$, 2.5 mM *trans*-2-pentenyl-CoA (**11**), and 10 μM recombinant Sfp, was incubated at 37 °C for 30 min. To collect the acylated ACP protein, 10% (v/v) trichloroacetic acid (TCA) solution was added, and the mixture was centrifuged (10 min at 13,000 × *g*). The precipitate was reconstituted in TcsC reaction mixture (100 μl), which contained 10 μg recombinant TcsC, 5 mM NADPH and 33 mM $NaHCO_3$. The reactions were run for 1 h at 30 °C to examine the reductive carboxylation activity of TcsC on *trans*-2-pentenyl-ACP_{tcsA}. After the reaction, the enzymatic reaction product was also concentrated by using TCA precipitation method described above. To check the dehydrogenation activity of TcsD on *trans*-2-pentenyl-ACP_{tcsA}, the precipitates obtained from the above Sfp-catalyzed reaction were separately reconstituted in TcsD reaction mixture (100 μl) containing 100 mM sodium phosphate buffer (pH 7.2), 6 μM phenazine methosulfate (PMS), 0.4 mM FAD, and 8 μg recombinant TcsD, then incubated at 37 °C

for 30 min, as previously reported[24]. Reactions to examine the enzymatic activity of TcsD (or TcsC) on propylmalonyl-ACP_{tcsA} (or *2E*-2,4-pentadienyl-ACP_{tcsA}) were sequentially conducted by dissolving the precipitate obtained by the TcsC-catalyzed (or TcsD-catalyzed) reaction into the above-mentioned TcsD (or TcsC) reaction mixture, which was then incubated at 37 °C for 30 min (or 1 h). The same reactions using boiled TcsC and TcsD were carried out as controls.

The molecular mass of 2-pentenyl-ACP_{tcsA} and its enzymatic reaction products were analyzed on a Waters/Micromass Quattro *micro* tandem ESI-MS instrument operated in the positive ion mode, scanning from 600 to 1,600 *m/z*. The optimized tune parameters were as follows: capillary and cone voltage at 2.0 kV and 40 V, respectively; cone gas and desolvation gas set at 150 and 650 l/h, respectively; and source and desolvation temperatures at 120 and 330 °C, respectively. The mass spectra were processed and deconvoluted using MassLynx MaxEnt 1 software from Waters. The uniform Guassian model and a resolution of 0.75 Da were used for MaxEnt 1 deconvolution (see **Figure 5**). Protein profiles from the reaction mixtures were examined by HPLC. Samples were separated on an XTerra C_{18} column (250 × 4.6 mm, 5 μm; Waters) interfaced with an UV detector (220 nm) using an isocratic elution of 60% (v/v) aqueous acetonitrile containing 0.1% formic acid at a flow rate of 0.1 ml/min over 40 min.

***In vitro* characterization of TcsC as 2-pentenyl-CoA carboxylase/reductase and TcsD as acyl-CoA dehydrogenase.** Recombinant TcsC was assayed using previously reported methods with modification[25,26]. TcsC (10 μg) was incubated with crotonyl- (**10**) or *trans*-2-pentenyl- (**11**) CoA (2 mM each) in reaction buffer (100 mM Tris-HCl, pH 8.0, 5 mM NADPH, and 33 mM $NaHCO_3$) at 30 °C for 1 h. Recombinant TcsD (8 μg) was incubated with **11** (2 mM) in reaction buffer (100 mM sodium phosphate buffer, pH 7.2, 0.4 mM FAD, and 6 μM PMS) at 37 °C for 30 min. Reactions were carried out as described above for the *in vitro* reaction using ACP_{tcsA} to qualitatively determine the preferred activities of both enzymes on acyl-CoAs or acyl-ACPs. Detection of TcsC-mediated production of ethylmalonyl- (**7**) or propylmalonyl- (**8**) CoA from 100 μl of reactants was carried out using HPLC-ESI-

MS/MS analysis as previously described[9].

Intracelluar CoA-ester profiles derived from FK506- and FK520-producing wild-type strains. Aliquots of cultures of the wild-type FK506 (**1**)-producing strain *Streptomyces* sp. KCTC 11604BP and the FK520 (**2**)-producing strain *S. hygroscopicus* var. *ascomyceticus* ATCC 14891 were taken at 3 d, and were subjected to silicon-oil layer centrifugation followed by a solid-phase extraction procedure, then analyzed by HPLC-ESI-MS/MS as described above[9] (see **Figure S20**). Authentic allylmalonyl-CoA (**9**) was chemically synthesized in this study (see the earlier section in **Supporting Methods; Figure S21**).

3-Dimensional (3D) modeling, docking and molecular dynamics simulation of 1, 2, 24, and 25 in the presence of FKBP12-calcineurins complex. The immunosuppressive activities of the mutasynthetic novel analogs **24** and **25** were predicted before they were subjected to *in vitro* bioassays. Structural scaffolds of the analogs along with the known immunosuppressants **1** and **2** were docked separately into the binding sites of the refined calcineurin A/B complex using the LigandFit[27] module in Discovery Studio 2.0 based on the crystal structure of the **1**/calcineurin complex[28] (PDB:1TCO). The scoring function with specific parameters for the complex containing **1** analogs was used to rank the docking poses. The conformation with the lowest binding energy and the greatest number of members in the cluster, indicating good convergence, was selected as the best conformation. The best orientation was identified and optimized using the scoring function based on the CHAMM force field[29] and energy minimization for induced-fit simulation[30]. The pose with lowest energy was selected as the initial conformation for further longtime molecular dynamics simulation.

The molecular dynamics simulations were performed with the AMBER 10 program[31]. The AMBER ff03 all atom force field31[32] was used for the protein and the general AMBER force field[33] was used for docked scaffolds. The energy minimization for each complex was performed by a combination of the steepest descent method for 5,000 steps and the conjugated gradient method for another 5,000 steps. After the minimization, each system was gradually heated from 0 to 300 K over 100 ps under the

isothermal-isochoric (NVT) ensemble condition and equilibrated at 300 K for 100 ps. Finally, 10-ns position-restrained molecular dynamics simulations were conducted at 1 atm and 300 K under the isothermal-isobaric (NpT) ensemble condition[34,35]. During the simulation, the SHAKE algorithm[36] was applied to constrain the covalent bonds to hydrogen atoms. The time step and nonbonding interaction cut-off radius were set to 2.0 fs and 10.0 Å, respectively. Coordinates were saved every 1.0 ps during the entire process (see **Figure S36** and **Supporting Notes**).

Calculation of the binding free energy obtained from the virtual fixation between each FK506 analog and the FKBP12-calcineurins complex can simulate the ligand affinities around the complex, thus enabling inference of the relative immunosuppressive activities of analogs **24** and **25** compared with those of **1** and **2**. The binding free energy between FK506 analogs and the calcineurin complex was calculated with the MM-PBSA approach[37-39] according to the following equation $\Delta G_{binding}=\Delta G_{MM}+\Delta G_{solv}-T\Delta S$; $\Delta G_{binding}$: binding free energy; ΔG_{MM}: molecular mechanical energy; ΔG_{solv}: solvation energy; $T\Delta S$: entropy contribution. The molecular mechanical energy is calculated by the following equation $\Delta G_{MM}=\Delta G_{elec}+\Delta G_{vdw}$; ΔG_{elec}: electrostatic energy; ΔG_{vdw}: van der Waals energy. The solvation energy is divided into two components; $\Delta G_{solv}=\Delta G_{elec.sol}+\Delta G_{nonpol.sol}$, where $\Delta G_{elec.sol}$ represents the electrostatic contribution to solvation energy, and $\Delta G_{nonpol.sol}$ means the nonpolar solvation term. Here, the polar contribution was calculated by solving the Poisson-Boltzmann equation using the PBSA program in AMBER 10[31], whereas the latter is determined using $\Delta G_{nonpol.sol}= \gamma(SASA)+b$, where γ represents surface tension, b is a constant, whereas SASA is the solvent-accessible surface area ($Å^2$) determined by the LCPO method[40]. The coefficients γ and b were set to 0.0072 kcal $(mol \cdot Å^2)^{-1}$ and 0, respectively[41]. Two hundred snapshots from the last 2.0 ns of the production stage were extracted for calculation of the binding free energy. The polar contribution term of the solvation energy was calculated using the PBSA program in AMBER 10[31]. Normal mode analysis was conducted to estimate entropic changes using the mode program[42] in AMBER 10[29]. Fifty snapshots of each system were selected for the entropy calculation[43-45] (see **Table S11** and **Supporting Notes**).

***In vitro* T-cell activation assay.** The relative immunosuppressive properties of the mutasynthetic analogs **24** and **25**, compared with authentic **1** and **2**, were determined using T lymphocytes as described elsewhere[46]. In brief, human T-cells (1 x 10^6 cells/well) were activated with CD3/CD28 antibodies (BD Pharmingen; 0.5 μg/ml for each), then treated with two different concentrations (0.1 and 1.0 nM) of **1**, **2**, **24** and **25** for 16 to 20 hr. After removal of cell debris by routine centrifugation, the supernatant was subjected to ELISA (R&D Systems) to quantify the level of interleukin-2 secreted from activated T-cells. The level of interleukin-2 obtained from T-cells activated with CD3/CD28 without further treatment with the above compounds was used as a control (see **Figure 8**).

***In vitro* neurite outgrowth assay using human neuroblastoma cells.** The relative nerve regeneration activities of the mutasynthetic analogs **24** and **25**, compared with authentic **1** and **2**, were determined using human neuroblastoma cells as described elsewhere[47,48]. The human neuroblastoma SH-SY5Y cells were plated in a 96-well plate (1x10^3 cells/well) and treated with nerve growth factor (NGF; KOMA Biotech; 10 ng/ml) to induce neurite outgrowth in the presence or absence of 1 nM **1**, **2**, **24** or **25**. The cells (n=90) were randomly photographed after 96 hr of cultivation, then the number of cells with outgrowth was counted. The neurite lengths were measured on photographic prints as previously described[47]. Duplicate wells were run in all experiments, and the entire experiment was replicated with three times. Neurite length estimated from samples treated with NGF alone was used as a control (see **Figure 8** and **Figure S37**).

Statistical analysis. For statistical comparisons of group differences, especially for both the T-cell activation and neurite outgrowth assays, quantitative data were analyzed by one-way analysis of variance (ANOVA) followed by Fisher's t-test according to the statistical program SigmaStat (Jandel Scientific; version 3.1).

Supporting Notes

The binding modes of 1 and its analogs. The effect of structural modification of the allyl group of **1** on its binding modes was investigated by analyzing molecular dynamics (MD) trajectories. Superimposition of the average structures of FK506 analogs showed that neither modification significantly altered the binding modes of the FKBP12-**1**-calcineurin complex. This finding indicates that the key residues of the calcineurin complex are relatively hydrophobic: Trp352 in calcineurin A, and Met118 and Val119 in calcineurin B. Among the amino acids in the active sites of the calcineurin complex, Ser353 is the only polar residue that provides an electrostatic interaction to orient the binding mode of **1** and its analogs. Before starting MD simulation, the hydroxyl group of Ser353 in calcineruin A pointed to the outer spheres of **1** and its analogs. After MD refinement, however, the hydroxyl group of Ser353 in both calcineurin-**1** and -**24** complexes was turned in the direction of their side chains, forming an electrostatic interaction as shown in **Figure S36a** and **c**. In contrast, the orientation of the hydroxyl group of Ser353 in the calcineurin-**2** and -**25** complexes remained outward as shown in **Figure S36b** and **d**. Although the conformations of **1** and **24** during MD simulation are similar, the average distance between the oxygen group of Ser353 and C37 of **24** (2.784Å) is shorter than that of **1** (2.983Å). Snapshots of the active site structure of all of the above simulations shown in **Figure S36** provide more detailed information regarding the interaction between the calcineurin residues and FK506 analogs including **1**.

Binding free energy analysis. Binding free energies of **1** and its analogs were calculated with the MM-PBSA method. The calculated binding free energies of FKBP12-FK506 analogs and the calcineurin complexes are -6.42, -6.03, -7.78 and -5.82 kcal/mol for **1**, **2**, **24**, and **25**, respectively, and are listed in **Table S11**. The calcineurin-FKBP12-**24** complex had the lowest binding free energy. The electrostatic interaction of Ser353 in calcineurin A with **24** and the relatively short distance between the oxygen atom of Ser353 and C37 of **24** might have contributed to this result.

Supporting References

1. MacNeil, D. J.; Gewain, K. M.; Ruby, C. L.; Dezeny, G.; Gibbons, P. H.; MacNeil, T. *Gene* **1992**, *111*, 61.

2. Motamedi, H.; Cai, S. J.; Shafiee, A.; Elliston, K. O. *Eur. J. Biochem.* **1997**, *244*, 74.

3. Muramatsu, H.; Mokhtar, S. I.; Katsuoka, M.; Ezaki, M. *Actinomycetologica* **2005**, *19*, 33.

4. Wu, K.; Chung, L.; Revill, W. P.; Katz, L.; Reeves, C. D. *Gene* **2000**, *251*, 81.

5. Walczak, R. J.; Hines, J. V.; Strohl, W. R.; Priestley, N. D. *Org. Lett*. **2001**, *3*, 2277.

6. Bierman, M.; Logan, R.; O'Brien, K.; Seno, E. T.; Rao, R. N.; Schoner, B. E. *Gene* **1992**, *116*, 43.

7. Zhou, P.; Florova, G.; Reynolds, K. A. *Chem. Biol*. **1999**, *6*, 577.

8. Yoon, Y. J.; Beck, B. J.; Kim, B. S.; Kang, H. Y.; Reynolds, K. A.; Sherman, D. H. *Chem. Biol*. **2002**, *9*, 203.

9. Park, J. W.; Jung, W. S.; Park, S. R.; Park, B. C.; Yoon, Y. J. *J. Mass Spectrom*. **2007**, *42*, 1136.

10. Park, J. W.; Mo, S.; Park, S. R.; Ban, Y. H.; Yoo, Y. J.; Yoon, Y. J. *Anal. Biochem*. **2009**, *393*, 1.

11. Liu, Y.; Hazzard, C.; Eustáquio, A. S.; Reynolds, K. A.; Moore, B. S. *J. Am. Chem. Soc.* **2009**, *131*, 10376.

12. Shirling, E. B.; Gottlieb, D. *Int. J. Syst. Bacteriol*. **1966**, *16*, 313.

13. Kieser, T.; Bibb, M. J.; Buttner, M. J.; Chater, K. F.; Hopwood, D. A. *Practical Streptomyces Genetics*; Ch. 19; John Innes Foundation: Norwich, England, 2000.

14. Oki, T.; Matsuzawa, K.; Kiyoshima, K.; Yoshimoto, A.; Naganawa, H.; Takeuchi, T.; Umezawa, H. *J. Antibiot. (Tokyo)* **1981**, *34*, 783.

15. Sambrook, J.; Fritsch, E. F.; Maniatis, T. *Molecular Cloning: A Laboratory Manual*, 3rd ed. ; Cold Spring Harbor Laboratory Press: Cold Spring Harbor, NY, 2000.

16. http://gate.smallsoft.co.kr:8080/pks

17. http://blast.ncbi.nlm.nih.gov/Blast.cgi

18. Mo, S.; Ban, Y. H.; Park, J. W.; Yoo, Y. J.; Yoon, Y. J. *J. Ind. Microbiol. Biotechnol*. **2009**, *36*, 1473.

19. Larkin, M. A.; Blackshields, G.; Brown, N. P.; Chenna, R.; McGettigan, P. A.; McWilliam, H.; Valentin, F.; Wallace, I. M.; Wilm, A.; Lopez, R.; Thompson, J. D.; Gibson, T. J.; Higgins, D. G. *Bioinformatics* **2007**, *23*, 2947.

20. Tamura, K.; Dudley, J.; Nei, M.; Kumar, S. *Mol. Biol. Evol*. **2007**, *24*, 1596.

21. Felsenstein, J. *PHYLIP (Phylogeny Inference Package) Version 3.6.* Distributed by the author; Department of Genome Sciences, University of Washington, Seattle, WA, 2005.

22. Ghatge, M. S.; Reynolds, K. A. *J. Bacteriol*. **2005**, *187*, 7970.

23. Quadri, L. E.; Weinreb, P. H.; Lei, M.; Nakano, M. M.; Zuber, P.; Walsh, C. T. *Biochemistry* **1998**, *37*, 1585.

24. Zhang, Y. X.; Denoya, C. D.; Skinner, D. D.; Fedechko, R. W.; McArthur, H. A.; Morgenstern, M. R.; Davies, R. A.; Lobo, S.; Reynolds, K. A.; Hutchinson, C. R. *Microbiology* **1999**, *145*, 2323.

25. Wallace, K. K.; Bao, Z. Y.; Dai, H.; Digate, R.; Schuler, G.; Speedie, M. K. Reynolds, K. A. *Eur. J. Biochem*. **1995**, *233*, 954.

26. Eustáquio, A. S.; McGlinchey, R. P.; Liu, Y.; Hazzard, C.; Beer, L. L.; Florova, G.; Alhamasheh, M. M.; Lechner, A.; Kale, A. J.; Kobayashi, Y.; Reynolds, K. A.; Moore, B. S. *Proc. Natl. Acad. Sci. USA* **2009**, *106*, 12295.

27. Montes, M.; Miteva, M. A.; Villoutreix, B. O. *Proteins* **2007**, *68*, 712.

28. Griffith J. P.; Kim, J. L.; Kim, E. E.; Sintchak, M. D.; Thomson, J. A.; Fitzgibbon, M. J.; Fleming, M. A.; Caron, P. R.; Hsiao, K.; Navia, M. A. *Cell* **1996**, *82*, 507.

29. Vanommeslaeghe, K.; Hatcher, E.; Acharya, C.; Kundu, S.; Zhong, S.; Shim, J.; Darian, E.; Guvench, O.; Lopes, P.; Vorobyov, I.; Mackerell, A. D. Jr. *J. Comput. Chem.* **2010**, *31*, 671.

30. Chang, C. E.; Gilson, M. K. *J. Am. Chem. Soc*. **2004**, *126*, 13156.

31. Case, D. A.; Darden, T. A.; Cheatham, T. E. III.; Simmerling, C. L.; Wang, J.; Duke, R. E.; Luo, R.; Crowley, M.; Walker, R. C.; Zhang, W.; Merz, K. M.; Wang, B.; Hayik, S.; Roitberg, A.; Seabra, G.; Kolossvary, I.; Wong, K. F.; Paesani, F.; Vanicek, J.; Wu, X.; Brozell, S. R.; Steinbrecher, T.; Gohlke, H.; Yang, L.; Tan, C.; Mongan, J.; Hornak, V.; Cui, G.; Mathews, D. H.; Seetin, M. G.; Sagui, C.;

Babin, V.; Kollman, P. A. *AMBER 10*; University of California, San Francisco, CA, 2008.

32. Duan, Y.; Wu, C.; Chowdhury, S.; Lee, M. C.; Xiong, G.; Zhang, W.; Yang, R.; Cieplak, P.; Luo, R.; Lee, T.; Caldwell, J.; Wang, J.; Kollman, P. *J. Comput. Chem.* **2003**, *24*, 1999.

33. Wang, J.; Wolf, R. M.; Caldwell, J. W.; Kollman, P. A.; Case, D. A. *J. Comput. Chem.* **2004**, *25*, 1157.

34. Wang, J.; Deng, Y.; Roux, B. *Biophys. J.* **2006**, *91*, 2798.

35. Cecchini, M.; Krivov, S. V.; Spichty, M.; Karplus, M. *J. Phys. Chem. B* **2009**, *113*, 9728.

36. Rychaert, J. P.; Ciccotti, G.; Berendsen, H. J. C. *J. Comput. Phys.* **1997**, *2*, 327.

37. Massova, I.; Kollman, P. A. *Perspec. Drug Discov. Design* **2000**, *18*, 113.

38. Wang, J.M.; Morin, P.; Wang, W.; Kollman, P. A. *J. Am. Chem. Soc.* **2001**, *123*, 5221.

39. Kollman, P. A.; Massova, I.; Reyes, C.; Kuhn, B.; Huo, S.; Chong, L.; Lee, M.; Lee, T.; Duan, Y.; Wang, W.; Donini, O.; Cieplak, P.; Srinivasan, J.; Case, D. A.; Cheatham, T. E. 3rd. *Acc. Chem. Res.* **2000**, *33*, 889.

40. Weiser, J.; Shenkin, P. S.; Still, W. C. *J. Comput. Chem.* **1999**, *20*, 217.

41. Weis, A.; Katebzadeh, K.; Söderhjelm, P.; Nilsson, I.; Ryde, U. *J. Med. Chem.* **2006**, *49*, 6596.

42. Brooks, B. R.; Janezic, D.; Karplus, M. *J. Comput. Chem.* **1995**, *16*, 1522.

43. Chang, C. -E. A.; Chen, W.; Gilson, M. K. *Proc. Natl. Acad. Sci. USA* **2007**, *104*, 1534.

44. Deng, Y.; Roux, B. *J. Phys. Chem. B* **2009**, *113*, 2234.

45. Karplus, M.; Kushick, J. N. *Macromolecules* **1981**, *14*, 325.

46. Choi, J. M.; Ahn, M. H.; Chae, W. J.; Jung, Y. G.; Park, J. C.; Song, H. M.; Kim. Y. E.; Shin, J. A.; Park, C. S.; Park, J. W.; Park, T. K.; Lee, J. H.; Seo, B. F.; Kim, K. D.; Kim, E. S.; Lee, D. H.; Lee, S. K.; Lee, S. K. *Nat. Med.* **2006**, *12*, 574.

47. Revill, W. P.; Voda, J.; Reeves, C. R.; Chung, L.; Schirmer, A.; Ashley, G.; Carney, J. R.; Fardis, M.; Carreras, C. W.; Zhou, Y.; Feng, L.; Tucker, E.; Robinson, D.; Gold, B. G. *J. Pharmacol. Exp. Ther.* **2002**, *302*, 1278.

48. Gold, B. G.; Densmore, V.; Shou, W.; Matzuk, M. M.; Gordon, H. S. *J. Pharmacol. Exp. Ther.* **1999**, *289*, 1202.